

DISSERTATION

**THE RESPONSE OF COARSE-BED RIVERS TO
LARGE FLOODS IN CALIFORNIA AND COLORADO**

Submitted by

John Pitlick

Department of Earth Resources

**In partial fulfillment of the requirements
for the Degree of Doctor of Philosophy**

Colorado State University

Fort Collins, Colorado

Fall, 1988

This is an authorized facsimile, made from the microfilm master copy of the original dissertation or masters thesis published by UMI.

The bibliographic information for this thesis is contained in UMI's Dissertation Abstracts database, the only central source for accessing almost every doctoral dissertation accepted in North America since 1861.

U·M·I Dissertation Information Service

University Microfilms International
A Bell & Howell Information Company
300 N. Zeeb Road, Ann Arbor, Michigan 48106
800-521-0600 OR 313/761-4700

Printed in 1993 by xerographic process
on acid-free paper

3266

Order Number 8911828

**The response of coarse-bed rivers to large floods in California
and Colorado**

Pitlick, John Charles, Ph.D.

Colorado State University, 1968

U·M·I

300 N. Zeeb Rd.
Ann Arbor, MI 48106

INFORMATION TO USERS

The most advanced technology has been used to photograph and reproduce this manuscript from the microfilm master. UMI films the text directly from the original or copy submitted. Thus, some thesis and dissertation copies are in typewriter face, while others may be from any type of computer printer.

The quality of this reproduction is dependent upon the quality of the copy submitted. Broken or indistinct print, colored or poor quality illustrations and photographs, print bleedthrough, substandard margins, and improper alignment can adversely affect reproduction.

In the unlikely event that the author did not send UMI a complete manuscript and there are missing pages, these will be noted. Also, if unauthorized copyright material had to be removed, a note will indicate the deletion.

Oversize materials (e.g., maps, drawings, charts) are reproduced by sectioning the original, beginning at the upper left-hand corner and continuing from left to right in equal sections with small overlaps. Each original is also photographed in one exposure and is included in reduced form at the back of the book. These are also available as one exposure on a standard 35mm slide or as a 17" x 23" black and white photographic print for an additional charge.

Photographs included in the original manuscript have been reproduced xerographically in this copy. Higher quality 6" x 9" black and white photographic prints are available for any photographs or illustrations appearing in this copy for an additional charge. Contact UMI directly to order.

U·M·I


University Microfilms International
A Bell & Howell Information Company
300 North Zeeb Road, Ann Arbor, MI 48106-1346 USA
313/761-4700 800/521-0600


COLORADO STATE UNIVERSITY

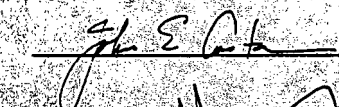
SEPTEMBER 19, 1988

WE HEREBY RECOMMEND THAT THE DISSERTATION PREPARED UNDER OUR SUPERVISION BY JOHN PITLICK ENTITLED RESPONSE TO LARGE FLOODS ON COARSE-BED RIVERS IN CALIFORNIA AND COLORADO BE ACCEPTED AS FULFILLING IN PART THE REQUIREMENTS FOR THE DEGREE OF DOCTOR OF PHILOSOPHY.

Committee on Graduate Work











Department Head

ABSTRACT OF DISSERTATION

THE RESPONSE OF COARSE-BED RIVERS TO
LARGE FLOODS IN CALIFORNIA AND COLORADO

For geomorphic purposes, the magnitude of a flood is best expressed by the ratio of the flood discharge, Q_f , to that of the mean annual flood, Q_{maf} . When indexed in this way, the magnitude of the T-year flood is much greater in basins where runoff is concentrated in time or space than in basins where runoff is seasonally or areally distributed. Thunderstorms in semi-arid basins of the Colorado Front Range may generate flash floods that exceed Q_{maf} by several factors of 10. Frontal storms in humid areas of northern California distribute their rainfall over large areas and generate floods that are generally less than 10-times Q_{maf} . Seasonal snowmelt in the alpine regions of Colorado produces floods that rarely exceed Q_{maf} by more than a factor of two. The effects of precipitation intensity attenuate with basin size, and the potential for floods much in excess of the mean annual flood is greatly reduced on rivers that drain more than about 1,000 km².

The response of individual rivers to floods depends on the power of the flood relative to the resistance provided by the channel. In Colorado, flash floods that occur on small, high gradient streams may have sufficient power to cause erosion. In northern California, lower magnitude floods often do not develop sufficient power to overcome the resistance of coarse-bed, high gradient streams. Floods on rivers with moderate slopes may widen their channels by bank erosion. Floods that carry very high loads deposit their sediment in intermediate or low gradient reaches where the friction losses from bedforms are high.

This study empirically verified the results of previous workers that the long-term yield of bed material by low gradient streams is optimized by flows that occur several days per year. However, the flow that yields the most bed material on streams with gradients in excess of about 1% may be an event that occurs once in a decade or once in a century. The discharge most effective for bed material transport may be very different from the bankfull discharge of high gradient rivers. Many high gradient rivers may have relict morphologies from past floods that extensively rework the valley floor and leave low-flow channels that are now filled to a bankfull capacity by more frequent events.

Rivers recover from the effects of floods or large sediment input at rates that vary depending on the magnitude of the initial perturbation, the rate at which sediment is supplied from upstream, and the frequency of flows in subsequent years that are competent to move the available sediment. In the headwater reaches of streams inundated with relatively fine sediment, recovery begins soon after the initial perturbation, and proceeds rapidly thereafter because the flows that are competent to move sediment occur frequently. In the downstream reaches of a river inundated with sediment in its headwaters are slower to recover because of the continued influx of sediment from upstream, and because the potential for sediment storage increases in a wider channel.

John Pitlick
Department of Earth Resources
Colorado State University
Fort Collins, CO 80523
Fall, 1988

ACKNOWLEDGEMENTS

This study was made possible with financial support provided by Dr. David Stevens of the National Park Service and Dr. Steve Mock of the U.S. Army Research Office (grant No. DAAG29-85-K-0108). Their contributions to this effort are gratefully acknowledged. A research grant from Amoco, Inc. made summer field work possible in 1987.

Dr. John Costa, Dr. Michael Harvey, Dr. Robert Jarrett and Dr. Malcolm Newson have shared their enthusiasm and ideas with me, and I am grateful for the logistical and technical assistance they have provided. Dr. Costa, Dr. Harvey, and the two other members of my committee, Dr. Stanley Schumm and Dr. Everett Richardson provided helpful comments on earlier versions of the dissertation.

Among the many individuals who assisted me in field work, I would like to thank Deborah Anthony, Bruce Brown, Steve Crews, Andrew Dephtereos, Danny Hagans, Dru Germanoski, David Jorgensen, Allan Pace, Bill Spitz, and Jeff Ware. My apologies to any of you that I might have forgotten; you all made the effort fun and productive.

Special thanks go to my friends and fellow graduate students, Terri and Gerald Craig, Steve Crews, Dru Germanoski, and David Jorgensen for the endless hours of discussion, proof-reading and advice. To work closely with people that share my own enthusiasm for rivers and rocks has been a most important and enjoyable aspect of graduate school.

And most of all, thank you Rebecca Thomas. You left town just long enough for me to get up a head of steam, and you returned just soon enough to keep me from being overwhelmed. Your timing is impeccable.

TABLE OF CONTENTS

<u>CHAPTER</u>		<u>PAGE</u>
I	INTRODUCTION	1
	1.1 Geomorphic Effects of Large Floods	2
	1.2 Channel Recovery Following Large Floods	3
	1.3 Objectives	5
II	STUDY AREAS AND METHODS	7
	2.1 Colorado Front Range	7
	2.2 California: the Sierra Nevada	12
	2.3 California: Klamath Mountains	17
	2.4 California: Coast Ranges	19
	2.5 Data Sources and Methods	20
III	FLOOD FREQUENCY ANALYSIS	23
	3.1 Flood Discharge	23
	3.2 Flood Frequency Analysis	25
	3.3 Regional Flood Frequency Analysis	27
	3.4 Floods, Climate and Drainage Basin Characteristics	36
	3.5 Discussion	47
	3.6 Summary	49

<u>CHAPTER</u>		<u>PAGE</u>
IV	GEOMORPHIC EFFECTS OF FLOODS	50
	4.1 Flood Discharge, Flood Power and Sediment Transport	51
	4.2 Channel Changes	58
	4.3 Flow Resistance and Sediment Transport in High Gradient Streams	68
	4.4 Summary	77
V	MAGNITUDE AND FREQUENCY OF COARSE SEDIMENT TRANSPORT	79
	5.1 Study Areas	82
	5.2 Procedures	82
	5.3 Results	84
	5.4 Summary	91
VI	CHANNEL RECOVERY FOLLOWING LARGE FLOODS OR HIGH SEDIMENT INPUTS	93
	6.1 Recovery Processes on Fall River Following the Lawn Lake Flood	94
	6.2 Recovery of Sierra Nevada Rivers from the Effects of Hydraulic Mining	106
	6.3 A General Model for Recovery of Streams with High Sediment Input	112
	6.4 Summary	121
VII	CONCLUSIONS	122
VIII	REFERENCES	132

LIST OF FIGURES

FIGURE	PAGE
2.1 Location map of study sites in the Colorado Front Range	8
2.2 Seasonal distribution of flood peaks on Colorado rivers	10
2.3 Location map of 4 study regions in California	13
2.4 Seasonal distribution of flood peaks on northern California rivers	14
2.5 Location map of rivers draining the northern Sierra Nevada	16
2.6 Location map of rivers draining the Klamath Mountains and Coast Ranges	18
3.1 Flood frequency curve for Plum Creek near Louviers, Colorado	26
3.2 Dimensionless flood frequency curves for selected gaging stations in the Colorado Foothills and Klamath Mountain Regions	28
3.3 Dimensionless flood frequency curves fit with weighted moments	33
3.4 Dimensionless flood frequency curves for 6 study regions	35
3.5 Morphometric relationships for the drainage basins of this study	42
3.6 Relations between flood variability, climate and drainage basin size	44
3.7 Relation between flood variability and drainage area in different regions	46

FIGURE	PAGE
4.1 Relation between drainage area and discharge for 25 flood sites	54
4.2 Relation between drainage area and unit stream power for 25 flood sites	54
4.3 Relation between shear stress and the size of the largest particles moved	57
4.4 Cross section adjustments on Scotchman Creek and the East Branch of the North Fork Feather River as a result of the February, 1986 flood	59
4.5 Changes in cross sectional area at 25 flood sites as functions of discharge, shear stress, particle size and valley width	61
4.6 Cross section surveys showing changes at the Butte Creek gaging station	65
4.7 Channel changes as a function of flood power index and valley width	67
4.8 Conceptual distribution of the different components of shear stress	71
4.9 Changes in the relative importance of the components of flow resistance	71
4.10 Flow resistance relations for static and mobile beds	73
4.11 Channel changes as a function of flow resistance	76
5.1 Conceptual magnitude/frequency relations	80
5.2 Location of sites used in magnitude/frequency analysis	83
5.3 Magnitude/frequency relations for the Van Duzen and N. Fork Yuba Rivers	85
5.4 Effective discharge relations for the Van Duzen and North Fork Yuba Rivers	86
5.5 Return period of the effective discharge as related to slope and sediment size	88
5.6 Changes on Scotchman Creek as a result of the February, 1986 flood	90

FIGURE	PAGE
6.1 Location map of Horseshoe Park study area	95
6.2 Grain size distributions of alluvial fan sediments, bed material and bed load	99
6.3 5-year trends in bed load at upstream and downstream sampling sites	100
6.4 Changes in channel cross sections in the storage zone reach of Fall River	102
6.5 Temporal changes in bed elevation within the storage zone reach	104
6.6 Location map of streams draining the foothills of the Sierra Nevada	108
6.7 Channel changes at cross sections on Greenhorn Creek	110
6.8 Temporal changes in incision rate at cross sections on Greenhorn Creek	111
6.9 Non-dimensional flow duration curves used in recovery analysis	114
6.10 Incision rate as a function of the number of days that the critical discharge for sediment transport was exceeded	118
6.11 Generalized model for channel recovery in streams inundated with sediment in their headwater reaches	120
7.1 Summary of the effects of climate and scale in flood geomorphology	128

CHAPTER I INTRODUCTION

Large floods have marked important points in human history but, in spite of decades of scientific study and speculation, their role in the evolution of landscapes remains unclear. This is due, in part, to the different scales of space and time considered in geomorphology (Schumm, 1985) and to the different objectives of various fluvial process studies. Present theories of landform evolution account for geomorphic catastrophes as events that may punctuate the progressive denudation of a landscape, and it has been suggested that the role of catastrophic events varies with scale and climate (Wolman and Gerson, 1978), or the state of the landform relative to a threshold of instability (Schumm, 1977).

Floods may be viewed, along with more frequent events, as agents of *landscape modification*. The forces generated by even modest-sized floods may exceed the critical resistance of the channel bed and bank materials and result in geomorphic changes that are unprecedented in historic times (Stewart and LaMarche, 1967; Anderson and Calver, 1977; Kelsey, 1980; Newson, 1980; Nanson, 1986). In other cases, large floods appear to have little effect on stream channels (Wolman and Eiler, 1958; Newson, 1980) yet their sinuous planforms provide clear testimony that channel adjustments do occur. Many alluvial rivers have morphologies that are apparently adjusted to frequent flows of moderate magnitude (Leopold and Wolman, 1960; Andrews, 1980) and it has been argued that this flow, by just filling the channel to its banks, is dominant in maintaining channel form. However, the frequency of bankfull flows varies widely between rivers (Williams, 1978), and because the bankfull flow is not always equivalent to the flow that is most effective in transporting sediment (Benson and Thomas, 1966; Pickup and Warner, 1976; Nolan, et al., 1987), it is unclear what role this discharge plays in maintaining channel form.

Floods, by their transportation of dissolved and clastic loads may also be viewed as agents of *landscape denudation*, and the amount of sediment yielded by rare events may be considered separately from their geomorphic changes. Individual flood events may transport many-times more sediment than occurs in an average year and may represent several decades-worth of normal denudation (Lusug, 1965; Ritter, 1974; Kelsey, 1980; J.E. Costa, pers. commun.). However, large floods generally do not perform enough geomorphic "work" to dominate the long-term sediment yield of many drainage basins (Wolman and Miller, 1960; Pickup and Warner, 1976; Andrews, 1980) and it appears that, on many rivers, lesser flows accomplish the bulk of landscape denudation.

This study examines the geomorphic response of gravel and cobble-bed rivers to recent floods in Colorado and California. The study considers not only the geomorphic effects of these floods, but also provides a context for their significance in terms of the water and sediment discharge of a river. Finally, the study examines the processes and rates of channel recovery in streams that have been subjected to large floods and high sediment loads. In attempting to bring together data and observations from many different rivers, this study represents a significant departure from the previous lines of research in flood geomorphology, some of which are reviewed in the following section.

1.1 Geomorphic Effects of Large Floods

Arguments for the geomorphic significance of large floods are often supported by the specific characteristics of the climatic or physiographic regimes in which they occur. The largest floods (in terms of unit discharge) occur in arid and semi-arid regions where the high precipitation intensity of storms and the lack of permeable soils and protective vegetation induces rapid surface runoff (Costa, 1987). However, the geomorphic effects of large floods in arid and semi-arid regions are highly variable (Schumm and Lichty, 1963; Burkham, 1972; Schick, 1974; Glancy and Harmsen, 1975; Baker, 1977; Kochel et al., 1982; Harvey, 1984; Osterkamp and Costa, 1987) due to large differences in storm duration, areal extent, and the characteristics of channel sediment and riparian vegetation.

Small drainage basins within humid climates may also exhibit catastrophic geomorphic responses because of their steep slopes, high runoff volume and, the presence of erodible soils or regolith. The failure of debris-filled hollows may result in debris flows that strip headwater tributary channels to bedrock. Notable examples are provided by Dietrich and others (1986) from the California and Oregon Coast Ranges and by Hack and Goodlett (1960), Williams and Guy (1970), and Kochel and Johnson (1984) from the Appalachians.

Finally, catastrophic floods may cause very significant geomorphic changes in areas with intense land use and erodible lithologies where the thresholds of landform stability are low (Kelsey, 1980; Pitlick, in press). Such conditions prevailed during a northern California winter storm and flood in 1964 that triggered massive landslides and resulted in wide-spread aggradation of stream channels (Hickey, 1969). The dramatic changes that occurred on Coffee Creek led Stewart and LaMarche (1967) to conclude that, in this environment, rare floods are most important for the development and adjustment of landforms. In describing hillslope and channel changes in the Van Duzen River Basin, Kelsey (1980) reported that the 1964 flood caused 49% more sediment to enter the Van Duzen River than would have normally occurred in the period 1941-1975. The sediment yield of this and other northcoast basins remain some of the highest in the United States.

1.2 Channel Recovery Following Large Floods

A topic closely related to the above concerns the persistence of features or the recovery of landforms following a catastrophic flood. Wolman and Gerson (1978) suggested that the geomorphic effectiveness of an event could be represented by the length of time required for the landscape to recover its prior condition. This definition of "recovery" is somewhat ambiguous but may include the re-establishment of pre-existing channel form and dimensions or the decline in sediment loads to pre-disturbance or background levels. Whatever the interpretation, it is implicit in the concept of recovery that geomorphic systems, if perturbed, will return to a condition of dynamic equilibrium whereby denudation proceeds by steady state processes. Wolman and Gerson went on to suggest that recovery

periods following catastrophic events will be on the order of decades in humid climates or in large drainage basins, and on the order of centuries in arid climates or headwater areas.

These generalizations are intuitively attractive, and data from a number of recent studies are available to test the recovery hypothesis as it relates to stream channels. The results of measurements at sites in Wales, U.K. (Newson, 1980) and Colorado (Pitlick, 1987) indicate sediment loads in disturbed streams may return to background levels within 5 years of very large floods that occurred within an otherwise stable landscape. These floods produced locally significant channel changes but stream banks and hillslopes quickly stabilized following passage of the flood. As a result, the in-channel sediment sources were rapidly depleted. These two landscapes differ in many respects but they share the common characteristics of being very stable and in both cases, their normal precipitation-runoff regimes are characterized by long periods of moderate stream discharge.

A slightly different picture emerges from northern California where studies have focused on the stream channel and hillslope recovery processes following the 1964 storm. In a study of sediment sources and storage in small drainage basins (< 50 km²) within the Redwood Creek watershed, Pitlick (in press) found that the majority of sediment delivered to stream channels by landslides exited these basins within a decade of the 1964 storm. Madej (1984) reported similar results for the upper reaches of the main stem of Redwood Creek. However, sediment loads in the downstream reaches of Redwood Creek remain some of the highest in the U.S. and recovery is projected to be of the order of a century or more (Madej, 1984). The downstream increase in recovery period is contrary to Wolman and Gerson's hypothesis that larger rivers will recover more rapidly but this is to be expected in rivers where sediment moves from headwater source areas to lower gradient reaches downstream. Lisle (1982) approached the recovery problem through a hydraulic geometry analysis of 12 northern California Rivers and he suggested that many northern California rivers recovered their pre-flood bed elevations within a decade because their sediment transport capacity was high during moderate, frequently occurring flows.

Relatively fewer studies of channel recovery have been conducted in arid climates, perhaps because, as suggested by Wolman and Gerson (1978), recovery is slower and may take decades. Studies by Schumm and Lichty (1963), Burkhart (1972), and Osterkamp and Costa (1987) provide thorough documentation of the processes of channel recovery in sand-bed streams. These authors all emphasize the role that riparian vegetation plays in stabilizing channel banks and bars and they report that a stable channel width may be re-established within several decades of major floods. Unlike coarse-grained rivers in arid environments (Baker, 1977), it appears that the recovery period in these sand-bed rivers may be much shorter than that suggested by the return period of the flood event itself.

The above examples, and those presented earlier from humid environments suggest that the rates and processes of channel recovery involve complex relationships between the frequency and size of inter-flood stream flows, the mobility of the sediment forming the channel bed and banks and the ability of vegetation to stabilize channel bars and banks. These factors are partly related to climate, but the problems of geomorphic effectiveness and recovery are more likely to be resolved by examining site-specific characteristics.

1.3 Objectives

Many of the above mentioned studies are essentially "case histories", and they are noteworthy because of their exceptional detail. In formulating their general models of flood effectiveness, Baker (1977) and Wolman and Gerson (1978) alluded to many of these case studies and presented convincing arguments that the roles of catastrophic vs. persistent geomorphic processes vary with climate or scale. These conclusions are based on observations and analyses that are largely qualitative, but because of their intuitive appeal, they have been very widely accepted. The present study pursues the ideas of Baker (1977) and Wolman and Gerson (1978) in a more rigorous or quantitative manner, and represents a first attempt at integrating the large number of factors that influence the geomorphic effectiveness of large floods. In moving away from the single basin or single channel reach approach that previous workers have taken, this study seeks to explain the adjustment of

Floods, by their transportation of dissolved and clastic loads may also be viewed as agents of *landscape denudation*, and the amount of sediment yielded by rare events may be considered separately from their geomorphic changes. Individual flood events may transport many-times more sediment than occurs in an average year and may represent several decades-worth of normal denudation (Lusug, 1965; Ritter, 1974; Kelsey, 1980; J.E. Costa, pers. commun.). However, large floods generally do not perform enough geomorphic "work" to dominate the long-term sediment yield of many drainage basins (Wolman and Miller, 1960; Pickup and Warner, 1976; Andrews, 1980) and it appears that, on many rivers, lesser flows accomplish the bulk of landscape denudation.

This study examines the geomorphic response of gravel and cobble-bed rivers to recent floods in Colorado and California. The study considers not only the geomorphic effects of these floods, but also provides a context for their significance in terms of the water and sediment discharge of a river. Finally, the study examines the processes and rates of channel recovery in streams that have been subjected to large floods and high sediment loads. In attempting to bring together data and observations from many different rivers, this study represents a significant departure from the previous lines of research in flood geomorphology, some of which are reviewed in the following section.

1.1 Geomorphic Effects of Large Floods

Arguments for the geomorphic significance of large floods are often supported by the specific characteristics of the climatic or physiographic regimes in which they occur. The largest floods (in terms of unit discharge) occur in arid and semi-arid regions where the high precipitation intensity of storms and the lack of permeable soils and protective vegetation induces rapid surface runoff (Costa, 1987). However, the geomorphic effects of large floods in arid and semi-arid regions are highly variable (Schumm and Lichty, 1963; Burkham, 1972; Schick, 1974; Glancy and Harmsen, 1975; Baker, 1977; Kochel, et al., 1982; Harvey, 1984; Osterkamp and Costa, 1987) due to large differences in storm duration, areal extent, and the characteristics of channel sediment and riparian vegetation.

Small drainage basins within humid climates may also exhibit catastrophic geomorphic responses because of their steep slopes, high runoff volume and the presence of erodible soils or regolith. The failure of debris-filled hollows may result in debris flows that strip headwater tributary channels to bedrock. Notable examples are provided by Dietrich and others (1986) from the California and Oregon Coast Ranges and by Hack and Goodlett (1960), Williams and Guy (1970), and Kochel and Johnson (1984) from the Appalachians.

Finally, catastrophic floods may cause very significant geomorphic changes in areas with intense land use and erodible lithologies where the thresholds of landform stability are low (Kelsey, 1980; Pitlick, in press). Such conditions prevailed during a northern California winter storm and flood in 1964 that triggered massive landslides and resulted in wide-spread aggradation of stream channels (Hickey, 1969). The dramatic changes that occurred on Coffee Creek led Stewart and LaMarche (1967) to conclude that, in this environment, rare floods are most important for the development and adjustment of landforms. In describing hillslope and channel changes in the Van Duzen River Basin, Kelsey (1980) reported that the 1964 flood caused 49% more sediment to enter the Van Duzen River than would have normally occurred in the period 1941-1975. The sediment yield of this and other northcoast basins remain some of the highest in the United States.

1.2 Channel Recovery Following Large Floods

A topic closely related to the above concerns the persistence of features or the recovery of landforms following a catastrophic flood. Wolman and Gerson (1978) suggested that the geomorphic effectiveness of an event could be represented by the length of time required for the landscape to recover its prior condition. This definition of "recovery" is somewhat ambiguous but may include the re-establishment of pre-existing channel form and dimensions or the decline in sediment loads to pre-disturbance or background levels. Whatever the interpretation, it is implicit in the concept of recovery that geomorphic systems, if perturbed, will return to a condition of dynamic equilibrium whereby denudation proceeds by steady state processes. Wolman and Gerson went on to suggest that recovery

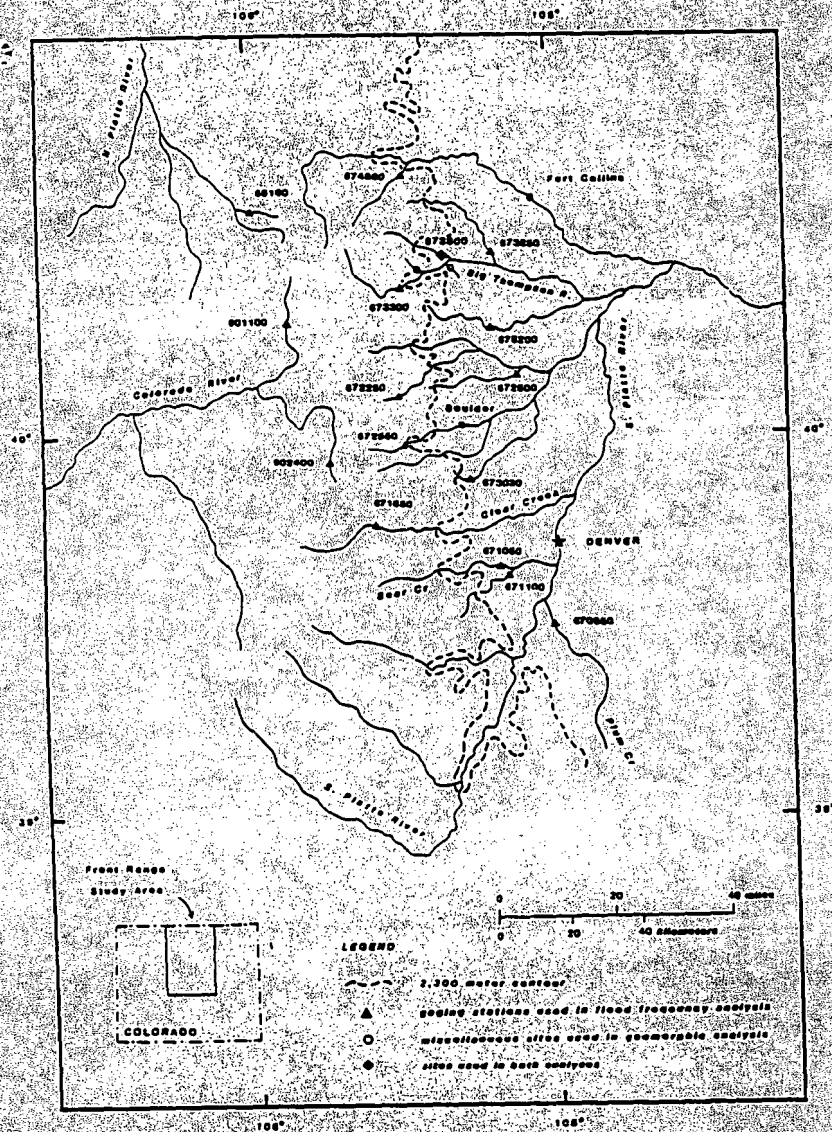


Figure 2.1. Location map of study sites within the Colorado Front Range. The dashed line indicates the approximate location of the 2,300 contour dividing the Alpine and Foothill study areas.

thunderstorms. In Colorado, thunderstorm activity is an almost daily occurrence from June through September and particularly severe storms may occur in the piedmont and foothill regions of the state (Costa and Jarrett, 1986).

Runoff in Colorado is produced by melting of the winter snowpack and by summer thunderstorms. Precipitation that falls as snow in the winter months does not become runoff until the spring melt. Snowmelt from lower elevations of the Front Range occurs in March and April. On some streams, these early spring flows constitute peaks in the annual flood series, but the volume of this early runoff is generally not large. The bulk of snowmelt runoff is produced by alpine headwater streams that usually reach their peak flows within a 1-month period between mid-May and mid-June (Fig. 2.2).

Front Range thunderstorms are often localized and produce highly variable amounts of runoff. In general, thunderstorms that occur in drainage basins with an average elevation of more than 2,300 m.a.s.l. are much less intense than those that occur at lower elevations of the Colorado Front Range (Costa and Jarrett, 1986). Thunderstorms that occur within the foothills and piedmont zones of the Front Range may generate severe flash floods, the most notable of which occurred on tributaries of the South Platte River in 1965 (Matthai, 1969), and on the Big Thompson River in 1976 (McCain, et al., 1979). Thus, peak flows of lower elevation foothill streams may occur in early spring due to snowmelt and at any time during the summer months due to intense localized thunderstorms (Fig. 2.2).

The distinction between snowmelt and thunderstorm generated flows is the basis for dividing the Front Range into "Alpine" and "Foothills" sub-areas that are roughly delimited by the 2,300-meter contour (Fig. 2.1). Peak flows of many Front Range streams may be derived from both snowmelt and rainfall sources that constitute a mixed population of streamflows (Elliott, et al. 1982) so only streams with predominantly snowmelt (alpine) or rainfall (foothill) sources of peak flow were used in the flood frequency analysis of this study. These sites are located on the main stems and tributary forks of Bear Creek, Clear Creek, Boulder Creek, the Big Thompson River and the Cache la Poudre River (Fig. 2.1).

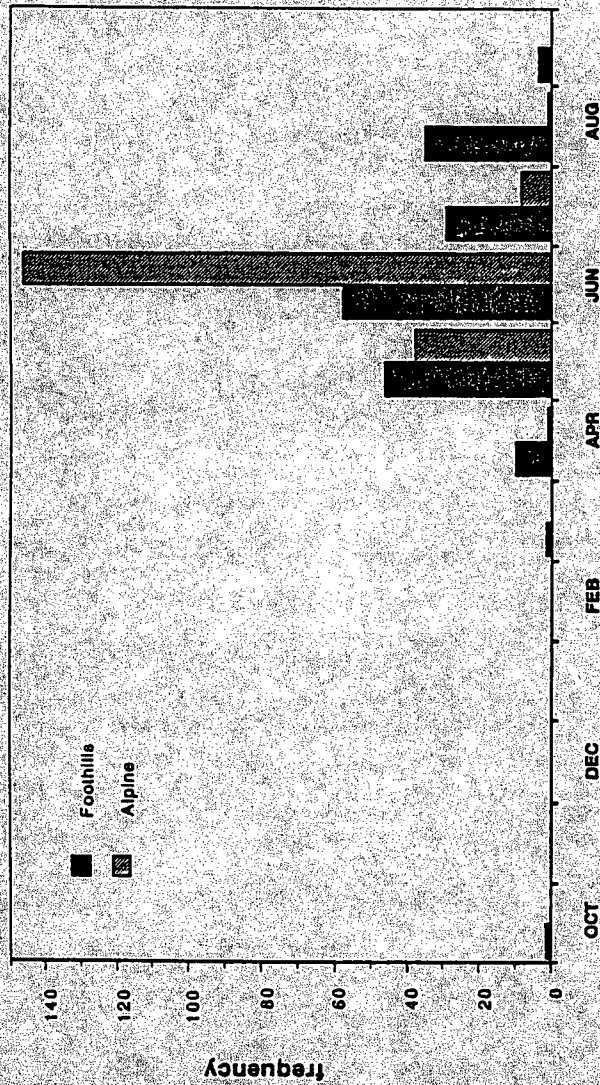


Figure 2.2. Seasonal distribution of annual flood peaks for selected rivers in Colorado. Peak flows on snowmelt-fed streams in the Alpine Region occur predominantly in June. Peak flows in the Foothills Region may be generated by late spring snowmelt or summer thunderstorms. Data were compiled from the WATSTORE file of peak flows for Colorado gaging stations.

Colorado has experienced a number of catastrophic floods within this century (Jarrett, 1987a). Two of the more recent floods are considered here in detail: the Big Thompson River flood of 1976 and the Lawn Lake dam-break flood of 1982 in Rocky Mountain National Park (Fig. 2.1). The Big Thompson flood was spawned by an intense thunderstorm which resulted in the largest natural disaster in Colorado history. During the storm, precipitation intensities within tributaries of the Big Thompson River were estimated to have reached 250 mm in 4 hours (McCain, et al., 1979). Peak flood discharges greatly exceeded the previously recorded maximums at gaging stations on the Big Thompson River, and unit discharges at ungaged tributary sites exceeded $75 \text{ m}^3/\text{sec}/\text{km}^2$ (McCain, et al., 1979). Shroba and others (1979) reported that erosion and deposition were sporadic within the channel of the Big Thompson River and its tributaries. Most low-order tributary streams scoured, some to bedrock, while the main stem channel had reaches that were alternately characterized by scour, lateral corrosion and fill. Several of the sites used for indirect discharge measurements of this flood were included in the analysis of the geomorphic effects presented in Chapter 4.

The Lawn Lake flood occurred in Rocky Mountain National Park on July 15, 1982 as the result of the failure of an 80-year old earthfill dam. This flood, though not a natural event, had the characteristics of a flash flood, and peak discharges were estimated to be 2 to 30 times larger than the 500-year flood (Jarrett and Costa, 1986). The Lawn Lake flood severely eroded the valley of Roaring River to its confluence with Fall River in Horseshoe Park where it deposited a large alluvial fan. Downstream of this fan, the 4 km reach of Fall River through Horseshoe Park was largely unaffected by the flood itself. This area has been the site of detailed geomorphic and sedimentologic studies that have documented the response of Fall River to a greatly increased sediment load in the first few years following the Lawn Lake flood (Blair, 1987; Pitlick and Thorne, 1987). The results of this work form the basis for the discussion of stream channel recovery processes in Chapter 6.

2.2 California: the Sierra Nevada

The study areas in California include the Sierra Nevada, Klamath Mountains and Coast Ranges (Fig. 2.3). The Sierra Nevada consist of Cretaceous-age plutonic rocks that are overlain or bounded by sedimentary, metamorphic and volcanic units. The northern Sierra Nevada is treated here as a separate region from the Central Sierra Nevada because of the abundance of metamorphic rocks and volcanic debris shed from the Modoc Plateau to the northeast. The central Sierra Nevada consists of Cretaceous age plutons, but the western foothills of the Sierra are underlain by abundant Tertiary fluvial sediments in which were located the placer deposits that initiated the great California Gold Rush of the mid 1800's.

The present relief of the Sierra Nevada, like the Colorado Front Range, is the result of Tertiary uplift and incision by the major rivers (Huber, 1981). Pleistocene glacial deposits are largely obscured by a dense coniferous forest but at least two glaciations are recognized in the Sierra Nevada (Bateman and Wahrhaftig, 1966). Evidence for glacial activity is present in headwater areas, where the soil cover has been stripped to expose bare granite. The lower elevations have occasionally thick and moderate- to well-developed soils.

Precipitation in the Sierra Nevada is derived from frontal storms that move onland from the Pacific Ocean, and almost all rain falls between October and May. The rapid rise in elevation leads to strong orographic effects and sharp precipitation gradients. Significant accumulations of snow occur at higher elevations, but because of the maritime climate of California, much of the wintertime precipitation falls as rain at lower elevations.

High flows in the Sierra Nevada occur mainly during the rainy winter months, although there is a small component of early spring snowmelt flow in some years (Fig. 2.4). In the Sierra Nevada, and throughout all of northern California, the largest floods occur in the winter months, when runoff from heavy precipitation is augmented by partial melting of the mountain snowpack. Rainfall intensities during these storms commonly exceed 300 mm per 24-hour period and condensation of warm, moist air causes melting of the snowpack.

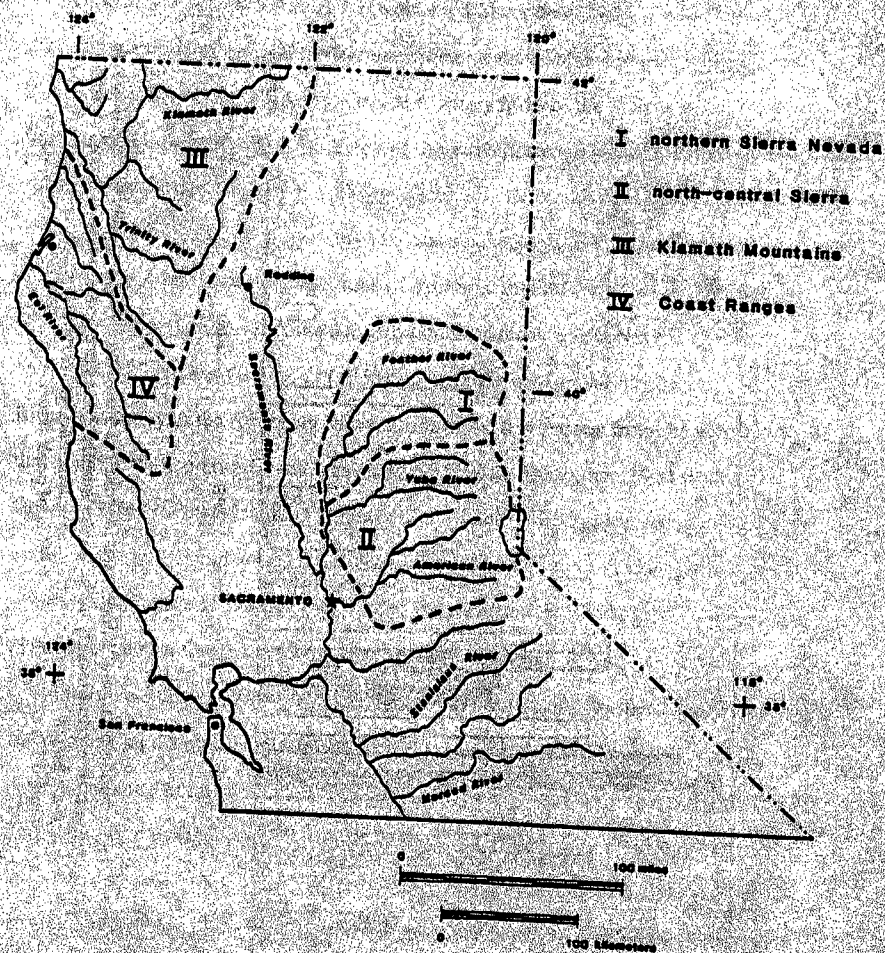


Figure 2.3. Location map of 4 study regions in northern California.

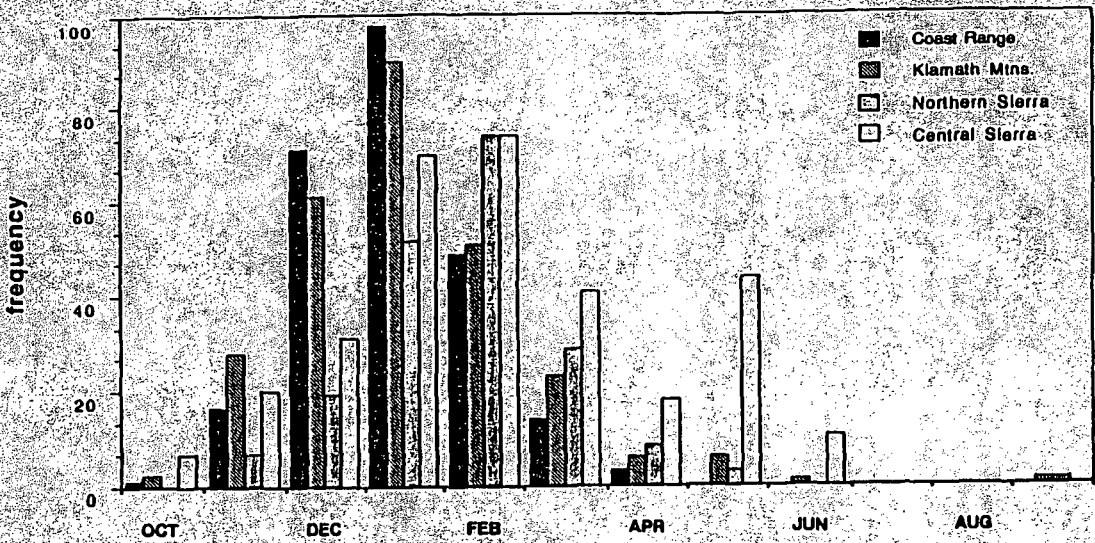


Figure 2.4. Seasonal distribution of annual flood peaks for selected Northern California rivers. Peak flows in these regions occur predominantly in the winter months due to precipitation from frontal storms. Peak flows on the Sierra Nevada streams are occasionally generated by spring snowmelt. These data were compiled from the WATSTORE file of peak flows for California gaging stations.

The streams and rivers studied in the northern Sierra Nevada are within the drainage of the Sacramento River and include tributary forks of the Feather River (Fig. 2.5). The rivers in the Central Sierra Nevada region include tributary forks of the American River, Bear River, and Yuba River (Fig. 2.5). Many of these rivers have gage records exceeding 70 years, and this makes the region well-suited for flood frequency analysis (Chapter 3) and greatly enhances the study of recovery processes (Chapter 6) in streams draining the Mother Lode, where a century ago, tons of hydraulic mining debris were deposited.

Major regional storms produced record floods on many Sierra Nevada rivers in 1964 and in 1986. Scott and Gravelle's (1965) account of a dam-break flood on the Rubicon River, a tributary of the American River, is one of the few reports from the Sierra Nevada that describe the geomorphic changes resulting from the December, 1964 storm. Scott and Gravelle (1965) estimated that the drainage of the Rubicon River received as much as 200 mm (8 inches) of precipitation in the 24-hour period before the Hell Hole Dam failed. The resulting flood surge of 7363 m³/s exceeded the mean annual flood of the Rubicon River gaging station near Geopetown by a factor of more than 30.

A storm in February, 1986 produced record floods on many northern Sierra Nevada rivers including the main stem and tributary forks of the Feather River (Fig. 2.5). Three-day rainfall totals of more than 500 mm (20 inches) were recorded at several gages in the headwaters of the North Fork Feather River (NOAA, 1986). Unit discharges at gaged sites did not exceed 1.0 m³/s/km², but the persistence of high flows caused significant erosion on the upper reaches of the North Fork Feather River. Flooding within the drainages of the Yuba River and the American River, to the south, was less severe than in the northern Sierra Nevada, but the 1986 flood was the second or third highest recorded on many rivers in this area. It was fortuitous that, in the summer prior to the 1986 flood, the writer began a study of streams in this area to examine their recovery from the effects of hydraulic mining. The availability of pre-flood data is invaluable for assessing the geomorphic effects of this flood (Chapter 4) and for assessing the processes of channel recovery (Chapter 6).

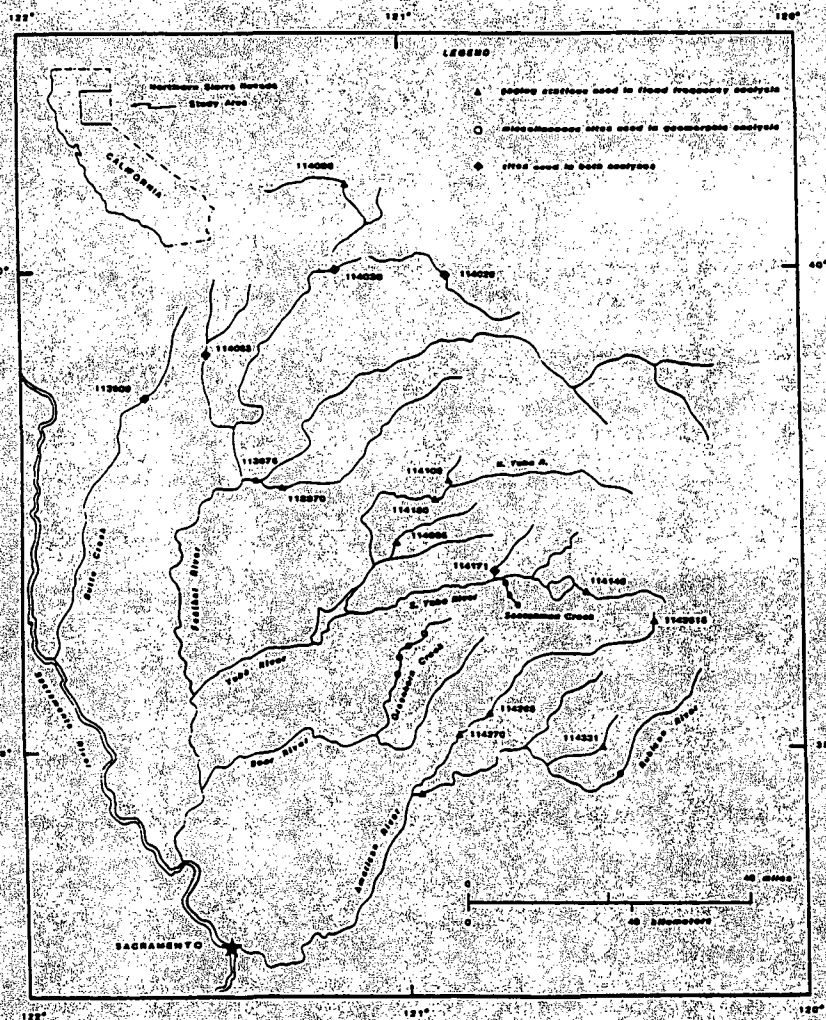


Figure 2.5. Location map of rivers draining the central and northern Sierra Nevada.

2.3 California: Klamath Mountains

The physiographic and climatic characteristics of the Klamath Mountains (Fig. 2.6) are similar in many respects to those of the Sierra Nevada. The Klamath Mountains consist of Cretaceous-age plutons intruded into complexly faulted and deformed Paleozoic sedimentary and metamorphic rocks (Irwin, 1966). Relief throughout the range is extreme, but erosion rates are not exceptionally high due to the relative competence of the bedrock. The Klamaths are densely forested, and soils are moderately to well developed. Runoff in the Klamath Mountains occurs in the winter months due to heavy, but not exceptionally intense precipitation that is often augmented by melting of the mountain snowpack. The rivers examined in this region include the main stems and tributary forks of the Klamath River, Trinity River and Smith River (Fig. 2.6).

Flood-producing storms occurred in the Klamath Mountains in December, 1964 and January, 1974. Stewart and LaMarche (1968) provide an excellent, detailed account of the geomorphic effects of the 1964 flood on Coffee Creek, a high gradient tributary of the Trinity River. A rainfall intensity of 125 mm (5 inches) in 24 hours generated a unit discharge of about $2.0 \text{ m}^3/\text{sec}/\text{km}^2$ near the mouth of Coffee Creek. Geomorphic changes on other Klamath Mountains rivers were not exceptional during the 1964 storm, but aggradation was noted at several of the gaging stations in this region (Hickey, 1969).

Record floods occurred on many Klamath Mountain rivers following several days of moderate precipitation and warm temperatures in mid-January, 1974. Rainfall totals for the 3-day period of the storm generally did not exceed 300 mm and the highest 24 hour rainfall recorded in the region was 172 mm (6.8 inches). However, climatic data from weather stations in the area indicated that minimum daily temperatures never fell below freezing during the period of January 13 to 19, and much of the storm runoff was likely produced from melting of the mountain snowpack. There were no reports of wide-spread erosion as a result of this storm, but the changes that occurred at the upstream Trinity River gage (Fig. 2.6) were significant and this site was included in the present study.

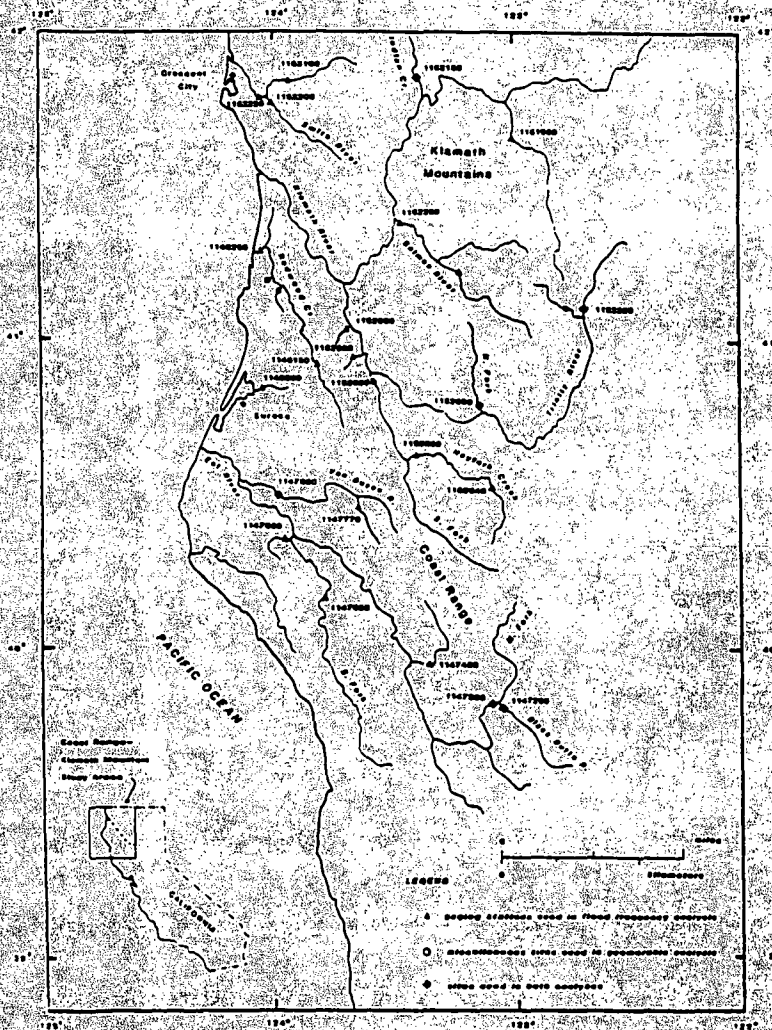


Figure 2.6. Location map of rivers draining the Klamath Mountains and Coast Ranges.

2.4 California: Coast Ranges

The Coast Ranges of California (Fig. 2.6) are underlain by weakly indurated sedimentary and metamorphic rocks. These lithologies were pervasively deformed as this terrain was accreted onto the continent and the present relief of the Coast Range is the result of recent uplift. The combined effects of erodible lithologies, high relief and high rainfall make this the most rapidly eroding area of the United States (Judson and Ritter, 1964) outside of the areas near Mount St. Helens in Washington State. As in other areas of California, runoff in the Coast Range occurs in the winter due to high rainfall that is sometimes augmented by snowmelt. The rivers examined in this region include the main stems and tributary forks of the Eel River, Van Duzen River and Redwood Creek (Fig. 2.6).

The Coast Ranges have experienced an exceptionally large number of floods within the last 30 years. Clearly, the most notable of these was the flood produced by the December, 1964 storm that affected all of northern California. Three-day precipitation totals exceeded 400 mm (15.7 inches) at many weather stations in the region, but unit discharges of north-coast rivers generally did not exceed $5 \text{ m}^3/\text{s}/\text{km}^2$. The suspended sediment discharge of the Eel River at Scotia for the 5-day period of December 19-23 was estimated to have been 16,400 metric tons/ km^2 , an amount equivalent to 9 years of normal suspended sediment yield (Brown and Ritter, 1971). While floods of similar size occurred in the mid-1950's and mid-1970's, the 1964 storm caused exceptional hillslope erosion and channel changes.

The geomorphic effects of the 1964 flood have been the focus of many studies (Hickey, 1969; Ritter, 1974; Harden et al., 1978; Kelsey, 1980; Lisle, 1982; Nolan, et al., in press) and it is still not clear why this storm produced such significant erosion. In many cases, timber harvesting operations, which had reached a peak in this region the decade before (Best, 1984), clearly exacerbated erosion associated with this storm (Kelsey, 1980; Kelsey, et al., in press; Pitlick, in press). However, many forested drainage basins also experienced severe erosion and the destabilizing effects of the prior storm events in the 1950's probably played a role in causing such severe erosion of the landscape.

2.3 Data Sources and Methods

A wide variety of hydrologic and geomorphic data were available from previously published studies of floods and their geomorphic effects (Chapter 1). However, the objectives of those studies were often very different, and the types of data collected were inconsistent. Where possible, data from previously published sources were used, but to be consistent with the objectives of the present study, additional data were often required.

Many of the sites used in this study are the locations of gaging stations presently or formerly operated by the U.S. Geological Survey. Data from these sites were used in the flood frequency analyses in Chapter 3. Approximately half of the sites used in the analyses of the geomorphic effects of floods (Chapter 4) are gaging stations, and the other half are miscellaneous sites established by the writer. In all cases, the data available from these sites allow for moderately accurate reconstruction of pre- and post-flood conditions.

Drainage Basin Characteristics: Included in the flood frequency analyses of Chapter 3 is a discussion of the characteristics of floods in relation to climate and drainage basin characteristics. Some of the data used in these analyses are available through the U.S.G.S. computerized retrieval system (WATSTORE). These data include: drainage basin area, average elevation, average channel gradient, channel length, mean annual precipitation, 24-hour rainfall intensity, average January temperature, percent forest cover and various flood frequency statistics. In cases where data were incomplete, the appropriate measurements were made on 1:24,000 topographic maps or were taken from climatic atlases. The drainage density of each basin was determined on 1:24,000 topographic maps by the line intersection method of Carlston and Langbein (1960). Patton and Baker (1976) report a standard error of less than 10% using the line intersection method; considering the tremendous savings in time, and the fact that it was used consistently for each basin, the method is considered appropriate for the present purposes.

Flood Frequency Statistics: Gaging station data on peak flows and flows of different duration were also available through WATSTORE. Included in the "Peak Flow" file for each gaging station are gage heights and discharges of peak flows for each year in the period of record, summary statistics and flood quantile estimates for the annual flood series, regionally derived estimates of the same, and a plotted flood frequency curve. Included in the "Daily Flow" files are discharge duration data, summary statistics for daily flows, the mean annual discharge for each year and, plotted flow duration curves. These data were used extensively in the analyses presented in Chapters 3, 5 and 6.

Flood Discharge: Records of the magnitude and duration of flood discharges at gaged sites are available in a variety of U.S.G.S. publications and from the local field offices that operate the gages. These records include flood hydrographs and estimates of the peak flow as derived from extension of the gaging station rating curve or by indirect discharge (slope-area) measurements made at or near the site. The latter provide particularly useful information on conditions at the site including photographs, assessments of scour or fill, and water surface profiles determined from trash and silt lines left by the flood.

A number of the sites considered in this study are not gaged, and peak flood discharges were estimated solely by indirect methods. The procedure adopted for these sites was as follows. First, the return period of the particular flood event was determined for gaged localities near the ungaged site. Then, using published multivariate relations for estimating the T-year flood from precipitation and basin characteristics (Waanenen and Crippen, 1977; Kircher, et al., 1985), the discharge for a flood with a return period specified as above was determined for the ungaged locality. Independent estimates of peak discharge at these sites were derived using the Manning formula and field measured values of slope and cross sectional area. This discharge was then compared for reasonableness with that derived from the multivariate relationship. Waanenen and Crippen (1977) report a standard error of less than 60% for discharges estimated with a multivariate relationship that includes basin area, mean annual precipitation and relief.

Channel Morphology: Channel cross sections at gaged sites were constructed using the actual discharge measurements made by the U.S.G.S. field personnel during their routine gagings. The bed elevations for each increment of channel width were determined by subtracting the measured flow depth from the gage height. Gaging measurements were usually restricted to the channel and generally were not made during the high flows that would inundate a floodplain. For this reason, the gaging station sites were surveyed to include the full width of the floodplain as well as the channel. Using the data from the field surveys and the discharge measurements, the configuration of flow over the channel and floodplain could be reconstructed for flood conditions. At the ungaged sites, the writer had conducted cross section and sediment surveys the year prior to the occurrence of the flood.

The longitudinal profile was surveyed at each gage site for which no slope-area measurements existed. The average slope for the reach was determined by the line best fit by eye through point measurements of water surface or channel bed elevation. Although it is only an approximation of the true energy slope, the average water surface or bed slope was all that was available for many computational purposes.

Sediment: The size of sediment comprising the channel bed, banks or terraces was determined by grid or bulk sampling. For very coarse sediments (cobbles and boulders), the size distribution was determined using the grid-by number sampling method of Wolman (1954). For sand and gravel mixtures, the coarse fraction was sieved and weighed in the field, and a split portion of the finer fraction was retained and sieved in the laboratory.

At each site visited by this author, the intermediate or b-axes of the 5 largest particles moved by the flood were also measured. Particle movement at these sites was indicated by the presence of moss and algae on the undersides of displaced boulders or cobbles. At other sites, where the channel scoured or filled appreciably, all the particles comprising the bed would have moved, and therefore, the decision as to whether a particle moved was not subjective. In those cases where sediment size data was taken from previously published reports, often the size of only the single largest particle moved was reported.

CHAPTER III FLOOD FREQUENCY ANALYSIS

When does a flood represent an unusual hydrologic event? Floods may be the result of several different precipitation and runoff processes, but how does one evaluate the hydrologic significance of a flood? Statistically, floods are the high-end members of the entire population of flows observed on a stream and thus the significance of the event can be considered in relation to some normative value, say an average flood, or in terms of its probability of occurring within a specified time span. This chapter focuses on a statistical analysis of floods with the intent of defining, as accurately as possible, both the magnitude and return period of the events. A technique for constructing regional flood frequency curves is presented as an alternative to single site frequency analysis, and this is followed by a discussion of specific attributes of flood frequency curves in relation to climate and drainage basin characteristics. Clearly, the flood event must first be placed in the proper hydrologic perspective before its geomorphic significance can be fully evaluated.

3.1 Flood Discharge

The discharges of very large floods are rarely measured directly. The difficulty of making accurate streamflow measurements during a flood can easily be envisioned, and the estimates of the peak flow are usually determined indirectly, after the flood waters have receded. At gaging stations, the peak flow is often estimated by extending the stage-discharge relation to the maximum gage height observed during the flood and adjusting this value with the discharge estimated by the "slope-area method" (Dairymple and Benson, 1967). Peak discharges at ungaged locations are commonly determined by the slope-area method along with estimates derived from regional rainfall-runoff models or multivariate relations of the type presented by Kircher and others (1985).

These indirect methods are all subject to error, the sources of which are many. For example, the accuracy of either a stage-discharge rating curve extension or the post-flood determination of cross-sectional area for use in slope-area calculations is dependent on whether large changes in channel bed elevation occurred during the flood. If significant scour occurs, then the recorded peak flood stage, and therefore the discharge estimated by extension of the rating curve, would be lower than if there had been no scour. At slope-area measurement sites, a similar problem exists if channel scour occurs after the high water marks were set. If the scoured channel bed and high water marks are used to compute the cross-sectional area of flow, then, obviously, the flood discharge will be overestimated. Costa (1983) addressed the "high water mark problem" in his analysis of paleoflood discharges but in most cases, this problem is untractable.

The accuracy of the slope-area method, which employs the Manning formula, is also dependent on the subjective choice of roughness coefficients used to compute the flow conveyance of the cross sections or subsections. Slope-area measurements have been interpreted to yield high estimates of flow velocity (Jarrett, 1987b) and low estimates of energy slope (Costa, 1987). Explicit evaluations of the error in slope-area measurements is not possible because channel roughness, flow velocity and energy slope are inextricably tied together. However, Kirby (1987) showed that the uncertainty in assessing the amount of channel scour or fill provided the largest source of error in estimating flood discharges.

The error in discharge estimates also influences the precision of the parameters used to characterize a flood frequency distribution, and the predictive ability of a flood frequency curve. In a study of Wisconsin gaging station records, Potter and Walker (1985) showed that indirectly-measured floods were often twice those of the largest directly-measured discharges, and that the inclusion of these large events significantly increased the skew of the annual flood series. Whether expressed in terms of discharge or return period, the error in flood measurements is difficult to evaluate, and it is understood that significant error may be associated with the estimates of flood discharge used in the present study.

3.2 Flood Frequency Analysis

The second aspect of flood hydrology, which is of concern is the statistical methodology for describing the characteristics of flood frequency distributions. In essence, these analytical techniques seek both a precise description of the observed data and an accurate prediction of an unknown value, such as a design flood with a specified return period. The most basic flood frequency techniques often fail in their ability to achieve these goals because the data are derived from small samples and do not represent the frequency distribution very well. These limitations can be summarized as follows.

The highest discharge occurring in each of n years of gaged record constitutes what is known as the annual series of peak flows. This series can be used to construct the probability distribution of floods at the gaging station if each event in the annual series is assigned a rank m with a probability of being exceeded in any year p given by:

$$p = m / (n + 1) \quad (3.1)$$

Equation 3.1 is the plotting position formula most commonly used to construct the flood frequency curve or cumulative distribution function (CDF) of the annual series. However, equation 3.1 has the obvious limitation that the return period of the largest flood, regardless of its "true" recurrence interval, is fixed by the length of record, n . This limitation is well illustrated by the flood frequency curve for Plum Creek near Louviers, Colorado (Fig. 3.1). In June, 1965, Plum Creek experienced its flood of record and the peak flow of 4,360 m³/sec was 35-times greater than the next highest discharge in the annual series. The Plum Creek gage record is 39 years long, so on the basis of equation 3.1, the 1965 flood would have a return period of 40 years. However, if the 1965 flood is treated as an outlier, and the flood frequency curve is fit using statistics derived from the rest of the gage record, then extrapolation to a magnitude of 4,360 m³/sec yields a return period for this flood of about 2,000 years. Clearly, there is a large difference between this value and the 40-year return period derived solely from the plotting position formula.

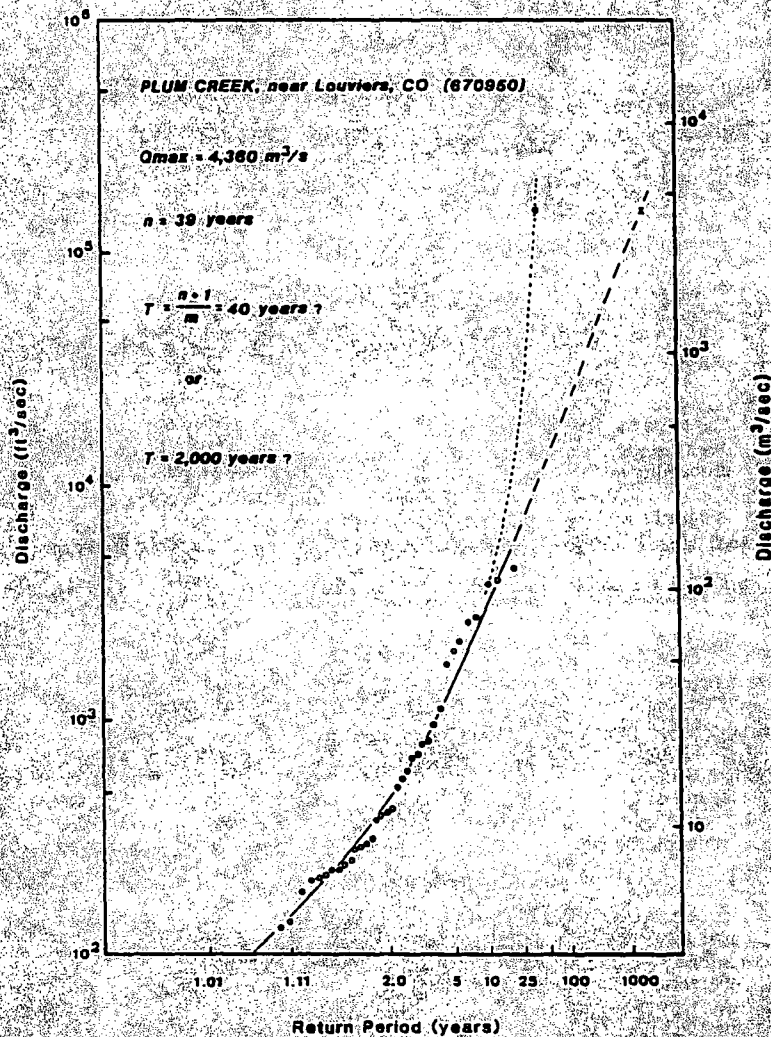


Figure 3.1: Flood frequency curve for U.S.G.S. gage on Plum Creek near Louviers, Colorado. Extrapolation of the systematic record to a flood discharge of 4,360 m³/sec gives a return period of about 2,000 years for the 1965 flood. Use of the Weibull plotting position [$T = (n+1)/m$] gives a return period of only 40 years.

Flood frequency analysis, like any statistical technique, is sensitive to the sample size, or the length of the gage record. In view of this limitation, several alternative methods have been adopted for determining the return period of infrequent events more accurately. These include the use of frequency distributions which account for extreme values, the use of flood frequency data from neighboring sites, and the incorporation of historic and paleo-hydrologic information into the gage record. For example, Osterkamp and Costa (1987) incorporated regional flood frequency data and presented geomorphic evidence to suggest a return period of 900-1,600 years for the 1965 flood on Plum Creek. Although there is considerable debate over the utility of incorporating historical and paleohydrological data (Hosking and Wallis, 1986a, 1986b; Stedinger and Cohn, 1986), it is generally agreed that regional techniques are preferable to single station flood frequency analyses (Potter, 1987).

3.3 Regional Flood Frequency Analysis

Within the past decade, there has been considerable research on the performance of different regionalization techniques but, as yet no consensus has been achieved as to which methods are most viable (Potter, 1987). All regional flood frequency techniques require that the region be homogenous with respect to the physical factors that generate floods. The regions considered in the present study were qualitatively established on the basis of their climate and physiography but no rigorous test of their homogeneity was applied. For any reasonably homogenous region, Potter (1987) suggests that the main source of variability in most regionalization procedures is in the precision of the at-site estimates of the mean, standard deviation and skewness of the flood frequency distribution. Consider, as an example, the characteristics of the dimensionless flood frequency curves of streams in the Colorado Foothills Region and the Klamath Mountain Region of California (Fig. 3.2). Each region is homogenous with respect to physiography and climate, but the flood frequency curves of the Colorado Foothills (Fig. 3.2A) are poorly defined because of the high variability in streamflow, while the flood frequency curves of the Klamath Mountains are better defined (Fig. 3.2B), because streamflows are less variable.

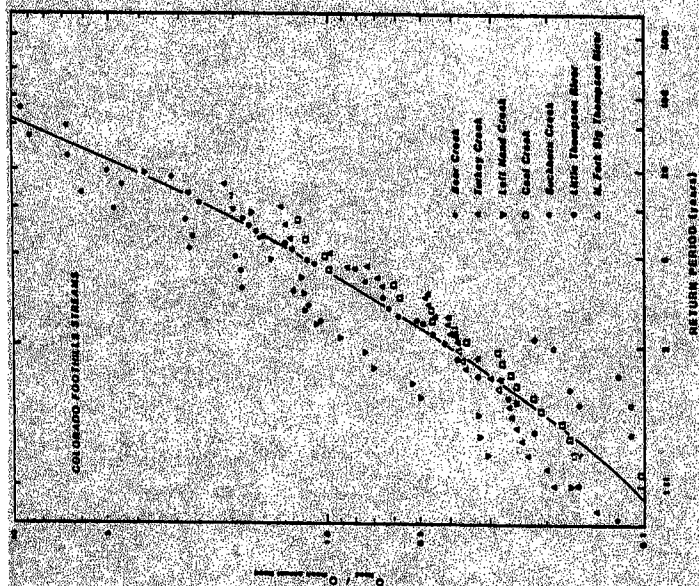
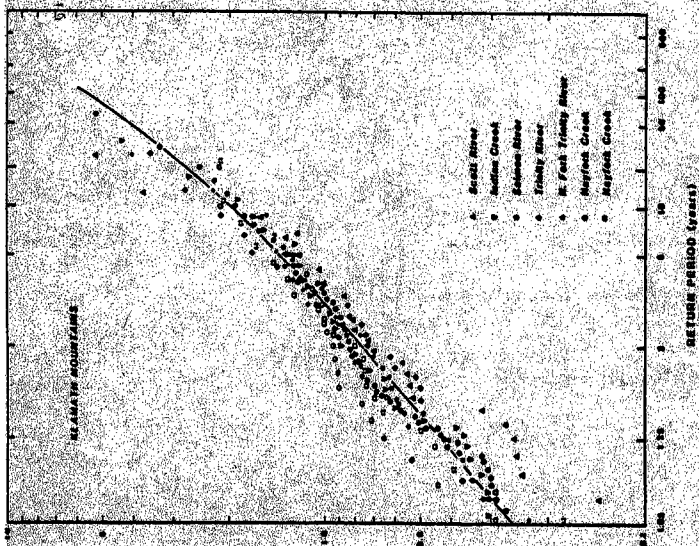


Figure 3.2. Dimensionless flood frequency curves for gaging stations in (A) the Colorado Foothills Region and (B) the Klamath Mountain Region of California. Note the wider spread of the data in (A) than in (B).

The procedure adopted for determining flood frequency curves for each of the 6 study regions is a modification of the index flood procedure recommended in Bulletin 17B of the *U.S. Water Resources Council* (1982). The procedure involved fitting each regional flood frequency curve with weighted averages of the standard deviation and skewness of the *Log Pearson Type III* distribution. No attempt was made to evaluate the performance of this method over others because the present analysis was simply intended to illustrate the differences in the flood frequency characteristics of the 6 regions considered in this study.

The regional flood frequency relationships were derived from at least 8 gaging stations with records of 10 years or longer in each region. The procedure for computing the regional relationships was as follows. The mean (\bar{z}_j), standard deviation (s_j), skewness (g_j) and coefficient of variation ($Cv = s_j/\bar{z}_j$) were computed from the logarithms (z_j) of the annual series of n floods at each of the $j = 1, 2, \dots, k$ gaging stations in the region:

$$\bar{z}_j = 1/n \sum z_j \quad (3.2)$$

$$s_j = \frac{[\sum z_j^2 - (\sum z_j)^2/n]^{1/2}}{n-1} \quad (3.3)$$

$$g_j = \frac{n^2 \sum z_j^3 - 3n \sum z_j \sum z_j^2 + 2(\sum z_j)^3}{n(n-1)(n-2)s_j^3} \quad (3.4)$$

$$Cv_j = s_j/\bar{z}_j \quad (3.5)$$

The values of these parameters were then weighted by $n_j/\sum n_k$, the proportionate length of record at each site in the region (Table 3.1). The site parameters, particularly s_j and g_j , are strongly influenced by the length of record n , and weighting them in this manner gives preference to stations with longer records.

The regional parameters \bar{S}' , \bar{Cv}' and \bar{g}' (Table 3.1, summary) were then formed as weighted averages of the site parameters:

$$\bar{S}' = \sum (n_j / \sum n_j) \times S_j \quad (3.6)$$

$$\bar{Cv}' = \sum (n_j / \sum n_j) \times Cv_j \quad (3.7)$$

$$\bar{g}' = \sum (n_j / \sum n_j) \times g_j \quad (3.8)$$

The discharge (in log units) of flows with specified return periods T were then computed at each station j in the region by:

$$(z_T)_j = \bar{z}_j + \bar{s}' K_T = \bar{z}_j (1 + \bar{Cv}' K_T) \quad (3.9)$$

where K_T is a coefficient that varies with the skewness and return period. Equation 3.9 has the advantage of incorporating both site and regional parameters to estimate the T -year flood. The terms in parentheses on the right side of equation 3.9 are weighted parameters and together represent a regional growth factor; the term \bar{z}_j is the site mean. The magnitude of the T -year flood was computed by first transforming the discharges from logarithmic to standard units ($Q_T = 10^{(z_T)}$) and then normalizing them by the mean annual flood, Q_{mar} . The resulting dimensionless flood frequency curves have common slopes and curvatures (defined respectively by the regional standard deviation and skewness) but with positions defined by unique values of Q_T to Q_{mar} (Fig. 3.3). Recall that the principal source of error in this technique lies in the computation of the at-site mean, the accuracy of which is a function of record length and flow variability. Thus, in the Foothills region of Colorado, where streamflows are more variable and the records are short relative to this variability, the flood frequency curves for individual sites cover a wide range (Fig. 3.3A). However, in California, where gaging records are longer and streamflow is less variable, the curves plot more closely together (Fig. 3.3B).

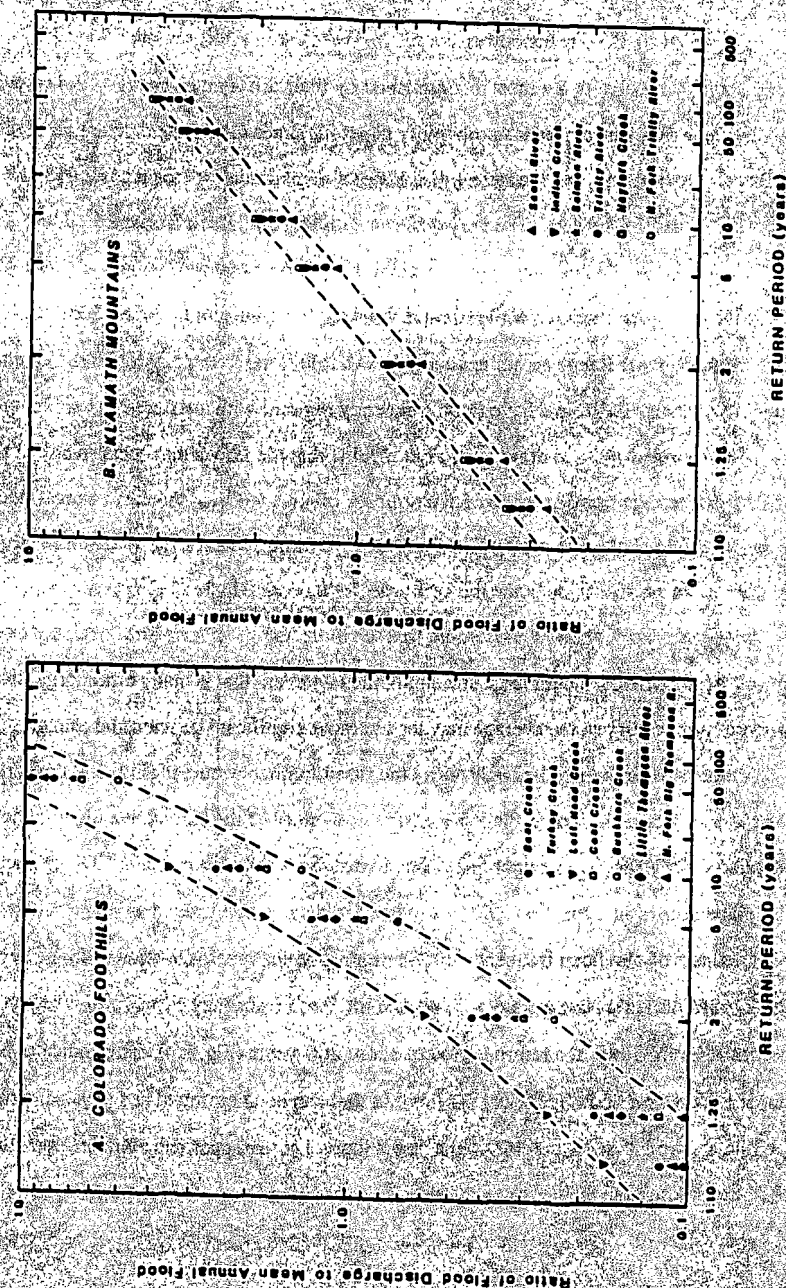


Figure 3.3. Dimensionless flood frequency curves for gaging stations in (A) the Colorado Foothills and (B) the Klamath Mountains. The curves in (A) and (B) were fit using regional, weighted averages of the standard deviation and skewness.

The median of the dimensionless site curves were taken as the regional flood frequency curves, and these curves are most distinguished by their different slopes (Fig. 3.4). Recall that the slope of a line plotted on probability paper indicates the standard deviation of the frequency distribution, and the steeper the slope of the cumulative frequency curve, the wider the spread in the data. The very different slopes of the flood frequency curves indicate flood magnitudes vary in each region. Floods on streams draining the Colorado Foothills are highly variable, while streams draining the high country or Alpine Region of the Colorado Front Range do not have highly variable flood frequency regimes. Rivers draining northern California have flood frequency regimes with intermediate variability.

The important point to draw from Figure 3.4 is that the floods that occur in any of these regions can be expressed in terms of a magnitude relative to Q_{maf} , the mean annual flood. For example, in Colorado, a 100-year flood on a Foothills stream may be 10-times larger than the mean annual flood while the 100-year flood on an Alpine stream may not be even twice the mean annual flood. Assuming that the morphology of a river reflects its past history of streamflows, both large and small, then an event that is many times larger than an event that occurs on the average may lead to more significant geomorphic changes.

A more subtle point to be made about the flood frequency curves (Fig. 3.4) concerns their shape. For a skew of 0, the log-transformed values of the cumulative distribution function (CDF) plot as a straight line; a positive skew results in a concave CDF and negative skew results in a convex CDF. Skewness can also be interpreted as representing the boundedness of the flood frequency distribution. The snowmelt-fed streams in the Alpine Region of Colorado have negative skews and the flood frequency curve for this region becomes asymptotic at a return period of about 200-years (Fig. 3.4). This indicates an upper limit to the flood frequency distribution that can be interpreted in a physical sense, i.e., the amount of snow that melts in a day is limited at the upper end by the temperature and amount of daylight. Conversely, the strong positive skew of the Colorado Foothills streams indicates a lower bound representing dry years in which the annual maximum flow would hardly be considered a flood.

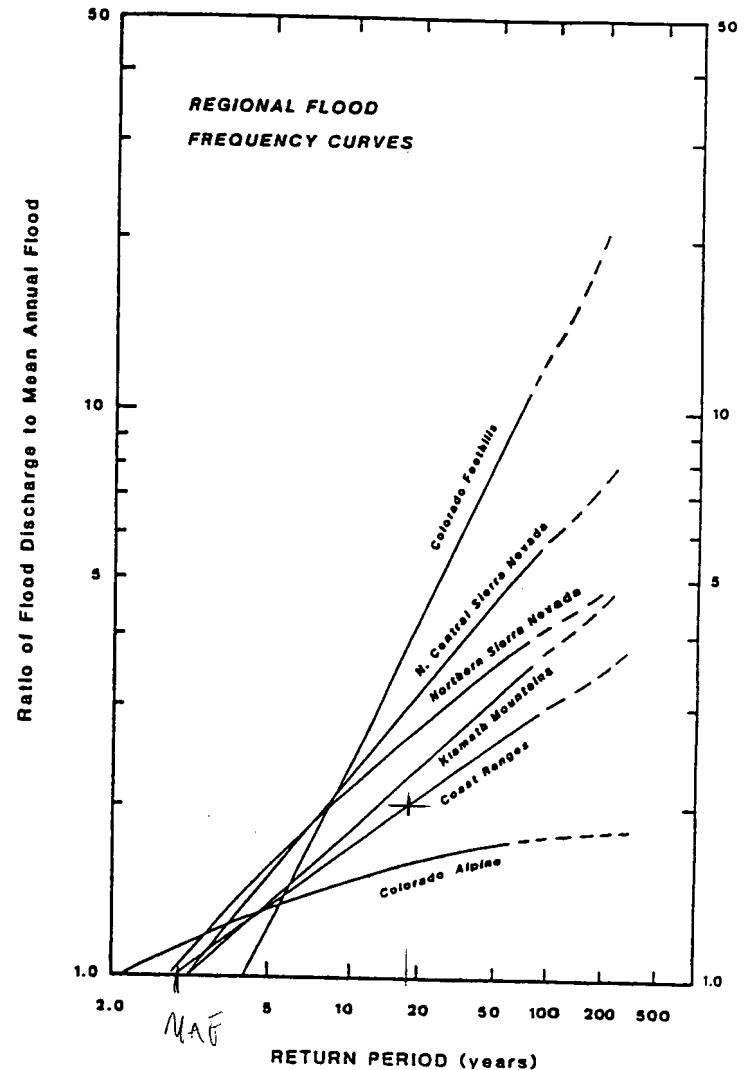


Figure 3.4. Dimensionless flood frequency curves for the 6 study regions.

SEE P. 47 -
SAYS COAST
RANGE CURVE
VALID FOR ALL
SIZE DRAINAGES

The median of the dimensionless site curves were taken as the regional flood frequency curves, and these curves are most distinguished by their different slopes (Fig. 3.4). Recall that the slope of a line plotted on probability paper indicates the standard deviation of the frequency distribution, and the steeper the slope of the cumulative frequency curve, the wider the spread in the data. The very different slopes of the flood frequency curves indicate flood magnitudes vary in each region. Floods on streams draining the Colorado Foothills are highly variable, while streams draining the high country or Alpine Region of the Colorado Front Range do not have highly variable flood frequency regimes. Rivers draining northern California have flood frequency regimes with intermediate variability.

The important point to draw from Figure 3.4 is that the floods that occur in any of these regions can be expressed in terms of a magnitude relative to Q_{maf} , the mean annual flood. For example, in Colorado, a 100-year flood on a Foothills stream may be 10-times larger than the mean annual flood while the 100-year flood on an Alpine stream may not be even twice the mean annual flood. Assuming that the morphology of a river reflects its past history of streamflows, both large and small, then an event that is many times larger than an event that occurs on the average may lead to more significant geomorphic changes.

A more subtle point to be made about the flood frequency curves (Fig. 3.4) concerns their shape. For a skew of 0, the log-transformed values of the cumulative distribution function (CDF) plot as a straight line; a positive skew results in a concave CDF and negative skew results in a convex CDF. Skewness can also be interpreted as representing the boundedness of the flood frequency distribution. The snowmelt-fed streams in the Alpine Region of Colorado have negative skews and the flood frequency curve for this region becomes asymptotic at a return period of about 200-years (Fig. 3.4). This indicates an upper limit to the flood frequency distribution that can be interpreted in a physical sense, i.e., the amount of snow that melts in a day is limited at the upper end by the temperature and amount of daylight. Conversely, the strong positive skew of the Colorado Foothills streams indicates a lower bound representing dry years in which the annual maximum flow would hardly be considered a flood.

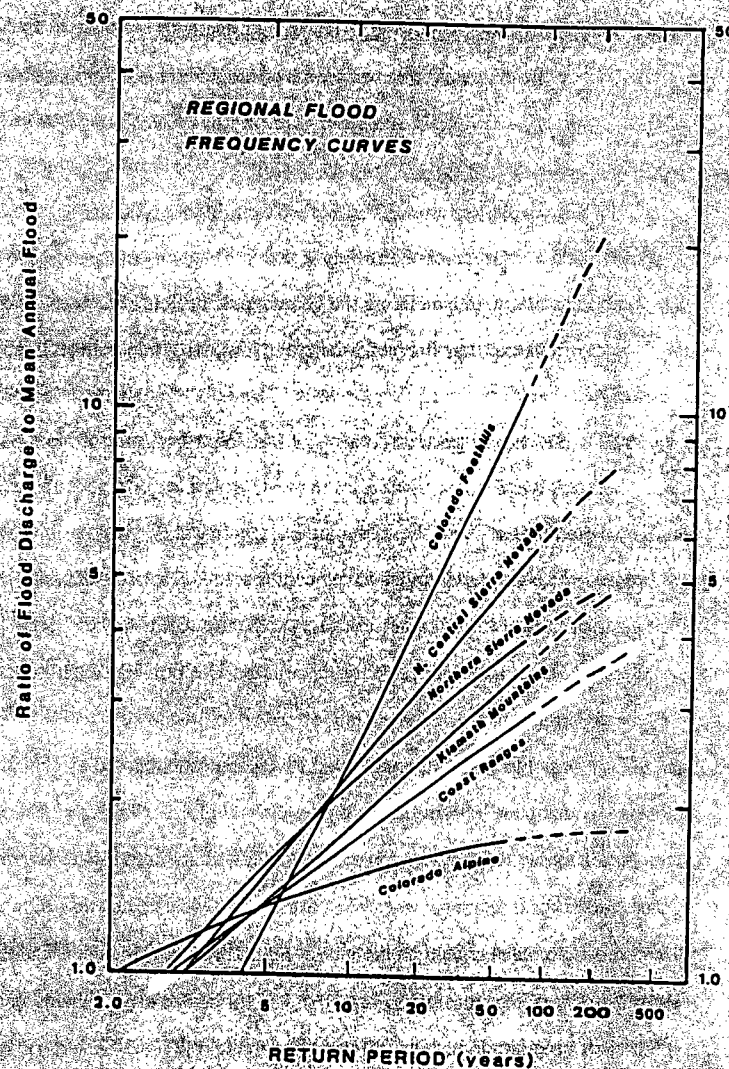


Figure 3.4. Dimensionless flood frequency curves for the 6 study regions.

SEE P 47 -
SAYS COAST
RANGE CURVE
VALID FOR ALL
SIZE DRAINAGES.

3.4 Floods, Climate and Drainage Basin Characteristics

A flood is the end result of a complex but integrated set of drainage basin processes that route precipitation inputs from headwater source areas, through the drainage network, and finally to the basin outlet. It is attractive, therefore, to interpret the differences in the regional flood frequency curves (Fig. 3.4) in terms of climatic and physiographic characteristics because these factors ultimately reflect the capacity of the drainage basin to produce runoff. Furthermore, in examining the geomorphic effects of floods, we should expect the drainage basin to express, at a meso-scale, the long-term importance of rare versus persistent hydrologic and geomorphic processes. The following analyses focuses on physiography and climate as large-scale controls of the flood-producing characteristics of a region.

Since the pioneering work of Horton (1945), geomorphologists and hydrologists have sought an understanding of the erosional drainage basin in terms its ability to transmit water and sediment. Numerous studies have been undertaken to establish links between climate, lithology, drainage basin characteristics, runoff, and sediment yield (see Abrahams, 1984, and Chorley, et al., 1985 for reviews). The important points to emerge from this work that concern the present study can be summarized as follows.

Drainage networks evolve according to the controls imposed by climate, relief, and lithology to form the patterns that are most efficient for conveying runoff and sediment through a basin. Of the morphometric variables that are used to describe the texture of the drainage network, drainage density has found the widest application. Drainage density decreases with mean annual precipitation (Gregory, 1976; Abrahams and Ponczynski, 1984) but may either increase (Gregory, 1976) or decrease (Abrahams and Ponczynski, 1984) with precipitation intensity depending on the role that vegetation plays in increasing infiltration and surface roughness and thereby reducing the rate and volume of runoff.

The density of stream channels dictates the hydrologic response of a basin and fine-textured drainage networks generally yield greater annual runoff volumes (Hadley and Schumm, 1961) and larger flood peaks (Carlson, 1963; Zimpfer, 1982). In semi-arid

areas of high drainage density and high relief, the lack of vegetation and low infiltration capacity of soils leads to a rapid concentration of runoff during storms and a high potential for the generation of flash-floods (Patton and Baker, 1976).

The drainage basin can also be viewed as a meso-scale landform sculpted by events of varying magnitude and frequency and thus the texture of the drainage network should reflect geomorphic processes. Chorley and Morgan (1962) argued that the drainage network is elaborated principally by high magnitude, low frequency storms because only these events have the power to incise new channels. The results presented by Patton and Baker (1976) and Abrahams and Ponczynski (1984) suggest that this is true in predominantly arid climates but Dietrich and others (1986) argue that infrequent events in humid environments may modify the drainage network as well via mass failure of debris-filled hollows in headwater basins. In summary, climate and physiography should dictate the hydrologic response of the drainage basin and, in turn, the drainage basin, as a distinct geomorphic unit, should reflect the importance of events of varying magnitude and frequency.

A straightforward test of these hypotheses follows. The analysis uses morphometric and hydrologic data that are easily obtained from topographic maps and climatic atlases to answer the following two questions: (1) do climate and physiography provide an explanation for flood variability within the study regions and, (2) do the characteristics of the drainage network provide large-scale evidence for the geomorphic effectiveness of events of varying magnitude and frequency? The analytical approach used is similar to that employed in regional flood or runoff studies where the goal has been to develop statistical relationships for predicting flood peaks on ungaged streams using climatic and physiographic data. The present analysis focuses not on the predictive ability of a multivariate relationship but rather on how climate and physiography control the variability of floods. The sole "flood" parameter considered is the coefficient of variation, C_v , which is the nondimensional parameter describing the spread of the flood frequency distribution. The coefficient of variation, in essence, provides an index of the "flashyness" of floods.

Experience has shown that the climatic and physiographic characteristics that are most useful for predicting flood peaks number about a dozen. The variables used in the following analysis were chosen from among those that have proven useful in the past (Benson, 1964; Thomas and Benson, 1970; Patton and Baker, 1976; Newson, 1978) and include drainage area A , average elevation E , relief R , channel slope S , basin length L_b , drainage density D , relief ratio R_b , ruggedness number HD , mean annual precipitation MAP , the 2-year 24-hour precipitation intensity $P2-24$, the average minimum January temperature $JMIN$, and the percent forest cover $FOREST$. An index of precipitation intensity PI , was derived from the ratio of $P2-24$ to MAP ; this represents the amount of annual rainfall that is likely to fall on a single day. These data are summarized in Table 3.2.

A correlation matrix of the morphometric and climatic variables is given in Table 3.3 with the significant correlations ($\alpha = 0.01$) noted in bold. Aside from those variables that have an obvious relation to each other, such as basin area and basin length, relatively few variables are highly correlated. In particular, C_v has a significant relationship to only A , MAP and PI . Flood variability does not appear to have a strong relation with the morphometric characteristics of the drainage basins considered here.

Recalling the results of previous workers, drainage density should increase with relief and, the ruggedness number should represent their mutual importance. In this analysis, drainage density is marginally correlated with relief (Fig. 3.5A) indicating a tendency for more efficient drainage with increasing steepness. However, in the steep drainage basins examined in this study, the importance of the ruggedness number as a measure of drainage texture is lost due to the overwhelming influence of relief. Note that relief increases with drainage area (Fig. 3.5B) as does the ruggedness number (Fig. 3.5C). However, drainage density is not significantly correlated with drainage area (Table 3.5) and thus adds nothing to the ruggedness number in its relationship to drainage area. Thus, as a measure of drainage texture, the ruggedness number may not provide much insight into runoff processes, particularly in areas of high relief and a narrow range of drainage density.

Table 3.2. Morphometric and climatic data for study basins in Colorado and California

STATION	ID	DA	E_b	H_b	S_b	L_b	D	R_b	HD	MAP	$P2-24$	PI	$JMIN$	FOREST
COLORADO ALPINE:														
N. Michigan Cr.	661600	55	2880	1265	0.040	9.8	3.61	0.140	4.56	660	36	0.054	5	89
Clear Cr.	671650	376	2890	1887	0.032	27.7	2.33	0.068	2.74	660	33	0.050	2	41
S. St. Vrain Cr.	672250	37	3188	1174	0.051	11.9	2.02	0.099	2.93	762	46	0.060	2	55
M. Boulder Cr.	672550	94	3048	1450	0.060	16.4	2.02	0.088	2.74	686	46	0.067	4	49
Big Thompson R.	673300	355	2743	2062	0.039	24.0	2.72	0.086	5.61	719	46	0.064	6	85
Catch in Poudre R.	674750	515	2765	1814	0.021	32.4	2.89	0.056	5.24	686	46	0.067	6	90
S.F. Cache	674860	234	2922	1818	0.049	22.9	3.87	0.080	7.04	650	43	0.066	8	95
Colorado R.	901100	264	2810	1391	0.015	29.1	2.92	0.048	4.06	701	36	0.051	4	48
Prater R.	902400	71	3069	1338	0.036	10.9	2.70	0.122	3.62	787	38	0.048	2	77
COLORADO FOOTHILLS:														
Head Cr.	671050	425	2586	2587	0.033	40.1	4.62	0.065	11.96	533	48	0.040	10	75
Turkey Cr.	671100	130	2195	1550	0.028	21.9	4.05	0.071	6.28	447	48	0.108	12	61
L. Head Cr.	672500	186	2109	1604	0.030	41.2	4.85	0.039	7.78	544	48	0.089	12	65
Coal Cr.	673030	39	2260	1205	0.039	10.8	3.51	0.112	4.23	503	48	0.096	12	85
NF Big Thump	673600	220	2719	2253	0.060	27.0	5.02	0.083	11.30	587	48	0.082	13	95
Buckhorn Cr.	673950	339	1999	1655	0.017	32.7	4.56	0.051	7.55	406	51	0.125	12	82
Little Thompson	674200	262	2019	1888	0.028	25.6	5.02	0.074	9.47	516	48	0.094	13	75
NORTH-CENTRAL SIERRA NEVADA:														
Oregon Creek	1140950	89	945	1232	0.032	24.2	6.91	0.051	8.51	1524	152	0.100	32	98
Gandy's Cr.	1141250	33	1250	1214	0.099	10.9	3.71	0.111	4.53	1905	114	0.060	24	86
N. Yuba R.	1141300	648	1341	1870	0.032	43.8	4.57	0.043	8.55	1524	114	0.075	24	97
S. Yuba R.	1141400	134	1890	1061	0.013	18.5	1.81	0.057	1.92	1648	127	0.079	16	90
Payman Cr.	1141710	60	1301	1128	0.065	16.4	4.66	0.069	5.26	1651	152	0.092	16	100
Ojoan Cr.	1142615	9	1951	596	0.099	3.1	2.59	0.195	1.54	1549	114	0.074	16	90
N. Shurtall Cr.	1142640	24	1158	382	0.029	12.1	2.80	0.032	1.07	1397	114	0.082	36	98
NF American R.	1142700	886	1219	2496	0.019	72.5	3.74	0.034	9.34	1575	127	0.081	37	90
Lang Canyon Cr.	1143310	47	1611	890	0.049	26.2	2.41	0.034	2.14	1575	140	0.089	16	100

KLAMATH MOUNTAINS:

Indian Cr.	1152150	311	823	1555	0.023	20.6	5.41	0.075	8.41	1905	127	0.067	28	95
S.F. Salmon R.	1152230	653	1006	2003	0.051	37.0	4.70	0.054	9.41	1473	89	0.060	28	97
Salmon River	1152250	1945	640	2298	0.013	62.5	4.61	0.037	10.60	1499	127	0.085	32	96
Trinity River	1152320	386	1344	1831	0.038	31.4	4.15	0.058	7.59	1524	97	0.063	26	93
Coffee Creek	1152370	277	0	1540	0.031	19.8	4.26	0.078	6.56	1473	91	0.062	25	95
N.F. Trinity R.	1152650	391	823	2324	0.015	33.5	5.02	0.069	11.66	1524	89	0.058	26	75
Hayfork Cr.	1152850	979	792	1398	0.009	48.3	4.90	0.029	6.86	1016	91	0.090	30	98

COAST RANGE:

		DA				L _B	D ⁴⁴ /km ²						FOREST	
Black Butte R.	1147290	420	762	1814	0.015	37.0	5.74	0.049	10.42	1270	127	0.100	28	98
M.F. Ecl. River	1147300	951	853	1829	0.025	37.0	5.27	0.049	9.64	1524	89	0.058	28	100
Van Duzen R.	1147750	221	838	1038	0.005	29.8	3.66	0.035	3.80	1905	114	0.060	36	95
S.F. Van Duzen	1147770	95	917	950	0.023	19.3	4.53	0.049	4.30	1778	109	0.061	36	100
Van Duzen R.	1147850	575	518	1537	0.012	49.9	4.15	0.031	6.38	1778	114	0.064	36	95
Redwood Creek	1148150	175	914	1391	0.031	26.6	5.47	0.052	7.61	1829	127	0.069	36	85
Redwood Creek	1148250	720	244	1648	0.006	80.3	4.79	0.021	7.89	1727	127	0.074	37	96
S.F. Trinity R.	1152000	2326	610	2227	0.008	101.4	3.93	0.022	8.76	1473	102	0.069	32	99
Willow Cr.	1152980	106	568	1331	0.045	13.7	5.08	0.097	6.76	1270	114	0.090	34	98
Campbell Cr.	1152995	18	579	1175	0.096	8.9	4.36	0.133	5.13	1397	91	0.065	34	100
M.F. Smith R.	1153100	337	518	1702	0.025	28.2	4.82	0.060	8.20	2642	152	0.058	38	95
S.F. Smith R.	1153200	754	472	1778	0.025	32.2	4.30	0.055	7.64	2540	152	0.060	38	98
Smith River	1153250	1577	457	1797	0.016	35.7	4.56	0.050	8.19	2565	152	0.059	38	100

Symbols: DA, drainage area (km²); E_B, average basin elevation (masl); H_B, relief (m); S_B, basin slope; L_B, basin length (km); D, drainage density (km/km²); R_B, relief ratio; HD, ruggedness number; MAP, mean annual precipitation (mm); P2-24, 2-year, 24-hour precipitation intensity (mm); PI, precipitation intensity index = ratio of P2-24 to MAP; JMIN, average January minimum temperature (°F); FOREST, percent forest cover.

Table 3.3. Correlation matrix for variables listed in Table 3.2. Log transformed variables are denoted with subscript z. Significant correlations (α = 0.01) are indicated in bold.

	Cv	A _z	E _{Bz}	S _{Bz}	L _{Bz}	H	D	R _{Bz}	HD	MAP	P2-24	PI	JMIN	FOREST
Cv	1.000													
A _z	-0.396	1.000												
E _{Bz}	0.174	-0.375	1.000											
S _{Bz}	-0.307	-0.575	0.351	1.000										
L _{Bz}	-0.292	0.901	-0.395	-0.584	1.000									
H	-0.171	0.773	-0.044	-0.184	0.688	1.000								
D	-0.026	0.354	-0.538	-0.085	0.369	0.325	1.000							
R _{Bz}	0.237	-0.636	0.489	0.634	-0.838	-0.209	-0.225	1.000						
HD	-0.086	0.695	-0.333	-0.166	0.648	0.840	0.745	-0.267	1.000					
MAP	-0.456	0.180	-0.782	-0.153	0.141	-0.126	0.251	-0.286	0.067	1.000				
P2-24	-0.269	0.119	-0.775	-0.118	0.170	-0.182	0.356	-0.377	0.095	0.899	1.000			
PI	0.702	-0.062	0.046	0.053	0.100	-0.015	0.313	-0.159	0.186	-0.323	0.057	1.000		
JMIN	-0.287	0.293	-0.914	-0.238	0.338	0.002	0.536	-0.484	0.310	0.795	0.811	0.019	1.000	
FOREST	-0.139	0.140	-0.614	-0.083	0.128	-0.076	0.409	-0.254	0.195	0.576	0.667	0.112	0.691	1.000

Symbols: Cv, Coefficient of variation; A_z, drainage area; E_{Bz}, average basin elevation; S_{Bz}, average basin slope; L_{Bz}, basin length; H, relief; D, drainage density; R_{Bz}, relief ratio; HD, ruggedness number; MAP, mean annual precipitation; P2-24, 2-year, 24-hour precipitation intensity; PI, precipitation intensity index = ratio of P2-24 to MAP; JMIN, average January minimum temperature; FOREST, percent forest cover.

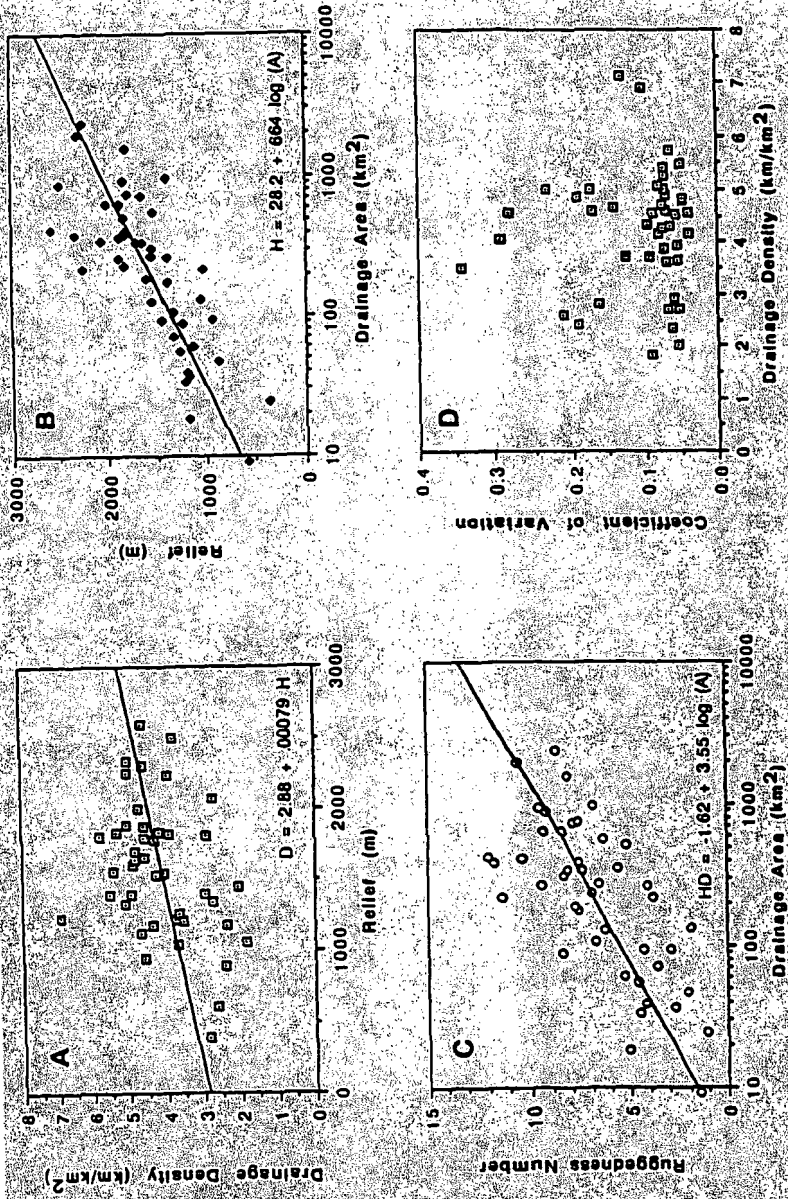


Figure 3.5 Selected morphometric relationships for data in Table 3.2. All relations except (D) are significant at the 0.01 level.

Patton and Baker (1976) interpreted high ruggedness numbers as an indication of high flash flood potential in a drainage basin. This conclusion is intuitively attractive and supports the widely held belief that a fine textured drainage network rapidly integrates runoff to produce a sharp flood peak. However their data set, like the one used in this study, is dominated by regions with very high relief but not very different drainage density. The results of Patton and Baker (1976) indicate poor correlation between drainage density and floods of varying magnitude, with the correlations being positive in some cases and negative in others. Their multivariate relations for predicting flood discharge from basin morphometry almost always include basin magnitude and ruggedness number, both of which increase with drainage area independently of changes in drainage density. It only makes sense that flood discharges should increase with drainage area and thus, the relationships between drainage network morphometry and flood characteristics that Patton and Baker describe are largely unsupported. It appears that drainage basin morphometry may have a more limited influence on flood characteristics than is widely thought and it is not surprising that flood variability, as indicated by C_v , was not highly correlated with drainage density (Fig. 3.5D) or many of the other morphometric variables used in this analysis.

Obviously, climatic factors must contribute to the flood characteristics of a region whether drainage basin morphometry has any influence or not. In general, rainfall becomes more temporally distributed and less seasonal as annual precipitation increases (Chorley, et al, 1986) and as would be expected, flood peaks become less variable with increasing mean annual precipitation, MAP (Fig. 3.6A). However, more intense rainfall does not necessarily produce a more flashy hydrologic response because precipitation intensity is highly correlated with MAP , and therefore, flood variability decreases with precipitation intensity, $P2:24$ (Fig. 3.6B). These relations are particularly evident if the snowmelt-fed streams of the Colorado Alpine region are excluded from the analysis.

The importance of precipitation intensity as a factor in producing floods becomes more apparent if $P2:24$ is expressed as a ratio to MAP . The resulting index of precipitation

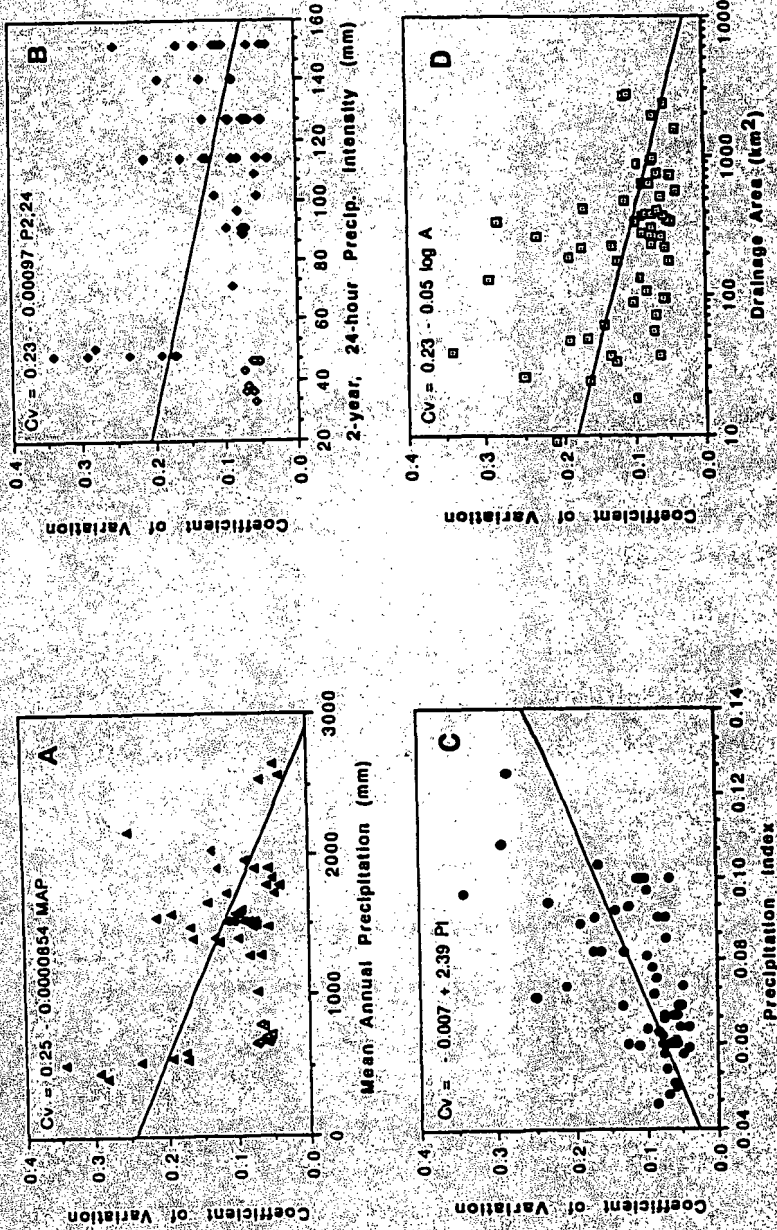


Figure 3.6. Relationships between the coefficient of variation and (A) mean annual precipitation, (B) precipitation intensity, (C) index of precipitation intensity, and (D) drainage area. The best-fit lines in (A) and (B) exclude the Colorado Alpine region.

intensity, *PI* provides a measure of event-distributed versus seasonally-distributed rainfall. Flood variability increases as more of the annual rainfall is concentrated into single events or a short season (Fig. 3.6C). The data in Figure 3.6c cluster into 3 groups defined at the upper end by the high *PI*-high *Cv* Foothills Region of Colorado where rainfall occurs during a short season with isolated events. The Sierra Nevada Regions represents an intermediate group characterized by seasonally distributed rain that falls in mountainous areas and produces floods that are moderately variable. Floods in the extra-humid regions of the California Coast Ranges and Klamath Mountains are very large, in terms of discharge but not in terms of relative magnitude because the moderately intense precipitation that produces flooding in this region is often distributed over a period of days or weeks.

The coefficient of variation *Cv*, decreases with increasing drainage area (Fig. 3.6D) indicating a tendency for floods to be less variable where runoff is more spatially distributed. This intuitive result becomes even clearer if the data in Figure 14d are treated separately by region (Fig. 3.7); it is again noted that the data form groups defined by three separate regression relations. In the Colorado Foothills Region, floods are produced by localized thunderstorms and flood variability decreases rapidly as basin size increases (Curve A, Fig.3.7). These localized storms result in a less integrated hydrologic response and flash floods attenuate in basins much larger than about 1,000 km², a point that is well illustrated by the 1976 Big Thompson River flood. The peak discharge at the point where the Big Thompson River issues from an incised canyon (*A* = 790 km²) was estimated to be 880 m³/s. This discharge was roughly 4-times larger than the previously recorded maximum. Because the storm was concentrated in mountainous areas, the flood peak attenuated rapidly as it moved eastward onto the High Plains. The peak discharge recorded near the confluence of the Big Thompson and South Platte Rivers (*A* = 2,145 km²), was 70 m³/s, a discharge that was less than one-half the previously recorded maximum.

Flood variability decreases with basin size in the Sierra Nevada and Klamath Mountain Regions as well (Curve B, Fig.3.7). In these mountainous regions, the orographic effects

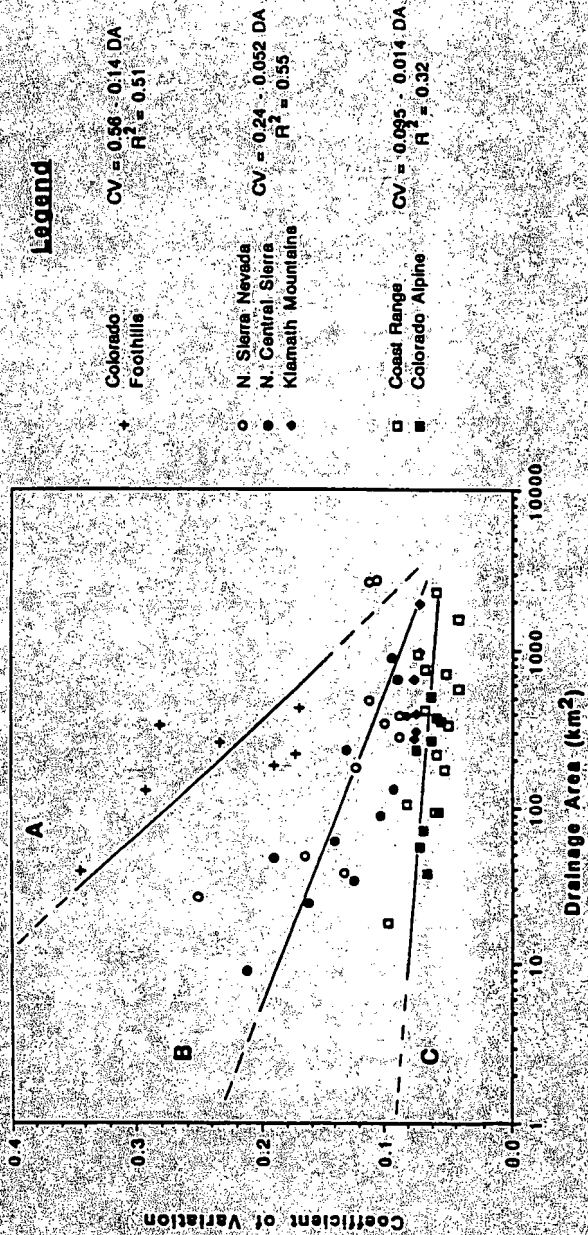


Figure 3.7. Relationships between the coefficient of variation and drainage area reflecting the spatial distribution of runoff process in different climatic regimes. Flood variability decreases rapidly with drainage area in the Colorado foothills (curve A) and in the Sierra Nevada and Klamath Mountains (curve B). In the California Coast Range and Colorado Alpine (curve C) to drainage area (curve C).

ZWD - @ORU
 1964
 $50,500 / 278 \text{ mi}^2$
 $= 181 \text{ cfs/mi}^2$
 $N = 55 = 178$

and high relief concentrate precipitation and runoff in smaller ($< 100 \text{ km}^2$) basins. However, runoff in this region may be augmented by snowmelt and this results in a more integrated hydrologic response and lower variability of floods in larger drainage basins.

Flood variability is independent of basin size in the California Coast Ranges and the Colorado Alpine Regions (Curve C, Fig.3.7). In the Coast Ranges, the wide-spread effects of moderately intense precipitation attenuate little with increasing drainage area. For this reason, the unit discharge of 2.65 cms/km^2 (242 cfs/mi^2) that was recorded at the Eel River gage at Scotia, Ca. in December, 1964 (drainage area = $7,700 \text{ km}^2$), stands as one of the highest recorded in the United States (Matthai, 1969). In the Colorado Alpine region, the peaks in runoff are not highly variable for the obvious reason that snowmelt is controlled by areally-integrated factors like snowpack depth and springtime temperature.

A final point with regard to the above discussion concerns the accuracy or validity of the regional flood frequency curves derived earlier (Fig.3.4). Clearly, in the Foothills of the Colorado Front Range, where precipitation and runoff processes are highly localized, the flood characteristics vary with drainage area and the regional frequency curve can be interpreted as a relation that is valid for a basin of "average" size. There is no way of explicitly defining an average-sized basin in this region and the problem is exacerbated by the relatively few number of stations with long records. In the Sierra Nevada and Klamath Mountains, the regional flood frequency curves would be valid for basins of a much larger range in size. Finally, in the California Coast Ranges and the Colorado Alpine, the regional flood frequency curves would probably be valid for all sizes of drainage basins.

3.5 Discussion

The lack of any meaningful relationships between flood variability and drainage basin characteristics is counterintuitive and unexpected given the results of previous workers. It stands to reason that basin characteristics should dictate, to some extent, the hydrologic responses that are eventually manifest as large floods. As an evolving landform, the drainage basin should reflect geomorphic processes of varying magnitude and frequency.

However, it would be an oversimplification to interpret these results as an indication that physiography plays no role in runoff characteristics or that the discharge of a rare flood depends solely on the intensity and volume of rainfall (Benson, 1964). Clearly, the areal distribution and intensity of precipitation play a large role in the generation of floods but this result is of no surprise.

The foregoing analysis is perhaps most limited by the scale at which the physiographic characteristics of drainage basins can be adequately described. Freeze (1980) modeled runoff processes at the hillslope scale and demonstrated that, whether the product of infiltration excess (Horton, 1933) or saturation excess (Dunne, 1978), runoff is very sensitive to the spatially varying hydraulic conductivity of the soil, as defined by both its porosity and moisture content. Freeze showed that simulated runoff volumes had a higher standard deviation, i.e. were more variable, when generated from a hillslope with homogenous properties than when generated from a hillslope with heterogeneous properties. Thus, "a homogenous hillslope propagates the full range of climatic variability to the streamflow peaks, whereas a heterogeneous hillslope acts in a certain sense as an attenuating medium" (Freeze, 1980, p. 405).

At the scale of the present study, the importance of rock type and its influence on soil characteristics could not be adequately assessed and it was assumed that, although undoubtedly important, lithology exerted less of an influence on runoff than did climate. Previous workers have found significant relations between bedrock lithology, basin morphometry and runoff (Hadley and Schumm, 1961) but, generally the rock type and its influence on soil characteristics can be usefully described only in a qualitative sense. Most of the basins considered here are underlain by crystalline rocks, with the exception of the California Coast Ranges which are underlain by weakly to moderately-indurated sedimentary and metamorphic rocks. On the basis of Freeze's comments, it might be inferred that these rock types, although homogenous in a large-scale sense, are sufficiently heterogeneous to eventually dominate runoff production from a basin.

3.6 Summary

For geomorphic purposes, the magnitude of a flood may be best expressed as the ratio of the flood discharge to that of a flood expected to occur on average, i.e. the mean annual flood. This definition was arrived at through a regional flood frequency analysis that demonstrated widely different flood characteristics in each of the regions considered in this study. In semi-arid regions such as the Foothills of the Colorado Front Range, streamflow is highly variable and the 100-year flood may be 10-times larger than the mean annual flood. Peak flows on the snowmelt-fed streams draining the Alpine Region of the Colorado Front Range have a relatively narrow range of discharge and the 100-year flood is not even twice the mean annual flood. Streams in mountainous areas of California have flood frequency distributions with intermediate variability and the 100-year flood is several-times larger than the mean annual flood.

Attempts to relate the flood frequency characteristics of these regions to drainage basin morphometry were unsuccessful. It was suggested that in many environments, transient runoff processes are responsible for the eventual translation of precipitation into a flood peak and that these runoff processes may not manifest themselves as part of the channel network of the drainage basin. Further, drainage basin characteristics do not appear to provide large-scale evidence for the geomorphic importance of high magnitude, low-frequency events as was hoped.

The flood characteristics of the regions considered in this study appear to be most related to climatic factors and scale effects. Flood variability decreases with precipitation amount and intensity but increases as precipitation becomes less seasonally and more event-distributed. The spatial distribution of precipitation and runoff also have an influence on the flood characteristics of a region. Highly intense but localized precipitation results in a poorly integrated drainage basin response that rapidly attenuates downstream. Spatially-distributed runoff, such as occurs during large-scale frontal storms and seasonal snowmelt, results in floods that attenuate slowly or not at all with increasing drainage area.

CHAPTER IV GEOMORPHIC EFFECTS OF FLOODS

As agents of geomorphic change, floods are well known for their spectacular landscape modifications. The last three decades have seen significant advances in our understanding of floods, but the hydraulic and sediment transport processes that lead to catastrophic responses during floods are poorly understood. Within the regional controls imposed by climate, geology and, to a lesser extent scale, it is clear that individual river reaches exhibit considerable variability in their geomorphic responses to floods. This variability is the result of complex interactions among hydraulic, geomorphic and sedimentologic factors. The present study considers several aspects of these interactions but moves away from the single basin, single reach approach and seeks a generalized understanding of the response of rivers to floods in terms of relationships between the driving and resisting forces.

What is meant by the "geomorphic response" to a flood? Previous workers have explored different aspects of flood geomorphology including (1) their extraordinary rates of sediment transport, (2) the changes in morphology that result from channel avulsions or massive inputs of sediment from hillslopes and (3) the changes at channel cross sections due to scouring, filling or bank erosion. The focus of the present chapter is on changes produced at channel cross sections, largely because of the nature of the data set and also because changes in channel planform were not common on the rivers examined. Several aspects of sediment transport will be considered but the more general topic of sediment yield and floods will be taken up in the following chapter. The following analysis is based on the premise that changes in the channel cross section can be related to the balance between *driving forces* as represented by the hydraulics of the flow and the *resisting forces* as represented by the local sedimentologic and morphologic characteristics.

4.1 Flood Discharge, Flood Power and Sediment Movement

The regional flood frequency relationships developed in Chapter 3 provided a means for determining the magnitude of an extraordinary flood. It was also noted that floods of similar return period have magnitudes that differ greatly depending on the climatic characteristics of a region. Thus, a more useful geomorphic definition of the magnitude of a flood is not in terms of its return period but rather in terms of its exceedence of the mean annual flood. For the 25 sites considered in this study, the floods had magnitudes of 2 to greater than 200-times the mean annual flood (Table 4.1). However, most sites experienced floods that were less than 5-times the mean annual flood and although these were unprecedented events in many cases, they would not be considered "super floods".

Additional insight into the relative magnitudes of these floods is gained from their comparison with the previously recorded maximums in the United States (Fig. 4.1). With the exception of the Rubicon River flood (Site 9, Table 4.1) which was the result of a dam failure, and the Big Thompson Flood (Sites 23-24, Table 4.1) which was a "cloud-burst" flood, the majority of the rainfall-runoff floods considered in this study fall well below the envelope curve defining the upper limit of flood discharge for a given drainage area. The floods used by Costa (1987) to define the upper limit of this curve come exclusively from arid and semi-arid areas while many of the floods considered here occurred in humid climates, and they are not extraordinary in terms of unit discharge.

The discharge of a flood is but one measure of its magnitude, but discharge alone is not particularly meaningful in a geomorphic sense because changes in channel geometry come about only if the thresholds of bed and bank stability are exceeded and sediment transport occurs. The initiation of particle motion and the related problems of sediment transport can be thought of as functions of water discharge or flow velocity, but they are more appropriately related to the forces imposed by the flow on the channel bed as represented by the average shear stress, τ or the power expended per unit width of stream, w .

Table 4.1: Summary of hydraulic and morphologic data for floods at selected sites in California and Colorado

Site #	Location	DA	Q _f	Q _{max}	Q _f /Q _{max}	w _v	w _c	R	d	v
1	Scotchman Creek, Site 1	9.8	27	5.9	4.5	12.0	7.8	0.94	1.06	2.09
2	Scotchman Creek, Site 2	11.5	31	7.1	4.3	39.1	10.0	0.69	0.70	1.12
3	Scotchman Creek, Site 3	12.1	32	7.5	4.2	62.6	10.5	0.56	0.57	0.89
4	Greenhorn Creek, Site 1	24.6	52	11.9	4.4	14.0	8.0	1.61	1.90	1.97
5	Greenhorn Creek, Site 2	25.7	55	12.7	4.3	20.5	12.0	1.08	1.14	2.37
6	Greenhorn Creek, Site 3	32.1	67	15.9	4.2	93.2	20.0	0.69	0.70	1.02
7	Greenhorn Creek, Site 4	44.0	84	21.0	4.0	77.1	29.5	1.15	1.17	0.93
8	Poolman Creek	60.0	128	34.0	3.8	17.5	8.2	2.11	2.28	3.21
9	Rubicon River	505	7363	230.5	31.9	191.4	60.4	6.18	6.34	6.07
10	Spanish Creek	477	555	179.2	3.1	42.3	14.4	3.32	3.55	3.70
11	E.Br. N.F. Feather River	2655	1796	482.7	3.7	104.0	72.0	3.81	3.90	4.43
12	W.Br. Feather River	285	736	262.4	2.8	47.2	22.9	4.72	4.72	3.30
13	Butte Creek	381	623	206.3	3.0	65.4	35.0	2.52	2.60	3.66
14	Collee Creek	277	504	109.9	4.6	56.5	35.7	1.58	1.62	5.50
15	Trinity River	386	751	212.4	3.5	118.0	32.0	1.58	1.59	4.01
16	N.F. Trinity River	391	1014	248.8	4.1	36.5	26.5	4.48	5.19	5.35
17	Indian Creek	311	1104	253.5	4.4	31.0	17.4	5.19	7.29	4.89
18	Tom McDonald Creek	17.7	40	19.8	2.0	26.0	11.0	0.76	0.74	2.08
19	Bridge Creek	30.0	60	30.4	2.0	25.0	11.0	1.11	1.17	2.04
20	Van Duzen River	575	1379	625.9	2.2	198.0	80.8	3.11	3.20	2.18
21	Black Butte River	420	821	339.8	2.4	51.5	50.6	4.06	4.54	3.51
22	M.F. Bel River	950	3738	1168.0	3.2	92.0	85.4	6.74	6.94	5.85
23	Loveland Heights Tributary	3.5	133	0.5	260	21.1	12.8	1.20	1.27	4.96
24	Dark Gulch	2.6	96	0.4	234	13.4	10.7	1.06	1.32	5.41
25	N.F. Big Thompson River	205	247	9.3	26.6	35.4	15.2	1.55	1.60	4.36

Symbols: DA, drainage area (km²); Q_f, discharge of flood (m³/s); Q_{max}, mean annual flood (m³/s); Q_f/Q_{max}, ratio of flood discharge to mean annual flood; w_v, total valley width (m); w_c, channel width (m); R, hydraulic radius (m); d, average flow depth (m); v, average flow velocity (m/s)

Table 4.1, continued

Site #	slope	f _f	F _r	τ	ω	τ*	τ* _c	D _{max}	D ₈₄	D ₅₀	ΔXSA	ΔBE
1	0.0497	0.840	0.688	458	957	0.065	0.023	434	160	97	0.15	0.02
2	0.0092	0.399	0.430	62	70	0.010	0.013	390	110	46	-30.54	-0.57
3	0.0140	0.779	0.379	77	68	0.013	0.015	360	118	50	-3.30	-0.05
4	0.0235	0.762	0.497	371	733	0.031	0.014	733	220	96	0.10	0.01
5	0.0090	0.136	0.727	95	226	0.020	0.017	300	90	47	-6.74	-0.37
6	0.0101	0.524	0.392	68	70	0.021	0.014	200	60	26	-59.19	-0.64
7	0.0101	1.063	0.276	114	106	0.039	0.015	180	45	25	17.71	0.22
8	0.0431	0.694	0.705	892	2861	0.165	0.030	334	220	105	2.13	0.13
9	0.0165	0.217	0.780	1000	6072	0.042	0.015	1456	416	208	117.15	0.61
10	0.0076	0.145	0.648	248	916	0.035	0.027	438	240	120	0.10	0.01
11	0.0105	0.160	0.724	392	1737	0.014	0.011	1682	360	160	51.18	0.52
12	0.0168	0.571	0.485	778	2567	0.128	0.019	374	160	68	-0.90	-0.03
13	0.0051	0.075	0.737	126	462	0.015	0.011	508	140	48	-16.89	-0.48
14	0.0163	0.067	1.398	253	1391	0.016	0.010	990	220	90	1.03	0.23
15	0.0051	0.040	1.016	79	316	0.009	0.014	568	155	72	13.09	0.46
16	0.0063	0.077	0.807	277	1481	0.050	0.012	342	82	38	36.84	1.09
17	0.0173	0.124	0.685	372	1817	0.047	0.015	488	220	66	15.05	1.06
18	0.0098	0.135	0.763	73	152	0.031	0.017	147	44	23	42.53	1.33
19	0.0102	0.213	0.618	111	227	0.018	0.010	378	72	35	29.50	1.55
20	0.0025	0.129	0.394	76	166	0.020	0.016	232	86	35	0.10	0.01
21	0.0041	0.106	0.556	163	573	0.096	0.009	105	30	9	44.94	0.86
22	0.0070	0.108	0.720	463	2708	0.079	0.008	360	104	24	99.21	1.12
23	0.0770	0.295	1.446	906	4497	0.054	0.008	1040	300	67	-8.16	-0.39
24	0.1295	0.367	1.679	1347	7291	0.051	0.008	1620	463	103	-3.31	-0.25
25	0.0181	0.116	1.119	275	1201	0.019	0.011	916	210	92	0.10	0.01

Symbols: slope (m/m); f_f, Darcy-Weisbach friction factor; F_r, Froude Number; τ, shear stress, (N/m²); ω, unit stream power (W/m²); τ*, dimensionless shear stress; τ*_c, critical dimensionless shear stress; D_{max}, average size of 5 largest boulders moved (mm); D₈₄, D₅₀, size fractions for which 84% and 50% of the bed material particles are finer (mm); ΔXSA, change in cross-sectional area (m²); ΔBE, change in average bed elevation (m)

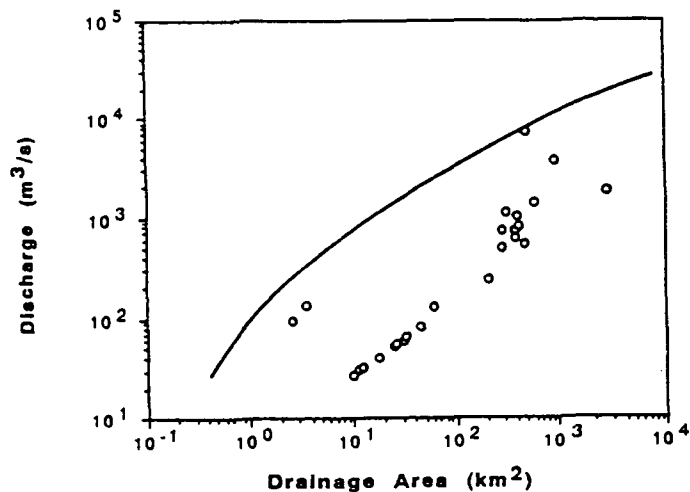


Figure 4.1. Relation between drainage area and flood discharge for the 25 sites examined in this study and the envelope curve for the largest floods in the conterminous United States (after Costa, 1987).

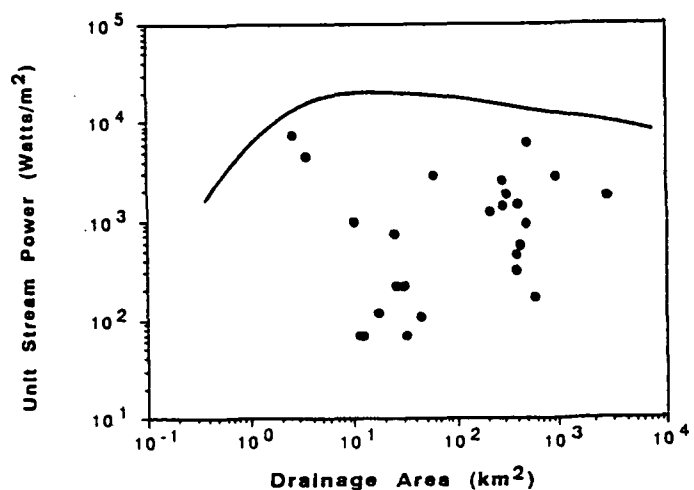


Figure 4.2. Relation between drainage area and unit stream power for the 25 sites examined in this study. The envelope curve defines the maximum unit stream power in rivers of different size (after Baker and Costa, 1987)

The average bed shear stress is given by:

$$\tau = \gamma R S \quad (4.1)$$

where R is the hydraulic radius, S is the slope of the energy gradient and γ is the specific weight of water. In practice, the mean depth is often used in place of R , the water surface slope is used as an approximation for S , and γ is $9,810 \text{ N/m}^3$ for flows with low sediment concentrations. A quantity that is closely related to shear stress and one that is also used in sediment transport problems is unit stream power ω , defined by Bagnold (1966) as:

$$\omega = \gamma R S V \quad (4.2)$$

where V is the average flow velocity. Values for τ , and ω are given in Table 4.1.

It is easily shown that where the combined effects of S , R and V are optimized, ω will reach a maximum (Bull, 1979). The empirical results of Graf (1983) and Baker and Costa (1987) indicate that ω is maximized in drainage basins of between 10 and 100 km^2 . In Figure 4.2, the calculated values of unit stream power at each of the 25 flood sites are compared with the envelope curve of Baker and Costa (1987) that defines the upper limits of unit stream power for a given drainage area. Many of these sites fall within the optimum size range, but because the unit flood discharges were not exceptional, the stream powers developed were much less than those used to define the limiting curve.

The force that a flow exerts on the channel bed and banks is resisted by the structural properties of the perimeter sediments. In gravelly rivers, the noncohesive sediment mixtures that comprise the channel bed derive their strength from the weight and imbrication of the particles on the bed. The force required to overcome the resistance of the particles is, therefore, related to their size and is expressed by the dimensionless shear stress, τ^* :

$$\tau^* = \gamma R S / (\gamma_s - \gamma) D_i \quad (4.3)$$

where γ_s is the specific weight of the sediment (assumed to be about $26,000 \text{ N/m}^3$) and D_i is the diameter of grains in size fraction i . The critical shear stress τ_c required to initiate

movement of sediment in size fraction i is represented by the critical dimensionless shear stress $\tau_{c_i}^*$, where the subscript c denotes the critical condition. The relation between shear force and particle size is the basis for initial motion criteria, sediment transport formulae, the evaluation of streamflow competence and the paleological reconstruction of flood discharges. At each of the 25 study sites, the largest particles moved by the floods were measured directly in the field or determined indirectly from sediment size data found in published reports. These data are presented in Table 4.1 along with data for other size fractions determined in the field by point or bulk sampling of the bed material.

The size of the largest particles moved at these sites ranges from 100 to over 1600 mm. In Figure 4.3, the size of the largest particles moved is compared with the maximum shear stress generated by the flood. Also shown on Figure 4.3 are limiting lines presented by Williams (1983) that define a zone of potential movement for a given particle size and shear stress. The lower line defines the minimum shear stress required to initiate particle motion, and corresponds closely to a critical dimensionless shear stress $\tau_{c_i}^*$, of 0.01. The upper line defines the maximum shear stress for which particle motion did not occur. The data from the 25 sites plot within the zone of potential movement defined by Williams (1983). However, the data span the full width of this zone and in many cases, the maximum shear stress generated by these floods moved particles far smaller than could have moved or, put another way, the minimum shear stress required to move the largest particles was often exceeded. The reasons for this are many and will be discussed later in this chapter.

In summary, the floods considered in this study were not, in most cases, exceptional in terms of their unit discharge or in terms of the unit stream power or shear stress developed. These floods were competent to move boulder-sized bed material, but in many cases, the available shear stress was in excess of the minimum required to initiate motion of larger particles. Nonetheless, spectacular geomorphic changes took place at some of these sites, the complex reasons for which are explored in the next section.

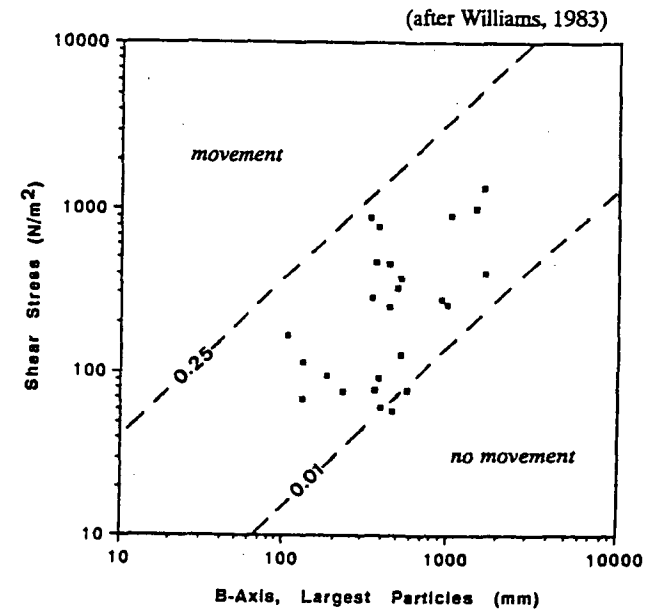


Figure 4.3. Relation between the maximum shear stress and the size of the largest particles that were moved at each of the 25 flood sites. Most points represent the average value of measurements on the 5 largest particles that moved; in a few cases, only the size of the largest particle moved was recorded. The diagonal lines represent minimum and maximum shear stresses required for movement of particles of a given size (after Williams, 1983). Values of the critical dimensionless shear stress at these limits are also shown.

4.2 Channel Changes

Floods may induce a number of geomorphic responses. The fluvial adjustments that result from scouring or filling of the bed, or from lateral erosion of the channel banks and deposition of mid-channel or lateral bars are most simply represented by changes in channel cross sections. Scour and lateral erosion may result in significant widening of the channel and reduction of the average bed elevation (Fig. 4.4A). Deposition of lateral bars may result in an increase in average bed elevation and a reduction of the low-flow channel width but a maintenance of the high-flow or bankfull channel width (Fig. 4.4B).

In cases where the cross section adjustment is very large, as depicted in Figure 4.4A, the choice of an appropriate cross sectional area to use for computational purposes becomes quite subjective. The convention adopted here was to choose the channel perimeter as the boundary defining the highest average bed elevation, whether the bed experienced scour or fill. In adopting this convention, it was assumed then that the high water marks were set when the bed was at its maximum elevation. There are two justifications for adopting this convention. First, the use of high water marks at cross sections that were deepened by scour may result in inordinately large cross sectional areas and high flood discharges. Costa (1983) followed this line of reasoning in concluding that the flood discharges on tributaries of the Big Thompson River were overestimated. The second justification is provided by the work of Harvey and others (1987). These authors conducted detailed channel surveys over a 3-month period to document topographic adjustments of a meandering, sand-bed stream at four different stages of flow. Their results suggest that the topography of a highly mobile bed adjusts to an equilibrium condition defined by the water-surface elevation. At the highest flow, their study reach had aggraded an average of 0.5 m and the bed elevation was at a maximum. As the flow receded and the water surface was lowered, the channel bed scoured. The hypothesis offered for these trends was that the bed topography adjusts by either scour or fill to maintain a velocity gradient and shear stress

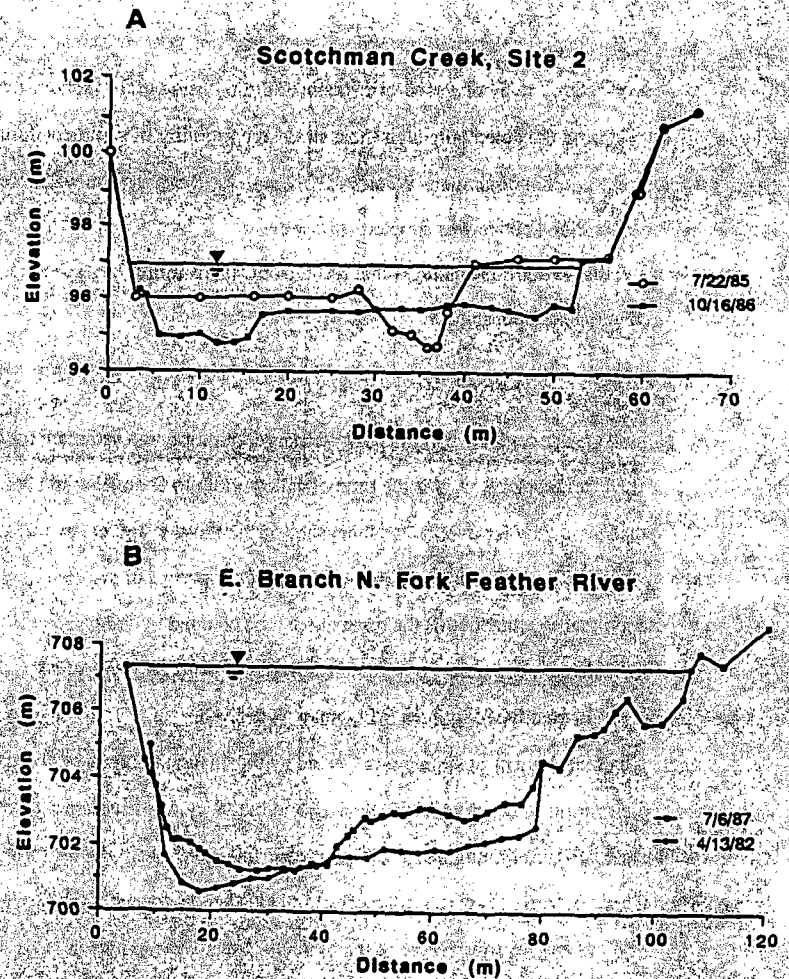


Figure 4.4. Cross section measurements showing the adjustment of two rivers in the Sierra Nevada to the February, 1986 flood. (A) Scotchman Creek was widened and scoured while (B) the East Branch of the North Fork Feather was narrowed by the deposition of a large lateral bar in the channel.

that is just right for the particular conditions of sediment size and flow resistance. Extrapolating the results from a study of a sand-bed stream to these coarse grained rivers may be tenuous but considering the potentially high shear stress and mobility of sediment during a flood, the scales are not that dissimilar. Whatever the case, some convention was necessary and the one described above was adopted uniformly.

Conceptually, the geomorphic changes that result from floods might be expressed as a generalized multivariate relationship:

$$\text{Channel Change} = f(Q_p, Q_d, Q_s, s, w_{v,c}, \tau, \omega, D_i, v, \dots \text{etc.}) \quad (4.4)$$

where Q_p , Q_d and Q_s are respectively, the peak discharge, duration and sediment load of the flood, s is the channel slope, $w_{v,c}$ is the ratio of valley width to channel width and would represent the capacity for overbank conveyance of the flow, τ and ω are measures of the force of the flood, and D_i and v are respectively, the properties of sediment and riparian vegetation that together define the resistance of the channel boundary. From this simple list of variables, other quantities such as critical dimensionless shear stress τ^* , Froude number Fr , or relative roughness R/D_i , may be derived.

Channel adjustments are most simply represented by the change in cross-sectional area or average bed elevation of the channel (Table 4.1), and in theory, these changes should reflect the balance between driving and resisting forces. In Figures 4.5A-D, the changes in cross-sectional area at each site are related to direct and indirect measures of the driving force of the flood and the resisting forces of the channel. Negative changes in cross section area indicate channel scour, and positive changes represent channel fill. The driving force of a flood can be expressed indirectly by the ratio of the flood discharge to the mean annual flood (Fig. 4.5A), and directly by the bed shear stress (Fig. 4.5B). The resisting forces of the channel bed can be expressed directly by the size of the sediment moved by the flood (Fig. 4.5C), and indirectly by a ratio of the valley width to the channel width (Fig. 4.5D). The latter variable would reflect the ability to dissipate flood energy in overbank areas.

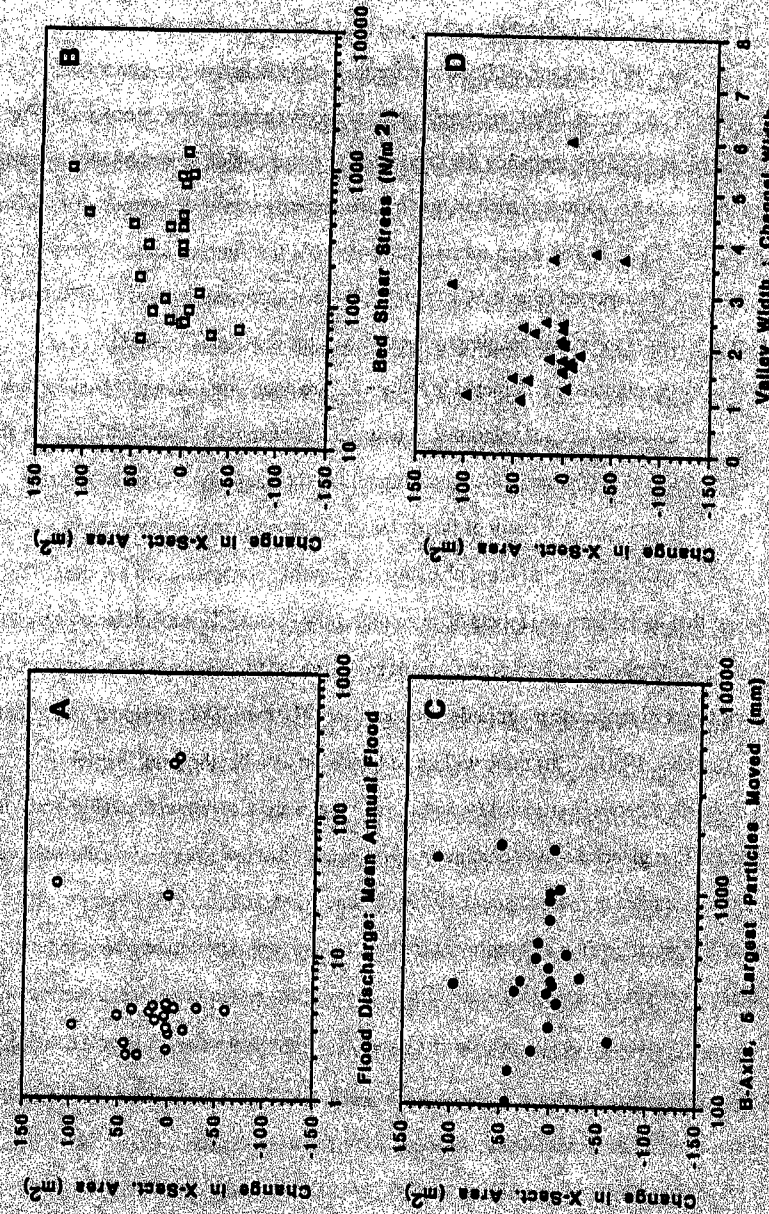


Figure 4.5. Changes in cross-sectional area at 25 flood sites as functions of (A) the ratio of flood discharge to mean annual flood, (B) average bed shear stress, (C) the largest particles moved, and (D) the ratio of valley width to channel width. A negative change in cross section area indicates erosion and a positive change in cross section area indicates deposition.

The most significant channel changes occurred at discharges that were only several times larger than the mean annual flood and for the same discharge, some channels experienced scour, others filled, and some cross sections changed little or not at all (Fig. 4.5A). There is a general tendency for deposition to occur at high values of shear stress, but a number of sites with very high values of shear stress experienced very little erosion or deposition (Fig. 4.5B). There is a similar trend of deposition with an increase in the size of the largest particles moved (Fig. 4.5C). Finally, there is a general trend of erosion with increasing width of the valley relative to the width of the channel (Fig. 4.5D).

Many of the relationships depicted in Figure 4.5 are counterintuitive and bear further explanation. Consider first the relationship between the change in cross sectional area and the ratio of the flood discharge to the mean annual flood (Fig. 4.5A). That many cross sections changed little as the result of floods that were several times larger than an average flood may be an indication that these channels have morphologies that are adjusted to rare events, or that their forms are relicts of prior high flow events. This result is contrary to the widely held belief that the morphology of self-formed alluvial rivers is the result of frequent flows of moderate magnitude (Leopold and Wolman, 1960; Wolman and Miller, 1960; Andrews, 1980). This topic will be addressed in detail in the next chapter.

The relation between shear stress and the change in cross sectional area (Fig 4.5B) is puzzling at first glance because channel erosion occurred at low values of shear stress and deposition occurred in some channels at high values of shear stress. However, as with many problems of erosion and sediment transport, it is more useful to express the total available shear stress τ , relative to the critical shear stress τ_c required for sediment motion:

$$q_s = k(\tau - \tau_c)^n \quad (4.5)$$

where q_s is the unit sediment discharge and n and k are constants. In addition, the total available shear stress is not all used for sediment transport because of losses due to the fluid drag on bedforms, obstructions, and channel bars. This topic will be addressed in detail in the next section of this chapter, but suffice to say at this point that at sites where

frictional losses were negligible and the critical shear stress approximately equaled the total shear stress, erosion occurred. At sites with high shear stress, either deposition occurred or there were no channel changes even though the critical shear stress was, in most cases, greatly exceeded. In the former case, much of the total available shear stress was lost to form drag and sediment transport; in the latter case, much of the total available shear stress was lost to the resistance created by very large boulders in the stream bed.

The general trend of deposition with increasing grain size (Fig. 4.5C) can be more easily explained by the fact that, in general, it is harder to move larger-sized sediment. However, following the same line of reasoning as above, rivers carrying significant amounts of sand and fine-gravel bed material may aggrade if there are large losses in the available shear stress due to the increased resistance from bed forms and channel bars.

The general trend from deposition in channels with narrow floodplains to erosion with increasing valley width (Fig. 4.5D) is also puzzling. A river flowing within a narrow valley would be expected to deepen or erode its banks during a flood because the flow cannot be dispersed over-bank. The observed trends may reflect several different processes. If a channel carrying a high bed material load adjusts its bed topography to the water-surface elevation (Harvey, et al., 1987), then an incised channel might well aggrade as the flood stage rises. Clearly this process cannot dominate over the long-term because, within the fluvial system, steep channels are not zones of aggradation. Aggradation can occur in steep channels if the flow is highly charged with sediment derived from hillslope sources. This represents a transient condition however, because the amount of sediment supplied to steep streams is limited by hillslope weathering and transport processes, the rates of which are much slower over the long term than those at which fluvial processes operate. Many high gradient streams in the Coast Ranges of California (Sites 18-22, Table 4.1) aggraded during the 1964 storm, a fact attributed by many observers to be the result of massive sediment inputs by landslides (Kelsey, 1980; Lisle, 1982). That many of these channels

aggraded under conditions of relatively high shear stress (Fig. 4.5D) is a reflection of the large losses in fluid drag due to bed forms created by the oversupply of sediment.

Once out of the headwater reaches, rivers become more sinuous and their alluvial valleys become wider. The observed tendency for erosion by rivers with wider valley floors (Fig. 4.5D) may be explained by two different effects associated with distal river reaches having floodplains and erodible channel banks. As described above, deposition in the headwater or tributary reaches of a river may leave the downstream reaches starved of sediment. Under supply-limited conditions, rivers will erode their beds if the critical condition for bed material motion is reached. Clearly, most rivers are not supply-limited in their downstream reaches and this condition cannot be dominant in the long-term development of an alluvial floodplain because these are zones of net deposition within the fluvial system. The flows that are competent to transport sediment in tributary channels may occur on a relatively frequent basis (say, several days per year) and may remove the majority of sediment stored in tributary channels within decades or less (Pitlick, in press). As this sediment moves to the downstream river reaches, it is deposited and the channel bed may be rebuilt to an elevation that, over the long-term, represents an equilibrium condition. As an example of this process, Butte Creek, a tributary of the Sacramento River in California (Site 13, Table 4.1), scoured its bed an average of 0.5 m during the February, 1986 flood (Fig. 4.6). This cross section was re-surveyed 18 months later and by that time, the bed had restored its pre-flood elevation by filling during less-than bankfull flows (Fig. 4.6). Presumably, the source for this sediment was from aggraded reaches not far upstream.

A second factor that contributes to the trend of erosion with increasing valley width is the tendency for rivers to attack their banks more vigorously as their gradient decreases and they become more sinuous. High gradient streams often have channel margins comprised of bedrock that is not easily eroded while low gradient streams often have sinuous channels carved into floodplain alluvium. The channel changes that occurred at sites on Greenhorn Creek (Site 6, Table 4.1) and Scotchman Creek (Site 2, Table 4.1; Fig 4.4A) were largely

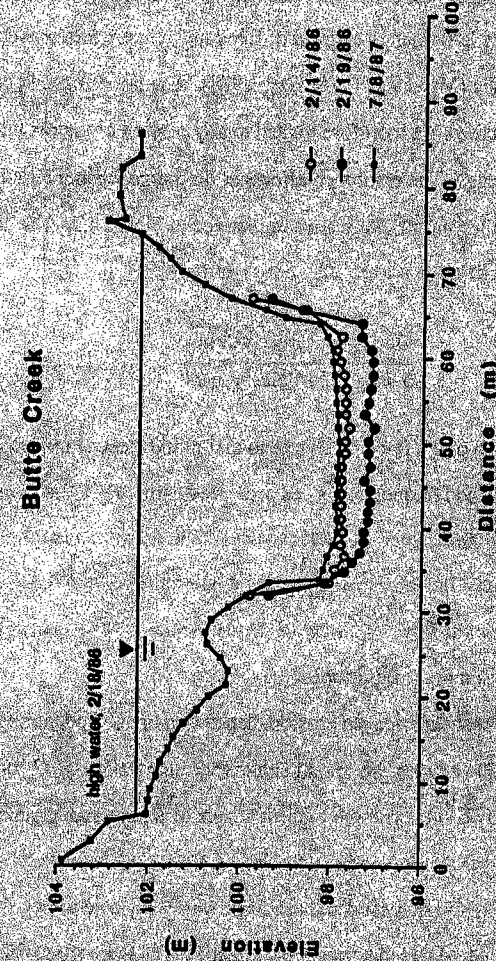


Figure 4.6. Cross section surveys at the U.S.G.S. gaging station on Butte Creek near Chico, California. Note that the bed scoured an average of about 0.5 meter during the February, 1986 flood. By the time of the next survey in July, 1987, the pre-flood bed elevation had been restored.

74,000 AC

due to erosion of unconsolidated sand and gravel bank materials. The sinuosity of rivers is clear testimony of their ability to erode their banks and it is likely that in many cases, the shear stress required to erode either the cohesive fine-grained sediments or non-cohesive gravels that comprise channel banks are exceeded only during large floods.

Because alluvial rivers have many "degrees of freedom", unique solutions to their geometry are indeterminate (Maddock, 1970; Hey, 1978). The flood-induced changes that occur at channel cross sections are therefore related to any number of factors working alone or in consort with each other. The combined effects of discharge, channel gradient, sediment size and channel/valley morphology are summarized in Figure 4.7. The ordinate is represented by an "index of flood power" Ω_i , derived from:

$$\frac{Q_f / Q_{maf} \cdot \text{reach slope}}{5 \text{ largest particles moved}} \quad (4.6)$$

where Q_f / Q_{maf} is the ratio of the flood discharge to that of the mean annual flood as determined from the regional flood frequency curves presented earlier (Fig. 3.4), and the reach slope and average size of the 5 largest particles moved are as measured in the field. This variable represents a ratio of the forces generated by the flood relative to the resistance of the bed material. The abscissa (ratio of valley to channel width) represents the importance of different valley and channel configurations.

The channel reaches that experienced erosion, deposition or no change roughly cluster into groups (Fig. 4.7). The erosion group had either very high values of Ω_i or relatively wide valley floors. The two sites with the highest values of Ω_i are high gradient tributaries of the Big Thompson River that scoured deeply during the 1976 flood. At these sites, the mean annual flood was greatly exceeded and the flood was easily able to overcome the resistance of the boulder-sized bed material in the channel. The three sites with relatively wide valley floors and moderate gradients are Sierra Nevada streams that are still filled with sand and gravel-sized sediment that was deposited during

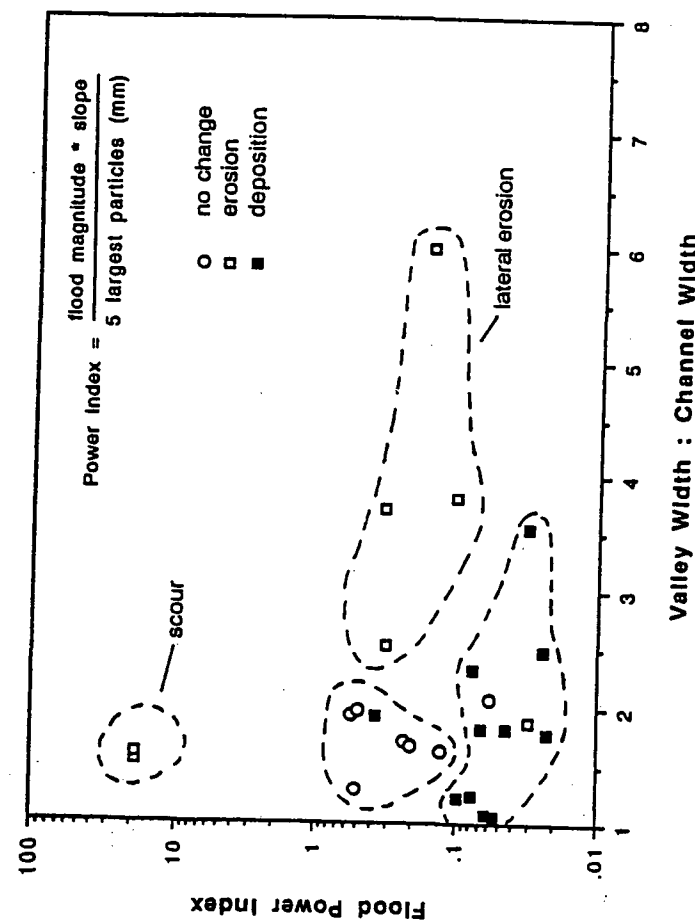


Figure 4.7. Channel changes as a function of an index of flood power and the ratio of the valley to channel width.

the period of hydraulic mining 100 years ago. The floods that occurred in February 1986 were only about 4-times greater than the mean annual flood on Greenhorn Creek and Scotchman Creek (Table 4.1), but their channels widened significantly because the unconsolidated sediments comprising the channel banks were vigorously eroded. Lateral erosion may be the most common response to floods on meandering, gravel-bed rivers because they often have banks comprised of non-cohesive, coarse-grained basal sediments overlain by cohesive, fine-grained sediments. On this type of river, the rate of bank erosion and meander bend migration is controlled primarily by the size of the sediment in the basal layer and the frequency that it is mobilized (Nanson and Hickin, 1986).

The sites at which little or no erosion took place had intermediate values of Ω . These sites may represent the case where the slope, sediment size and form of the channel are adjusted to high flow conditions and are marginally affected by a flood. At yet lower values of Ω , many sites experienced deposition. These sites are primarily on low gradient reaches of California Coast Range streams where deposition occurred because the flood magnitude was not high relative to the size of sediment supplied to the reach.

4.3 Flow Resistance and Sediment Transport in High Gradient Streams

High gradient streams may have the potential to optimize unit stream power (Bull, 1979) but their cobble and boulder beds create hydraulic conditions that are much different from those of lowland rivers. In addition, many of the rivers chosen for this study carried extraordinary sediment loads during the floods of interest. The bias towards rivers with coarse beds and potentially high sediment loads introduces several complex but interesting problems of flood geomorphology. Some of these problems have already been alluded to but, they were not explored in detail. The following discussion elaborates on the topics of flow resistance and sediment transport in high gradient streams. These problems have been the focus of much research in engineering and geomorphology but the results have not been applied in previous flood studies.

Consider first the relation between shear stress and the movement of large particles. Data presented earlier showed a wide range in the amount of shear stress used in the movement of large particles (Fig. 4.3). The data from the 25 study sites fell within the zone of potential sediment movement defined by Williams (1983) but the available shear stress was often in excess of the minimum required to move the largest particles. The reasons for this have to do with the sorting and imbrication of the bed material, the exposure of the larger particles, and the use of average rather than instantaneous values of bed shear stress. A solution to the latter problem is not possible with the present data but the effects of particle exposure and sediment sorting can be partially accounted for with the results of recent studies by Parker and others (1982), Andrews (1983) and Carling (1983), all of whom have investigated the problems of particle entrainment in gravel-bed rivers.

Defining the critical condition at which sediment movement just begins is a difficult if not impossible task. In the above studies, particle motion was detected by sampling the bed load in traps or portable samplers and it was assumed that the particles in motion were entrained under the conditions of average shear stress observed at the time. In the present study there were no means of directly verifying the critical conditions; it can only be said that the shear stress at a particular site attained a given maximum and that particles of a given size either did or did not move.

The minimum critical dimensionless shear stress required to move the largest particles D_{max} can be estimated by using any one of the empirical relations developed by the above authors. These equations take the general form:

$$\tau_c^* = k (D_1 / D_{50})^n \quad (4.7)$$

where k and n are constants; n takes on values that approach 1.0 indicating that particles within a bed of mixed sizes begin to move at approximately the same shear stresses.

The critical dimensionless shear stress τ_c^* for the largest particles D_{max} was computed using the relation given by Andrews (1983) and the size characteristics of the bed material at each site (Table 4.1). For motion of the largest particles, the predicted values of $\tau_{c_{max}}^*$

cluster about 0.01, the minimum value suggested by Andrews and the value that also defines the lower limit of critical shear stress suggested by Williams (Fig. 4.3). Also listed in Table 4.1 is the dimensionless shear stress τ^* (eqn. 4.3) that was available to move the largest particles. It is clear from these data that τ^* commonly exceeds τ_{*c}^* , and sometimes by an order of magnitude. This is particularly true on the streams with gradients higher than 1% and bed material coarser than cobbles (b-axis > 256 mm).

Two possible explanations are available for the disparity between the available shear stress and the critical shear stress required to move the largest particles. First, larger particles than those that moved may not have been available for transport. In general, this was not the case because larger particles were present in the channel bed but there was clear evidence (e.g. algae growing on the top side of an imbricate boulder) that they were not moved by the flood. Second, it is possible that not all of the total shear stress is available for sediment transport. As the following discussion will point out, this may be particularly true for floods on high gradient streams with coarse bed material and high sediment loads.

The shear stress represented by $\tau = \gamma R S$ is the total drag force exerted by the flow per unit area of channel bed. However, the total shear stress τ is actually a stress that is distributed among a number of different elements (Einstein, 1950). The components of the total shear stress include the drag due to sediment grains on the bed τ_g or in saltation τ_s , both small- and large-scale bedforms τ_f , the internal fluid shear or spill τ_i , etc. (Fig. 4.8). Only the grain component of shear stress τ_g is used in bed material transport. The shear stress exerted on each of these components is opposed by resistance elements that are likewise distributed. The total flow resistance is distributed as grain resistance, form resistance and spill resistance (Leopold, et al., 1960). Conceptually, the importance of the various components of flow resistance changes with increasing discharge (Fig. 4.9). The common assumption is that the total flow resistance in channels with static beds and moderate slopes (< 1%) is provided solely by the grains (e.g. Hey, 1979).

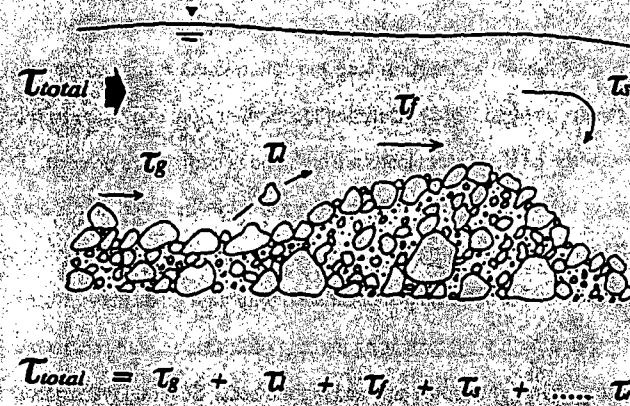


Figure 4.8. Components of shear stress distributed conceptually between sediment grains, bed forms and internal fluid spill or distortion.

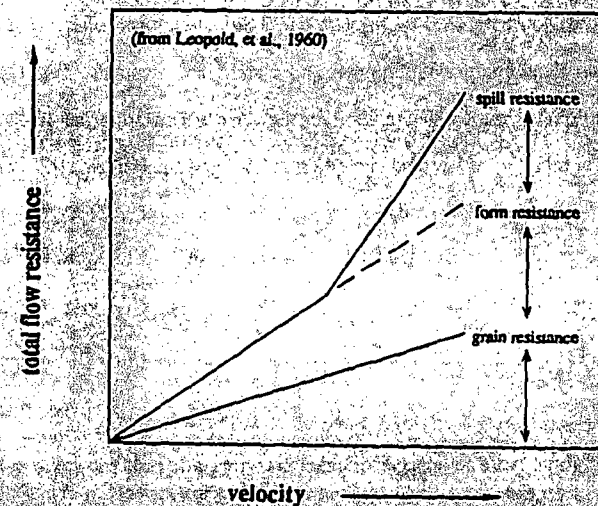


Figure 4.9. Changes in the relative importance of the components of flow resistance with increasing velocity or discharge.

Boulder and cobble-bed streams have gradients that commonly exceed 1% and roughness elements that are of the same scale as the flow depth. Flow resistance in these coarse bed rivers is dominated by the form drag and spill resistance induced by large-scale roughness elements (Bathurst, 1982). Defining the amount flow resistance in this type of river is further exacerbated if sediment loads are high and bed forms are present. During a flood, it is very likely that sediment loads will be high and the expectation that the total shear stress or flow resistance can be represented by that due solely to grains becomes suspect.

The problem of flow resistance on streams with high gradients and high sediment loads was investigated further by comparing the data of this study with previously published data obtained from rivers with both static and mobile beds. Several investigators (Limerinos, 1970; Leopold, et al., 1964) have developed resistance relations of the general form:

$$u/u_* = 1/\sqrt{f} = c + k \log (y/k_s) \quad (4.8)$$

where u is the flow velocity, u_* is the shear velocity ($u_* = \sqrt{gRs}$), f is the flow resistance computed from the Darcy-Weisbach relation ($f = 8gRs/v^2$), y is the height above the bed, k_s is the equivalent sand grain roughness, and c and k are constants. Equation 4.8 is the well known Prandtl-von Karman relation for the vertical distribution of stream velocity. The empirical relations of Leopold and others (1964) and Limerinos (1970) are similar in form and relate the total flow resistance to the mean flow depth, d or hydraulic radius R and D_{84} as the characteristic sediment size. The equation of Leopold and others is:

$$1/\sqrt{f} = 1.0 + 2.03 \log (d/D_{84}) \quad (4.9)$$

and Limerinos:

$$1/\sqrt{f} = 1.16 + 2.03 \log (R/D_{84}) \quad (4.10)$$

These relations were developed for channels with static beds and relative smoothness values (R/D_{84}) of greater than 1.0. The relations defined by equations 4.9 and 4.10 plot as virtually the same curve (Fig. 4.10A), and indicate that the total resistance offered by the grains decreases with flow depth. Thus, for a given grain size, a deep flow encounters a

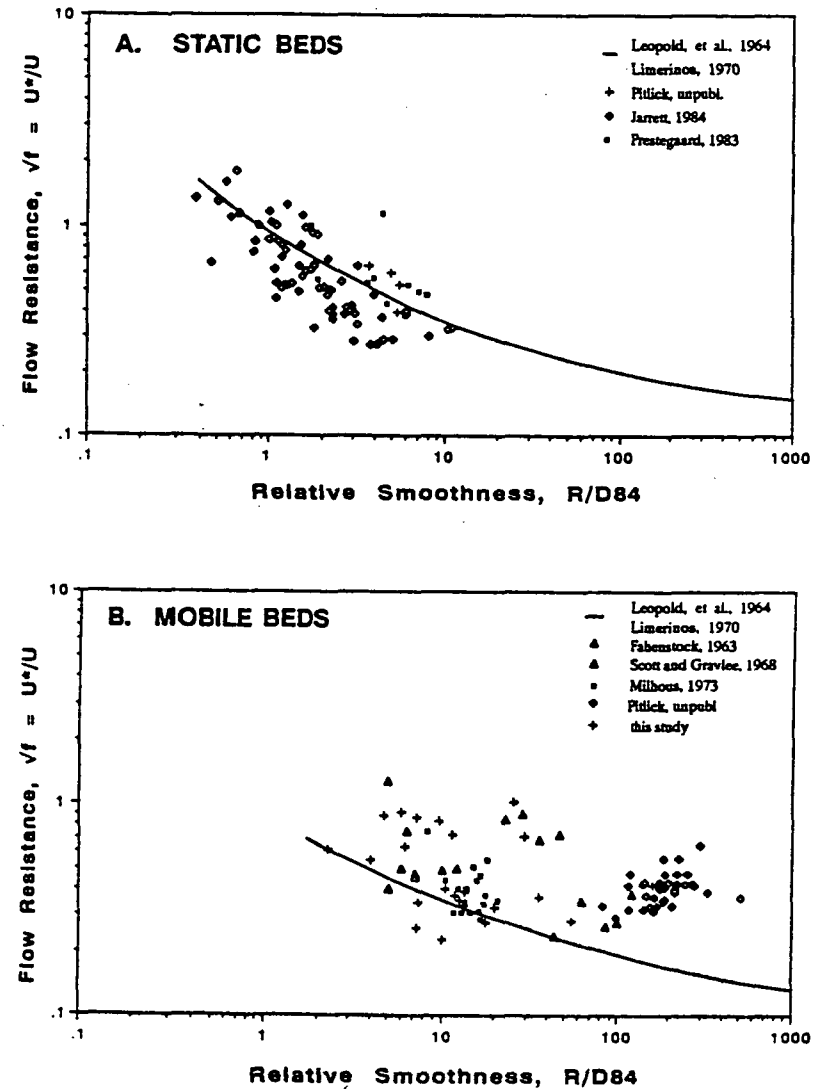


Figure 4.10. Flow resistance and relative smoothness relations for (A) static beds and (B) mobile beds.

relatively smoother bed than does a shallow flow, assuming that D_{84} is the appropriate measure of the equivalent sand roughness. Additional data from rivers with low relative smoothness and static beds are provided by Prestegard (1983), Jarrett (1985), and this author (Fig. 4.10A). These data conform very closely to the above relations and support the belief that the majority of the total flow resistance in streams with immobile beds is provided by the stationary bed material particles.

Field data from rivers with mobile beds are plotted in Figure 4.10B along with the data from this study and the reference curves defined by the above relations. The additional field data come from reports by Fahenstock (1963), Scott and Gravelle (1968), Milhous (1973) and this author. Note that the total flow resistance, in many cases, is far greater than that defined by the reference curve for flow resistance due to grains alone. The data that plot to the far right in Figure 4.10B (labeled "Pitlick, unpubl.") are from a sand bed stream where bed forms were present. These data were purposely included to show the obvious increase in flow resistance from the effects of bed forms. The data from many of the flood sites plot far above the reference curve as well.

In rivers with very coarse bed material, the additional flow resistance may be derived from spill around large boulders and from the step-pool bed topography. At particle Reynolds numbers of about 10^5 , flow separation occurs around large boulders and this causes a drastic reduction in particle drag. Flow separation explains why, at $Re > 10^5$, the critical dimensionless shear stress of the larger particles has been observed to be greater than 0.1 (Ashida and Bayazit, 1973; Bathurst, et al., 1987); compare this with the value of 0.01 suggested by Andrews (1983). The step-pool topography and bar forms of high gradient streams contribute additional flow resistance in the way of large-scale bed forms. At bankfull flows, the resistance created by channel bars may be of the same order as grain resistance (Prestegard, 1983). At yet higher flows, it can be speculated that the form resistance induced by the step-pool topography of a very steep stream may be of the same scale of roughness as that of a relatively shallow flow over a sand bed stream with dunes.

In rivers with very high sediment loads, additional flow resistance may be derived from the saltating and suspended sediment load as well as from bed forms. The flood sites with high relative smoothness and excess flow resistance (Fig. 4.10B) are mainly on rivers in the northern California Coast Ranges where sediment loads during the flood were very high. The sediment load, because it has mass and is moving slower than the water, extracts momentum from the flow. If a river is moving high quantities of bed material then it is also likely that bed forms are present. If the sediment is sand-sized, then the bed forms would be small scale. With gravel-sized and coarser sediment, the bed forms are large scale channel bars that contribute to the flow resistance in the manner described above.

The channel changes that occurred at the 25 flood sites can be partially explained by the relative distribution of the components of flow resistance. The computed values of flow resistance and relative roughness for the 25 flood sites are given in Figure 4.11A with each site keyed according to whether it experienced erosion, deposition or no change. In Figure 4.11B, these changes are generalized in terms of the relative importance of spill, grain, and form resistance. It is hypothesized that, at sites with low values of R/D_{84} , much of the total flow resistance was expended as spill resistance, much less was due to grain roughness (Fig. 4.11B) and no erosion took place. These were sites where larger particles could have moved under the available shear stress but did not. At slightly higher values of R/D_{84} , a greater proportion of grain resistance was available and erosion occurred (Fig. 4.11B). These were sites where the critical shear stress approximately equaled the available shear stress. Finally, deposition occurred at sites with high values of R/D_{84} and high sediment load due to the presence of bed forms. The increased resistance from bed forms decreased the available proportion of grain resistance and deposition resulted (Fig. 4.11B).

It is also interesting to consider why, under conditions of similar flow resistance and relative smoothness, some sites experienced erosion while others did not change. If a transient sand or gravel sediment load were introduced to boulder-bed reaches with high spill resistance, erosion might have occurred. The finer sediment would have the effect of

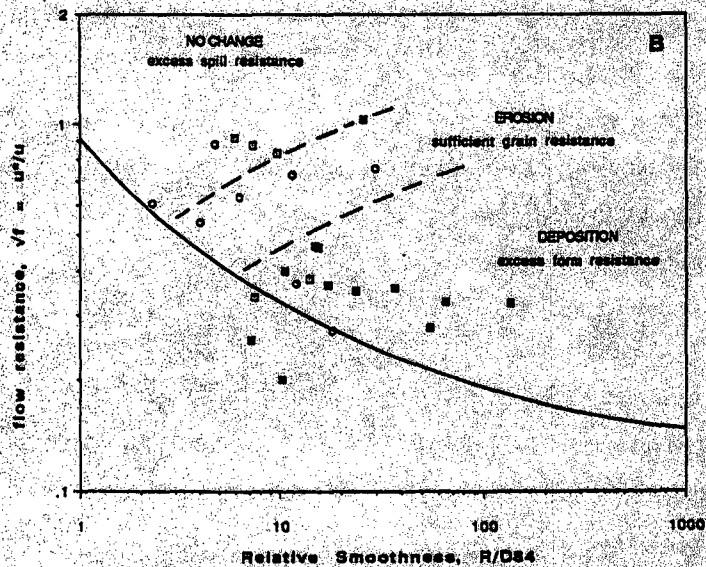
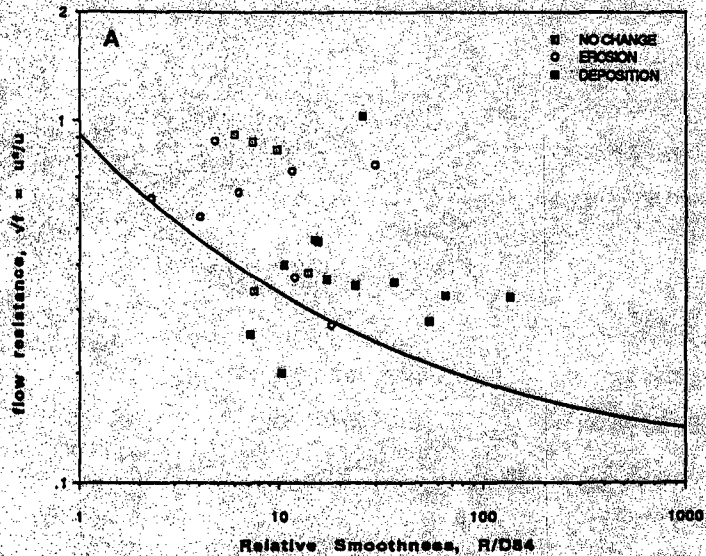


Figure 4.11. Relations between relative smoothness and flow resistance at 25 flood sites keyed in (A) as to whether they experienced no change, erosion or deposition and in (B), these changes are expressed as general functions of flow resistance.

making the bed relatively smoother while changing the exposure of the larger particles little. This would result in a higher proportion of grain resistance and the potential for erosion.

These results have important implications for the use of flow competence relations in the computation of paleodischarges. Many empirical relations are available for predicting the shear stress, velocity or flow depth from sediment size (e.g. Baker and Ritter, 1975; Costa, 1983; Williams, 1983). The implicit assumption of these relations is that the largest particles moved were entrained at the maximum shear stress or discharge attained by a flood. The preceding discussion emphasizes the potential losses in total available shear stress due to spill resistance and form resistance. Failure to account for these losses would result in the underprediction of hydraulic conditions because the total shear stress may not have been wholly utilized to transport sediment of a given size. Flood deposits are often very coarse grained and their poor sorting is indicative of high sediment loads so the conditions alluded to above may be common during rare floods.

4.4 Summary

The geomorphic response of a coarse-bed river to a flood is only partly explained by large-scale factors such as basin size, relief, climate, geology, and vegetation. Within the constraints imposed by these factors, the response of any reach of channel depends also on the local gradient, channel morphology and the availability and mobility of sediment in the bed or banks. This chapter considered the flood-induced geomorphic changes at 25 sites in California and Colorado. For the most part, these floods were not exceptional in terms of their discharge per unit drainage area or in terms of their unit stream power. They were competent to move boulder-sized bed material, but in many cases, the available shear stress was far in excess of the minimum required to initiate motion of the largest particles in the stream bed. Nonetheless, spectacular geomorphic changes took place at some of these sites, the complex reasons for which were explored in detail.

The fluvial responses to large floods were explored in terms of the geomorphic adjustments that occurred at individual channel cross sections. General relations were derived from at-site data characterizing the flood magnitude, flow hydraulics, sediment transport and channel morphology. Many sites experienced no significant change from floods that were several times larger than a mean annual flood and it was suggested that many mountain streams are adjusted to these rare events. The conditions that led to scour, fill, or changes in channel width at the other sites depended on the local conditions of channel gradient, sediment size and floodplain width. Channel scour occurred on high gradient reaches where the flood discharge greatly exceeded that of the mean annual flood. Sites with intermediate gradients, gravel-sized bed material, and wide valley floors experienced lateral erosion. Deposition occurred at sites with low gradients and gravel sediment loads.

A detailed analysis of the relationship between flow resistance and channel morphology showed that the hydraulic and sediment transport conditions of floods cannot be represented. In streams with a step-pool bed topography, bouldery sediment and relative smoothness ($R/D_{84} < 10$), the potential loss of shear stress due to the elements is significant and a flood may entrain sediment far smaller than would be predicted with available competence relations. Under conditions of very high sediment transport and $R/D_{84} \gg 10$, the presence of large and small-scale bed forms and saltating bed material has a similar effect on increasing flow resistance and reducing the shear stress available for sediment transport. It was suggested that both conditions commonly occur during floods but that they have not been accounted for in previous flood studies. The additive effects of the individual components of flow resistance greatly increase the total resistance of flood discharges on high gradient streams. As a result, the total flood discharge may be greatly underestimated with a competence relation that assumes that all of the available shear stress is used in transporting sediment.

THUS ~ →
INCLUDING RARE
PERIODS IS NOT
INDICATIVE OF
LONG-TERM SED. YIELD

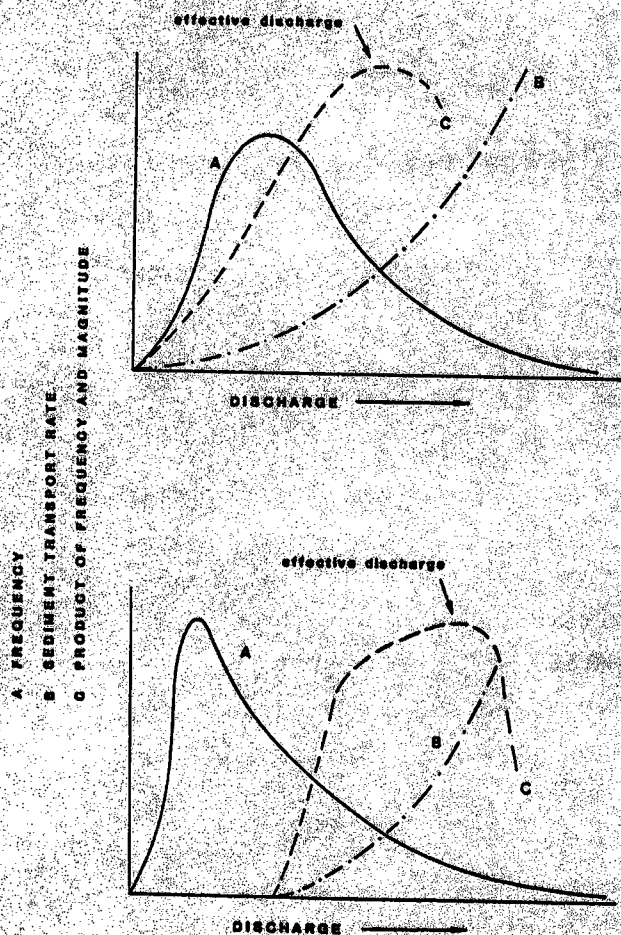
CHAPTER V

MAGNITUDE AND FREQUENCY OF COARSE SEDIMENT TRANSPORT

Rivers, by their transportation of dissolved and clastic loads, are the principal agents of landscape denudation. In their seminal paper, Wolman and Miller (1960) demonstrated that rivers accomplish the bulk of their "work" during relatively common events of moderate magnitude. Although rare floods may transport many-times more sediment than occurs in an average year (Lustig, 1965; Ritter, 1974; Kelsey, 1980), they do not occur with sufficient frequency to dominate the long-term sediment yield of many rivers (Wolman and Miller, 1960; Pickup and Warner, 1976; Andrews, 1980; Nolan, et al., 1987); lesser flows occur frequently but do not carry sufficient sediment. The flow that optimizes sediment transport is termed the "effective discharge" (Fig. 5.1A) and often falls in the range of events that occur a few or several days per year (Benson and Thomas, 1966).

There is a distinction between the flows that carry the most sediment and those that are most important for maintaining channel form. In many cases, the morphology of alluvial rivers can be related to a frequent discharge of moderate magnitude (Leopold and Wolman, 1960; Andrews, 1980). This flow is often one that just fills the channel to its banks and is sometimes equivalent to the flow that transports the most sediment (Andrews, 1980). The association between a flow that optimizes sediment transport and one that is dominant in maintaining channel morphology implies that the river is in adjustment with the long-term supply of sediment and water from upstream.

There has been wide acceptance of the Wolman and Miller concept and it has stood as a cornerstone of geomorphic thought for nearly 30 years. Whether the concept is universally applicable remains in question however. In many cases, the discharge that is most effective for sediment transport occurs more frequently than the bankfull discharge (Benson and



(after Wolman and Miller, 1980; and Baker, 1977)

Figure 5.1. Conceptual relations between the magnitude and frequency of sediment transport as envisioned by Wolman and Miller (upper diagram) and Baker (lower diagram). Curve A is the frequency of flow, curve B, the sediment transport rate, and curve C, the product of magnitude and frequency.

Thomas, 1966; Pickup and Warner, 1976; Nolan, et al., 1987) for reasons that may have to do with either the sediment transport or flow frequency relations that are used. A river's sediment load is commonly assumed to be carried largely (~90%) in suspension, but there is sufficient evidence to indicate that this generalization is not true for many streams and rivers (G. Williams, pers. com.). In other cases, suspended load may be the appropriate index of denudation but it is not clear what role suspended sediment plays in maintaining the form of many rivers, particularly those with gravel beds. Furthermore, given the difference in thresholds for coarse- and fine-grained sediment movement, Baker (1977) has suggested that the effective discharge for bed material transport may be a relatively rare event compared to the effective discharge for suspended sediment transport (Fig. 5.1B).

The magnitude-frequency analysis also requires that the frequency distribution or duration curve of daily flows be well established. The analyses of Andrews (1980) and more recently, Ashmore and Day (1988) indicate a sensitivity to the characteristics of the discharge duration curve. As discussed in Chapter 3, the frequency of flows of given magnitude is both climate- and scale-dependent. The return period of the effective discharge should, therefore, vary with climate and the size of the drainage basin.

Finally, the observations of this author (Chapter 4) and many other workers are that rare floods may result in geomorphic changes that appear unprecedented in historic time. Although they don't transport the bulk of a river's sediment load, floods may effect channel changes that persist for long periods, and it is unclear what role the lesser events play in maintaining channel form. The distinction between an events' sediment yield and its effectiveness in sculpting the land led Wolman and Gerson (1978) to conclude that rare events may be dominant in more arid climates and in smaller drainage basins.

Bearing in mind that runoff processes are both climate- and scale-dependent and that the morphology and stability of coarse-bed channels should depend primarily on the mobility of the bed material, this chapter focuses on the magnitude-frequency concept as it applies to the effective discharge of coarse sediment in high gradient streams.

5.1 Study Sites

This analysis incorporates data from seven USGS gaging stations on rivers draining mountainous terrain in northern California (Fig. 5.2). These rivers have moderately high gradients and gravel- to boulder-sized bed material (Table 5.1). The climate of northern California is strongly seasonal with the majority of rainfall and runoff occurring between the months of October and May. Floods in this region are produced from sustained frontal storms that may generate precipitation with intensities of over 400 mm in 24 hours and may cause significant melting of the mountain snowpack. The 100-year flood may exceed the mean annual flood on the rivers considered here by a factor of 3 to 6 times (Chapter 3).

Table 5.1. Summary data for magnitude/frequency analysis of selected rivers in California

Site	Station ID	DA (km ²)	slope	D ₅₀ (mm)	Q _b (m ³ /s)	Q _{e_b} (m ³ /s)	T _c (yr)
Merced R. ⁽¹⁾	112645	469	0.0200	253	N/A	> 200	> 75
N. Yuba R.	114130	648	0.0100	42	280	450	11.0
Indian Cr.	115215	311	0.0073	66	90	150	2.2
Butte Cr.	113900	381	0.0050	48	127	170	3.4
Trinity R.	115232	386	0.0050	72	85	250	5.8
Smith R.	115325	1577	0.0027	45	N/A	1440	1.70
Van Duzen R.	114785	575	0.0025	35	850	280	1.16

(1): slope and sediment size data were taken from Limerinos (1970).
N/A: a distinct bankfull elevation was not discernible or not available.

5.2 Procedure

The procedure employed in the magnitude and frequency analysis is straightforward. The frequency distribution of flows is determined from the discharge records of the gaging station. Included in the USGS computerized retrieval system, WATSTORE is an output file tabulating the frequency of mean daily flows in each of 34 discharge classes. The proportion of flows falling in a class is simply their frequency divided by the total number of days in the period of record. The frequency distribution is often expressed as a cumulative curve representing the duration of time that the flow is equalled or exceeded.

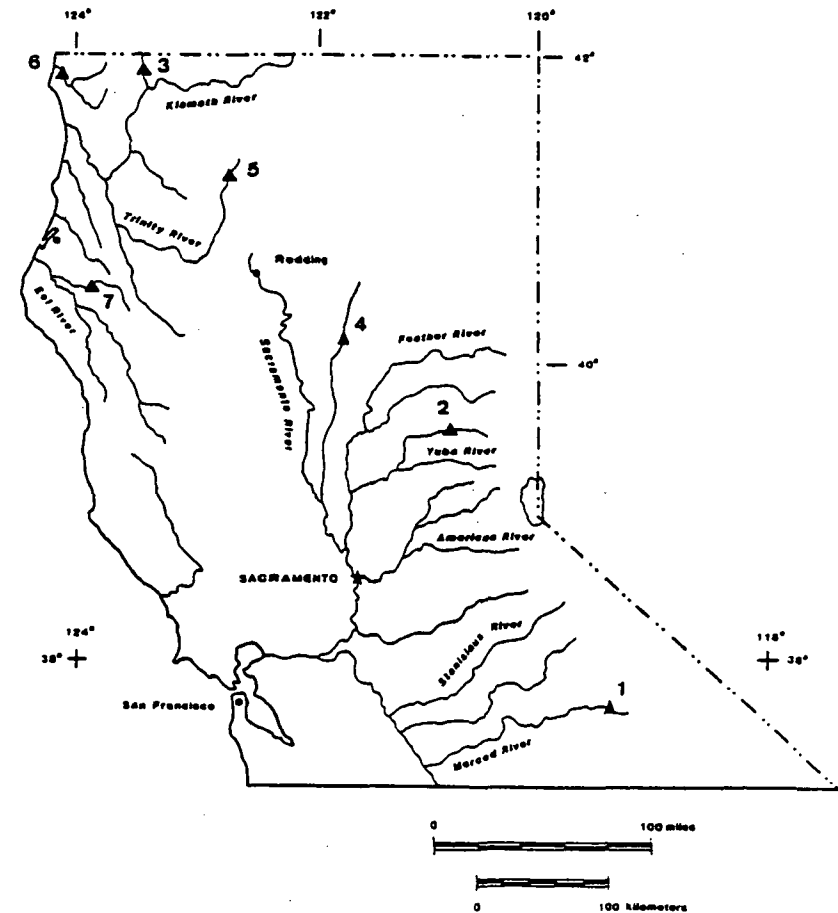


Figure 5.2. Location of sites used in magnitude/frequency analysis. Sites are keyed to information given in Table 5.1

Because the interest was on coarse sediment transport, for which few field data were available, the bed material transport rates at each site were computed using the equation of Meyer-Peter and Müller (1948). This relation (hereafter referred to as the MPM equation) requires that the slope, bed material size distribution, and channel roughness be known. The slope of the reach and the gage cross section were surveyed at all sites except the Merced River, the data for which were obtained from the report by Limerinos (1970). The bankfull stage was identified in the field and the bankfull discharge Q_b was found from the stage-discharge relation of the gage. The size distribution of the bed material was measured in the field with a grid-by-number sample. The channel roughness, represented by Manning's n , was determined from the hydraulic geometry relations of the gage, under the assumption of a constant slope. The bed material discharge was computed by the MPM equation for the median grain size only and not for individual grain size fractions.

Given a process rate, considered here to be the transport of bed material per unit width of channel q_s , and the relative frequency p_i of events within each discharge class i , the proportion of sediment yielded by flows of a given magnitude was computed from:

$$q_{s_i} = q_s \times p_i \quad (5.1)$$

The amount of sediment transported by events within each discharge class can be represented as a histogram or a frequency distribution of discrete events, and the flow at which the maximum value of q_{s_i} occurs is taken as the effective discharge Q_{ef} .

5.3 Results

The flow frequency distribution and sediment discharge relations for the Van Duzen River and the North Fork Yuba River (Fig. 5.3) are typical of most sites. The right-skewed flow frequency distributions deviate from the ideal form represented schematically in Figure 5.1. In both cases, the transport of bed material begins at threshold discharges that occur relatively infrequently (< 2% of the time), and thereafter increase as power functions of discharge, as required by the MPM equation and envisioned by Baker (1977).

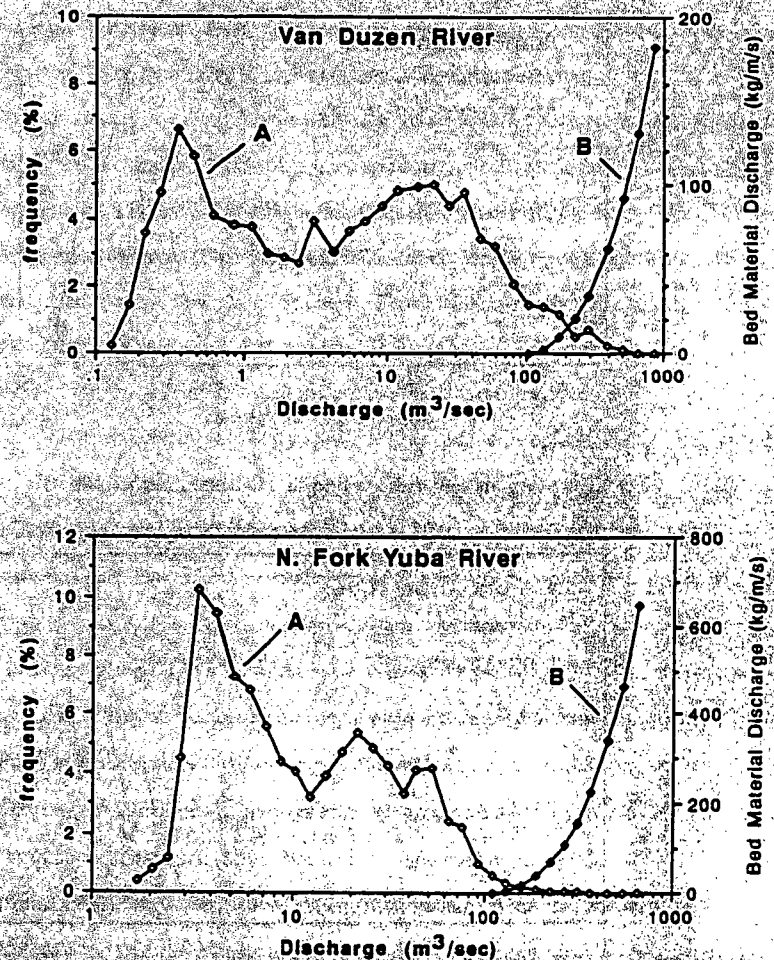


Figure 5.3. Flow frequency distributions and bed material discharge relations for the Van Duzen River and the North Fork Yuba River. Curve (A) represents the frequency of mean daily flows within each increment of discharge; curve (B) represents the bed material transport rate computed for each increment of discharge from the Meyer-Peter and Müller (1948) equation.

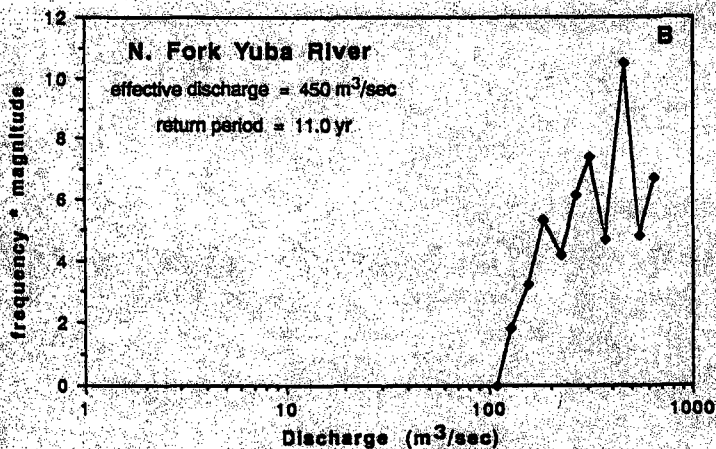
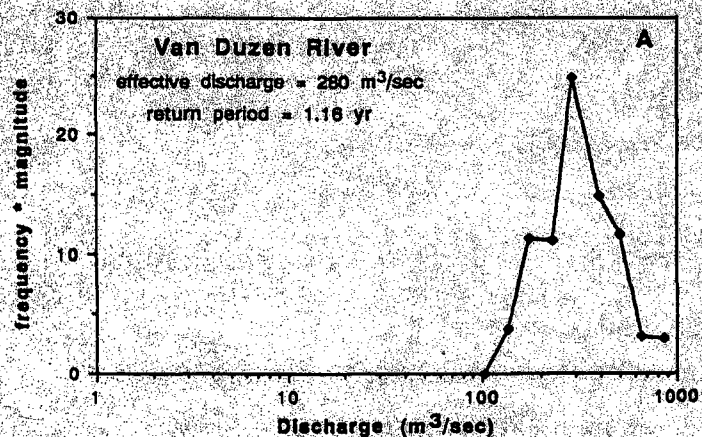


Figure 5.4. Magnitude and frequency relations for the Van Duzen River and North Fork Yuba River. The single peak in the magnitude-frequency relation of the Van Duzen River corresponds to a discharge with a return period of about 1.2 years. The magnitude-frequency relation for the North Fork Yuba River is more irregular but has a peak corresponding to a discharge with a return period of about 11 years.

The effective discharge is the point at which the product of magnitude and frequency is optimized. The magnitude-frequency relation for bed material transport on the Van Duzen River (Fig. 5.4A) has a single peak at about 280 m³/sec, a discharge corresponding to a flow with a return period of about 1.2 years. In the case of the North Fork Yuba River, the peak occurs at a discharge of 450 m³/sec and corresponds to a flow with a return period of approximately 11 years. The magnitude-frequency relation for the North Fork Yuba River is much more irregular (Fig. 5.4B) and indicates the sensitivity of this analysis to the characteristics of the flow duration curve. Flows within the upper discharge classes are sometimes unevenly distributed, and this produces peaks and troughs in the magnitude-frequency relation. Several other stations exhibited these irregularities but, in most cases, a single peak was discernible. The magnitude Q_{ep} , and return period T_{ep} , of the discharges most effective for bed material transport at other sites are given in Table 5.1.

The frequency of the discharge that is most effective for bed material transport appears to be scale dependent. If the return period of Q_{ep} is plotted as a function of channel slope and sediment size, then it is clear that the effective discharge becomes an increasingly rare event as the gradient and size of the bed material increase (Fig. 5.5). This result may appear intuitive at first, because it seems logical that larger discharges or forces would be required to initiate the motion of larger sized sediment. However, the entrainment of gravel and coarser-sized sediments involves complex processes that are generally not accounted for by simple competence (shear stress vs. particle size) relations (Chapter 4; Carson and Griffiths, 1985). However, the MPM equation includes terms that account for this complexity and thus the results shown in Figure 5.5, although partly an artifact of an empirical sediment transport equation, reflect processes that are observed in the field.

If most rivers carry the bulk of their total sediment load in suspension, as is often assumed, then these results may have little bearing on the Wolman and Miller concept as it applies to landscape denudation. However, if the relative proportions of suspended load and bed load are scale dependent, i.e. if the proportion of bed load decreases with drainage

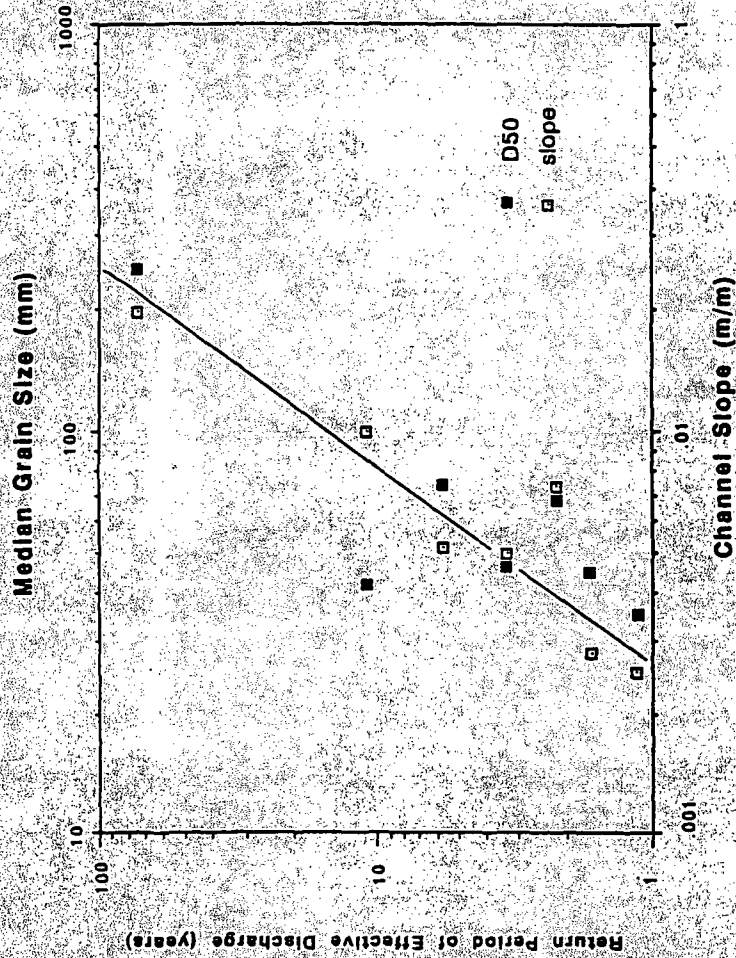


Figure 5.5. Relation between the return period of the effective discharge, channel slope and bed material size.

area, then the above results may also be significant in terms of defining the discharge that accomplishes the most geomorphic work. Data that would conclusively support any scale dependence on the relative proportion of suspended load and bed load in rivers are lacking. However, Ashmore and Day (1988) reported a tendency for the larger Canadian rivers to carry high suspended loads at low discharges, and they offer this as a possible explanation for why the duration of the effective discharge for suspended load increases downstream.

The relation between the effective discharge and the bankfull discharge is not clear (Table 5.1). In some cases, the bankfull discharge and the discharge that is most effective for transporting bed material are nearly equivalent and in other cases they are dissimilar. This analysis would suggest that any generalizations about the relation between the bankfull discharge and the discharge that is most effective for bed material transport are precluded. This may be due to uncertainties associated with the use of an empirical sediment transport equation, but field measurements of bed material transport are also subject to large uncertainty (Hubbell, 1987; Pitlick, 1988). These results suggest that the morphology of many high gradient rivers may bear little relation to a "regime" condition defined by either the dominant discharge or the effective discharge.

The morphology of many steep, cobble- and boulder-bed rivers may be relict from prior floods of extraordinary return period or hydrologic and sediment transport conditions that no longer prevail because of changing environmental conditions. Rare floods may extensively rework the channel and floodplain of a river but they probably do not leave the valley floor as a featureless plain. The deposition of large lateral bars or the formation of terraces by a sediment-charged flood would produce an irregular topography with one or more channels representing either high-flow thalwegs or features incised during the recessional stage of the flood. The morphology of these "relict" channels would be entirely the result of a rare flood event and it would be erroneous, in these cases, to assume that the "bankfull" flows are the dominant or channel forming events.

Scotchman Creek, Site 2

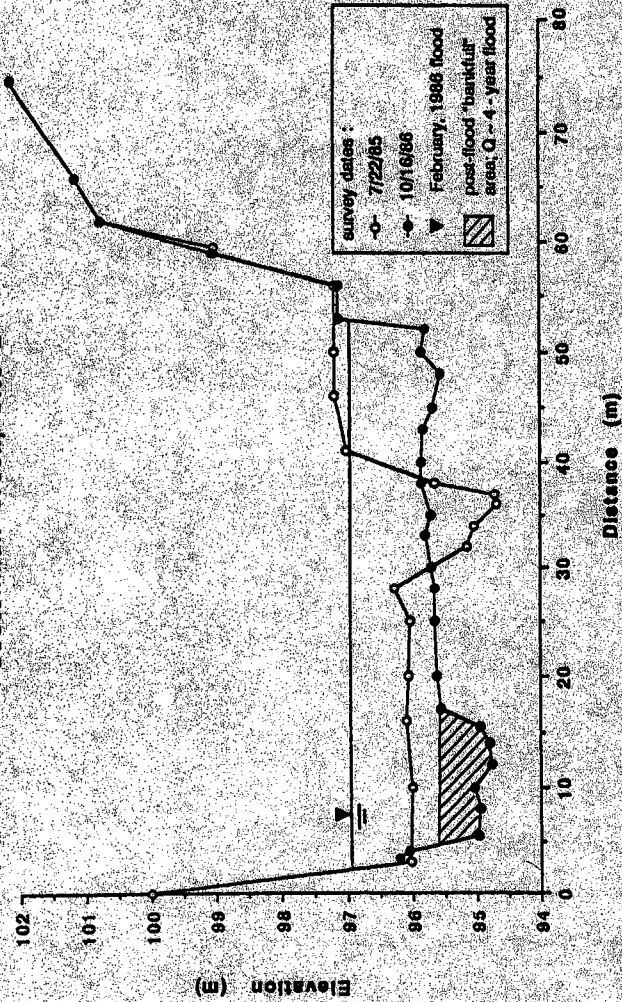


Figure 5.6. Cross section on Scotchman Creek, a Northern Sierra Nevada stream that was completely reshaped at this site as the result of a flood in February, 1986. The low-flow channel that remained after the 1986 flood would convey a discharge approximately equal to the 4-year flood.

An example of how a large flood may produce a low-flow channel that is filled to the bankfull capacity by more common events is shown in Figure 5.6. A flood in February, 1986 reworked the entire valley floor of Scotchman Creek, an 11.5 km² tributary of the South Fork Yuba River in the Sierra Nevada, California. The February 1986 flood affected much of northern California and was estimated to have a return period of about 25 years at this site. This author had surveyed cross sections on Scotchman Creek in 1985 and was able to re-establish their locations several months after the 1986 flood. At this site, the flood inundated the entire valley floor, completely reshaped the cross section and caused the channel to shift by about 25 meters. A large lateral bar was deposited adjacent to a channel that was presumably incised during the flood. The discharge that would fill the incised channel to its banks was computed indirectly to be about 9.7 m³/sec (using a cross sectional area of 7.2 m², the Manning formula to compute a velocity of 1.35 m/sec on a cobble bed with a slope of 0.009, and an "n" value of 0.05). This discharge would have a return period of between 2 and 5 years based on values computed from the regional regression relation of Waanannen and Crippen (1977). Thus, the flow that fills the channel of Scotchman Creek to its banks occurs on a relatively frequent basis but in actuality, this channel was formed as the result of a rare event.

5.4 Summary

The magnitude and frequency concept was examined as it applies to the transport of coarse sediment and the morphology of high gradient rivers. The discharge that is most effective for bed material transport Q_{eb} was computed using an empirical sediment transport equation and the flow frequency characteristics of 7 gaging stations in northern California. Q_{eb} becomes an increasingly rare event as the channel gradient and size of the bed material increase. The return period of Q_{eb} was less than 2-years on the rivers with channel slopes much less than 1%, but approached 100-years on a river with a 2% slope.

The discharge that is most effective for bed material transport is often very different from the bankfull discharge in high gradient, cobble-bed rivers. It was suggested that the morphology of many high gradient rivers may be relict from past floods that extensively rework the channel or floodplain. Large floods may produce low-flow channels that may be filled to the bankfull capacity by more common events, and it would be erroneous in these cases to assume that the "bankfull" flows are the dominant or channel forming events.

These results do not refute the findings of previous workers, but suggest that the magnitude and frequency concept proposed by Wolman and Miller (1960) is not readily applied to high gradient rivers with bed material that is mobilized only during rare floods. Further, if the ratio of bed load to suspended load increases towards the headwater reaches of a river, then these results suggest that the discharges that accomplish the bulk of landscape denudation may be increasingly rare events in smaller drainage basins.

CHAPTER VI

CHANNEL RECOVERY FOLLOWING LARGE FLOODS OR HIGH SEDIMENT INPUTS

The geomorphic effects of floods have been the focus of this and many other studies. However, post-flood studies of channel recovery rates and processes are relatively less common. The length of time required to recover from a flood, or any other catastrophe that alters the regime of a river, is important in both a practical sense and in terms of scaling the geomorphic effectiveness of the event (Wolman and Gerson, 1978). Disturbances caused by floods, landslides, volcanic eruptions and human activities may be short lived or they may propagate through a river system over periods of decades or centuries. Tracking the geomorphic adjustments that take place after a flood is often prohibited by the high costs of maintaining a long-term monitoring effort, and few data are available for testing the hypothesis of geomorphic recovery as applied to rivers.

It is implicit in the concept of recovery that geomorphic systems, if perturbed, will return to a condition of dynamic equilibrium whereby denudation proceeds by steady state processes. The length of time required to restore a landform or a process to its steady state condition depends on the magnitude of the initial perturbation and the rates at which post-event processes are capable of modifying or stabilizing the landscape. Wolman and Gerson hypothesized that the rates of landform recovery are both climate- and scale-dependant. In arid climates, hydrologic events that are capable of restoring landforms to their initial condition are less distributed in time or space so recovery is slower than in humid climates where runoff and sediment movement are more continuous.

The concept of channel recovery has been variously represented by changes in channel planform (Osterkamp and Costa, 1987), longitudinal profile and cross section morphology (Lisle, 1982), sediment storage (Madej, 1984), and sediment transport (Newson, 1980).

In this chapter, the topic of channel recovery will be addressed in terms of changes in sediment transport and cross section morphology with the focus primarily on the spatially and temporally varying processes of channel degradation following large sediment inputs. The process of channel recovery is first illustrated with pertinent data on sediment transport and channel changes on Fall River in Rocky Mountain National Park, Colorado, and is then extended to longer time periods (~ 100 years) with data from rivers draining the hydraulic gold-mining districts of the central Sierra Nevada, California. The chapter concludes with the presentation of a generalized model describing recovery in a fluvial system in terms of spatially and temporally varying rates of sediment transport.

6.1 Recovery Processes on Fall River Following the Lawn Lake flood

The Lawn Lake flood occurred on July 15, 1982 as the result of failure of an 80-year old earthfill dam in Rocky Mountain National Park. This flood, though not a natural event, had the characteristics of a flash flood and peak discharges were estimated to be 2- to 30-times larger than the 500-year flood (Jarrett and Costa, 1986). The flood severely eroded the valley of Roaring River to its confluence with Fall River in Horseshoe Park where it deposited a large alluvial fan (Fig. 6.1). Downstream of the alluvial fan, the 4 km reach of Fall River through Horseshoe Park was left virtually unchanged because the flood was of short duration, the flow was dispersed over a very wide and low-gradient valley floor, and because the channel was protected from erosion by coarse bed material, and heavily vegetated banks (Pitlick and Thorne, 1987). Further details of the flood, its geomorphic effects, and the sedimentology of the alluvial fan are available in the reports by Jarrett and Costa (1986) and Blair (1987).

The unique field settings of the Roaring River alluvial fan and the Horseshoe Park reaches of Fall River have provided outstanding opportunities to examine the processes of recovery in gravel-bed streams. Geomorphic studies in Horseshoe Park were initiated by this author in March, 1983, and were carried on through the 1987 summer field season.

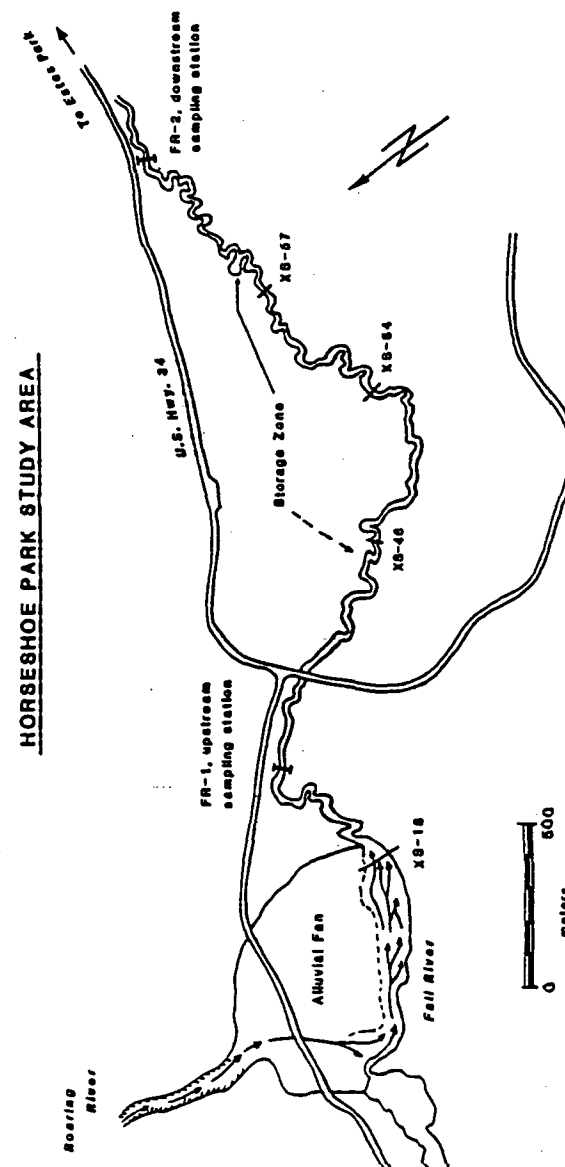


Figure 6.1. Location map of Horseshoe Park study area, Rocky Mountain National Park, Colorado.

Because the Lawn Lake flood occurred in mid-summer, and well after the peak in snowmelt runoff, there were few modifications of Fall River in Horseshoe Park prior to the Spring of 1983 when the site was chosen for field studies. The changes observed during the past 5 years can therefore be related to a well defined baseline. The area is also located within a National Park and human modifications of the flood deposits or the channel of Fall River have been minimal, and will most likely be maintained as they are. The accessibility and the natural setting of the field area has thus provided an opportunity to document the post-flood geomorphic response of a meandering river at a level of detail, that to this author's knowledge, is unprecedented in the United States.

Methods: The geomorphic response of Fall River has been monitored in Horseshoe Park using information from aerial and ground photographs, an array of channel cross sections, and an extensive set of water discharge and bed load measurements from sites on Roaring River and Fall River. Over 80 channel cross sections have been established between the Fall River-Roaring River confluence and the downstream end of Horseshoe Park (Fig. 6.1). Most of these cross sections were established in the first two years of the study and have been surveyed several times during each of the subsequent snowmelt periods. Selected cross sections have been used to monitor changes in bed material texture. A continuously-operating water stage recorder was installed on the U.S. Highway 34 bridge where it crosses Fall River (Fig. 6.1). The record from this site has been used to construct synthetic flood frequency and flow duration curves for Fall River using data from a U.S. Bureau of Reclamation Gaging Station 10 km downstream in the town of Estes Park. Water discharge and sediment load measurements have been made during the snowmelt periods at 1 site on Roaring River and 3 sites on Fall River. Suspended load measurements have been made using depth integrating samplers; bed load has been measured with portable Helley-Smith samplers. These data and the results of related work are available in a series of published and unpublished manuscripts by this author. A brief summary of this work is given below.

Hydrology: Roaring River and Fall River are snowmelt-fed streams that drain mountainous, alpine and subalpine terrain. These basins receive about 700 mm of precipitation annually, most of which falls as snow between the months of October and May above an elevation of about 2500 m.a.s.l. The annual hydrograph of Fall River is dominated by snowmelt runoff that typically peaks in mid-June. The peak flows of Fall River are like most alpine streams of the Colorado Front Range in that they are not highly variable and they rarely exceed the mean annual flood by more than a factor of 2 (Chapter 3).

A synthetic hydrologic record for Fall River in Horseshoe Park was constructed from the data obtained from the temporary gage at the U.S. Highway 34 bridge and from the 38-year record of the gaging station in Estes Park. During the 5-year study period, Fall River has experienced a typical range in snowmelt generated flows; runoff volumes were about equal to the long term average in 3 of the 5 years, well above average in 1983, and well below average in 1987 (Table 6.1). It is significant to note that the highest flows recorded within the 5-year study period occurred in 1983, the year immediately following the Lawn Lake flood. Many of the geomorphic changes that have occurred on Fall River since the Lawn Lake flood can be attributed to the fact that bankfull flows and high sediment transport rates persisted for nearly a month during the 1983 snowmelt runoff period.

Table 6.1 Summary of Hydrologic Data for Fall River in Horseshoe Park

Return Period (1)	Mean Daily Discharge (m ³ /sec)	Number of days flow equalled or exceeded in year				
		1983	1984	1985	1986	1987
1.50	6.31	26	2	4	18	-
2.22 ⁽²⁾	7.46	20	1	3	10	-
5.0	9.94	10	-	-	-	-
10	10.79	-	-	-	-	-
25	12.16	-	-	-	-	-
50	12.66	-	-	-	-	-

(1) determined from the annual maximum series of mean daily discharges

(2) mean annual flood

Sediment Transport: The severely eroded reaches of Roaring River and the unconsolidated deposits of the alluvial fan have provided abundant sediment to Fall River. Sediment yield from the canyon walls of Roaring River and the newly-incised channels of the alluvial fan was greatest during the period of peak snowmelt flow in June, 1983. Bed load was measured throughout this period at the sampling station located 400 m downstream of the alluvial fan terminus (FR-1, Fig. 6.1) and transport rates reached a maximum of 750,000 kg/day during the peak of the 1983 snowmelt. The distal alluvial fan sediments were the primary source of this sediment as indicated by the similarity in the texture of these deposits and the texture of the bed load measured at FR-1 (Fig. 6.2a). In subsequent years, the Roaring River gully has become more stable and channels on the alluvial fan have become armored with a coarse bed material that is mobile only during the highest flows. The bed load measured at FR-1 in recent years has had a size distribution that reflects the sub-armored bed material as the primary source of sediment from the alluvial fan (Fig. 6.2b).

Rapid stabilization of the upstream reaches of Fall River has resulted in a progressive decline in sediment loads at the FR-1 sampling site (Fig. 6.3a). This decline appears to be relatively independent of hydrologic trends because in several years, particularly in 1986, flows were above average, yet sediment loads continued to decrease. The sediment load of Fall River in 1983 was estimated to be at least 1000-times higher than before the Lawn Lake flood, but within 4 years, bed load transport rates had returned nearly to background levels. Rapidly declining sediment yields (Newson, 1980), sediment storage (Pitlick, in press), or rill formation (Collins and Dunne, 1986) have been reported in other disturbed landscapes. The landscape elements examined in these studies were located, like Fall River, within a proximal zone of the fluvial system where the available energy was high, and the rapid return to steady-state conditions was enhanced by the mobility of the sediment. Although, small landscape elements may be sensitive to large perturbations (Wolman and Gerson, 1978) they may also have the capacity to recover their pre-event condition very rapidly if the sediment in the system is mobile over a wide range of flows.

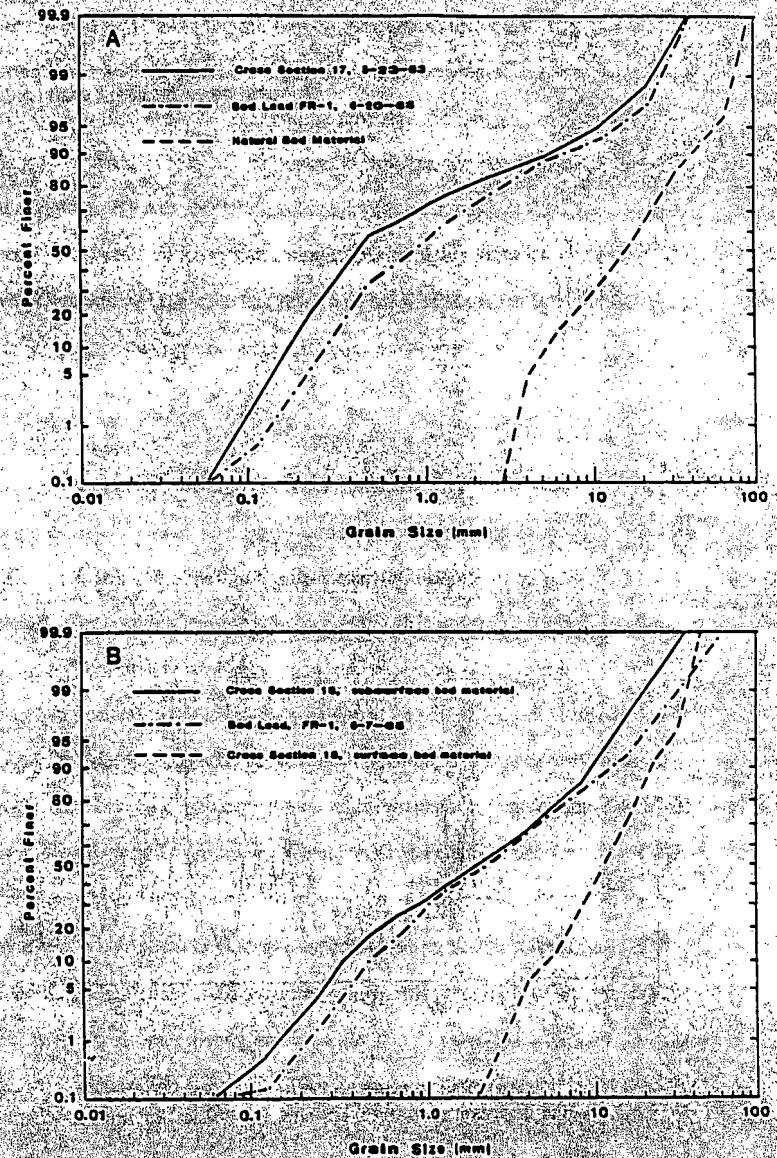
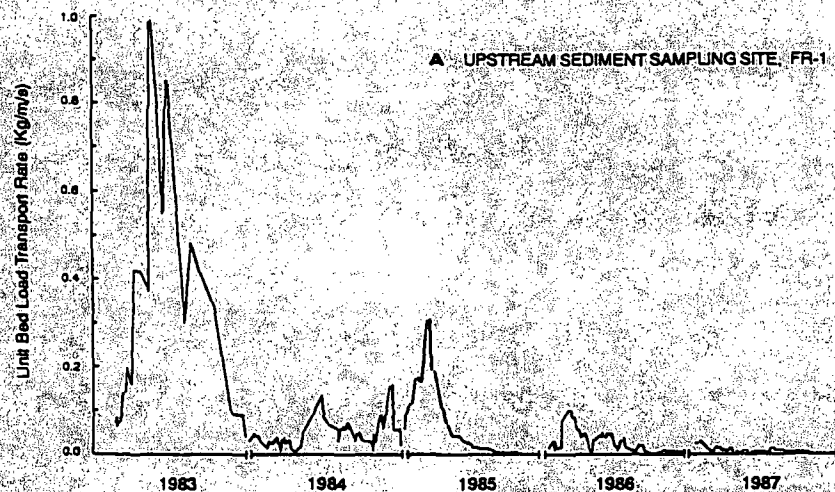


Figure 6.2. Grain size distributions for alluvial fan sediments and bed load sediment in (A) the early part of the study period, and (B) in more recent years.



B DOWNSTREAM SEDIMENT SAMPLING SITE, FR-2

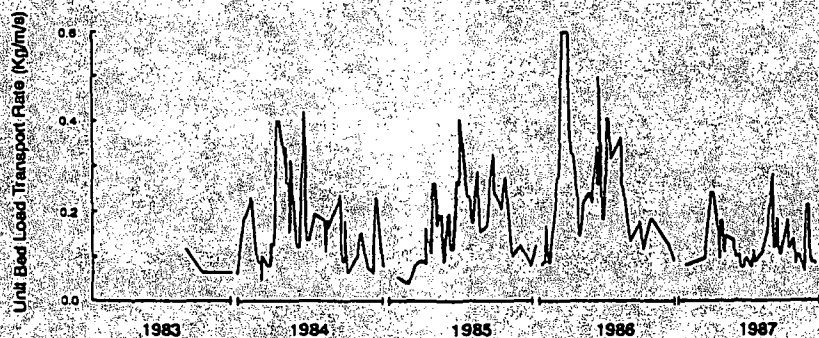


Figure 6.3 Trends in sediment transport in the years since the Lawn Lake flood at (A) the upstream measurement site, FR-1; and (B) at the downstream measurement site, FR-2. Sediment loads declined rapidly at FR-1 as the alluvial fan stabilized, but have remained high at FR-2 because of continued sediment supply from the storage zone reach upstream.

In the first year following the Lawn Lake flood, the coarse sediment yielded from Roaring River and the alluvial fan moved rapidly downstream. The high sediment loads of the 1983 snowmelt were not maintained through the low gradient, sinuous reaches of Fall River downstream of the U.S. Highway 34 bridge, and the channel aggraded to the level of the floodplain. By August, 1983, a 2 km-long sediment storage zone had formed, and the channel pattern of Fall River had changed from highly sinuous to quasi-braided. In subsequent years, this storage zone has acted as a sediment source for the distal reaches of Fall River by progressive erosion from upstream to downstream. The terminus of the storage zone has remained in the same location as where it first formed, and there has been no downstream migration of sediment as a wave. Sediment stored in this reach has not yet been exhausted and is being conveyed slowly through the lower reaches of Fall River. Bed load measurements have been made at the downstream end of the study area since 1983 (FR-3, Fig. 6.3b), and although highly variable, indicate little in the way of a trend toward recovery. The contrast between the data from this site and the data from the upstream site (Fig. 6.3a) illustrates how channel recovery may involve temporally disjointed processes that are very sensitive to the spatially varying characteristics of river slope and planform.

Channel Morphology: The concept of recovery can also be formulated in terms of changes in channel morphology, but as with sediment transport, this also involves spatially and temporally varying processes. Changes in the channel pattern and cross-section form of Fall River have been monitored throughout the Horseshoe Park study area, but channel adjustments within the sediment storage zone are particularly illustrative of the recovery processes. Two channel cross sections within this reach (Fig. 6.4) depict the changes that occurred as the channel first aggraded to the level of the floodplain, and then later degraded to the former bed. The initial cross-section surveys were conducted in early June, 1983, at which time the channel, not having been modified by the Lawn Lake flood, existed in its natural condition (survey of 6/7/83, Fig. 6.4a). By the end of the 1984 snowmelt period, the channel had aggraded to the level of the floodplain (survey of 7/20/83, Fig. 6.4a).

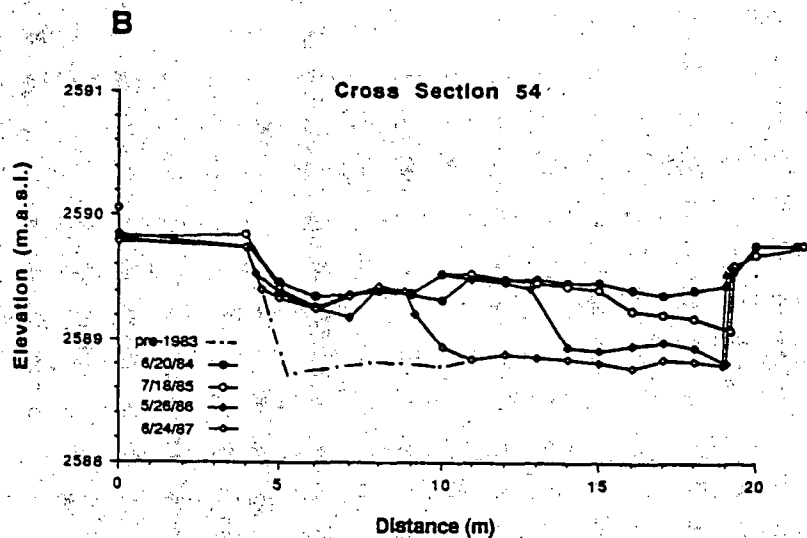
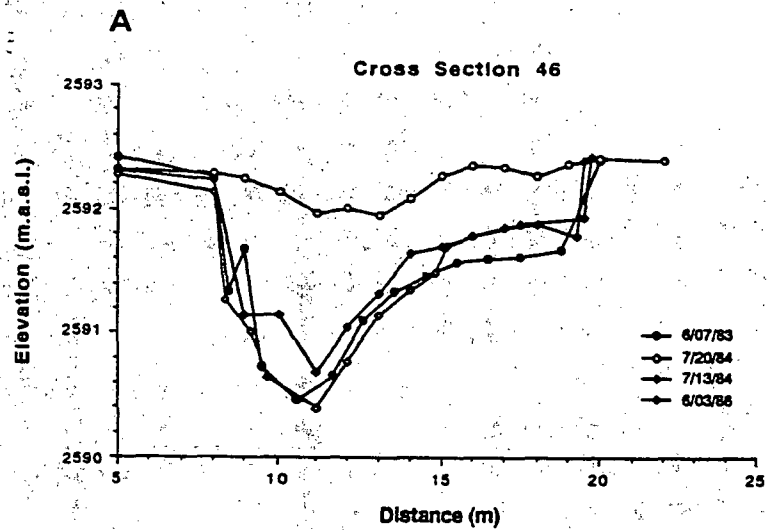


Figure 6.4. Fall River cross sections showing (A) rapid degradation in the upstream part of the storage zone, and (B) slower degradation in the downstream part of the storage zone.

Recovery of the pre-1983 channel configuration has proceeded at increasingly slower rates from the upstream to the downstream reaches of the storage zone. Cross sections in the upstream part of the storage zone (Cross Section 46, Fig. 6.4a), degraded rapidly due to decreased sediment supply from the alluvial fan and because the sediment comprising the channel fill ($D_{50} \sim 2.0$ mm) was mobile at flows that occurred about 50 % of the time. By the end of the 1984 snowmelt period, degradation had restored Cross Section 46 to about the same configuration as when it was first surveyed in June, 1983 (Fig. 6.4a).

In contrast to the rapidly-degrading cross sections in the upstream reaches of the storage zone, the medial and distal reaches of the storage zone have degraded more slowly. Cross sections within the downstream part of the storage zone were not surveyed in 1983 and their pre-aggradation form can only be inferred (Cross Section 54, Fig. 6.4b). However, the initial surveys in June, 1984, show the channel still aggraded to about the level of the floodplain. Degradation at Cross Section 54, located about half the distance between Cross Section 46 and the storage zone terminus, has proceeded gradually over the 4-year period of observation with each year seeing an incremental adjustment of the cross section. Channel recovery in the downstream reaches of the storage zone has proceeded slowly because of continued sediment supply from upstream and because the frequency of flows that are competent to move the sand and gravel-sized bed material decreases in the downstream direction.

The storage zone reach of Fall River illustrates how the rate of channel recovery, in this case represented by degradation, varies depending on location. The spatially varying rates of channel degradation are effectively summarized by serial changes in the average bed elevation through time at cross sections in the proximal, medial, and distal parts of the storage zone (Fig. 6.5). The recovery of pre-aggradation bed elevation occurred rapidly in upstream reaches of the storage zone, and an asymptote defining no change in the average bed elevation was reached about 1 year after the time of peak aggradation (Fig. 6.5a). In the medial reaches of the storage zone, the magnitude of the initial perturbation was not

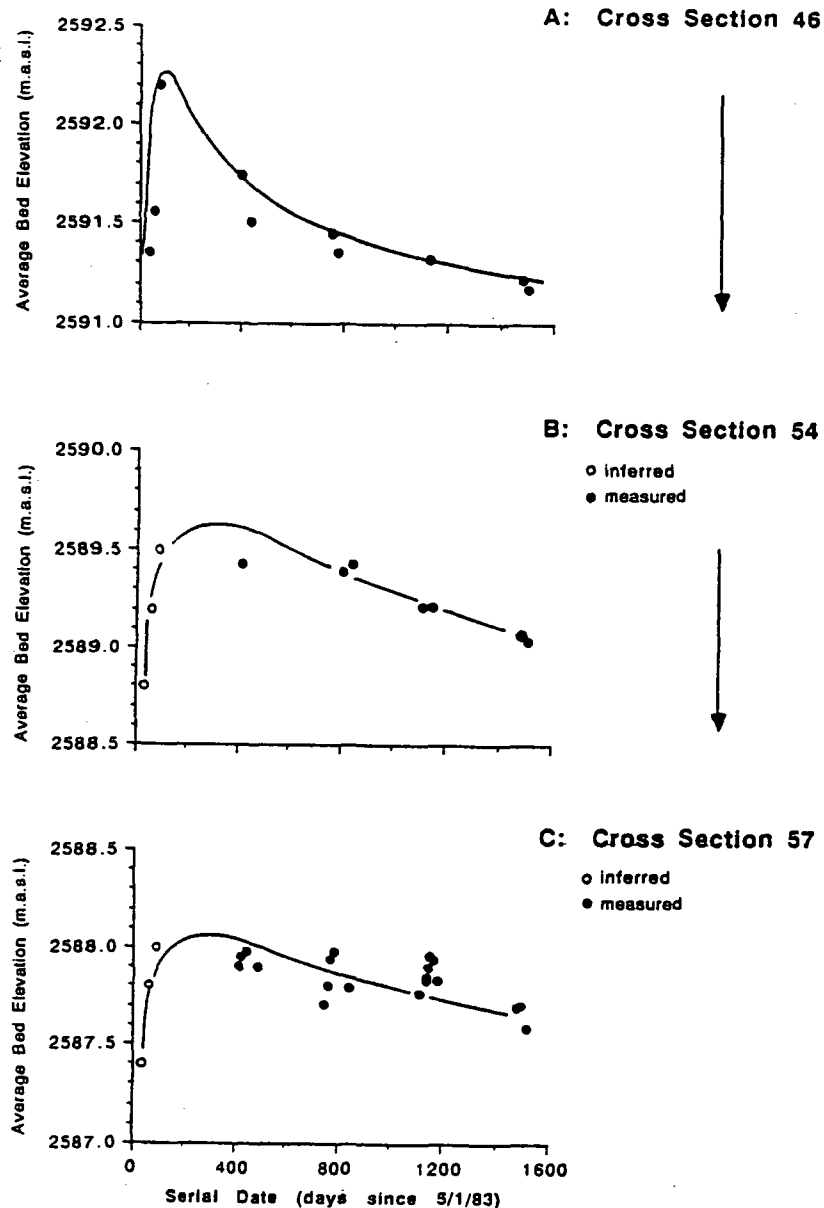


Figure 6.5. Changes in bed elevation through time at cross sections located from (A) the upstream to (B) the downstream parts of the storage zone.

known but recovery has proceeded more slowly than upstream, and appears to be reaching the asymptote of no change in bed elevation after about 5 years (Fig. 6.5 b). The recovery of bed elevations is proceeding at yet slower rates in distal reaches of the storage zone (Fig. 6.5c), and full recovery of pre-1983 bed elevations may be several years or a decade hence.

Downstream progressive trends of channel recovery appear to be common in rivers subjected to large and sudden sediment inputs in their headwater reaches. Similar trends have been reported for rivers in northwestern California (Kelsey, 1980; Madej, 1984), rivers draining Mt. St. Helens (Paine, 1985), and large, gravel-bed braided rivers in New Zealand (Griffiths, 1979; Beschta, 1983) and New Guinea (Pickup, et al., 1983). The results of these studies and the Fall River study would appear to contradict Wolman and Gerson's hypothesis that recovery rates are scale dependent, and specifically, that the downstream reaches of rivers should recover more rapidly from catastrophic events than would headwater reaches. However, Wolman and Gerson, in forming this hypothesis, were likely considering only the flood-induced changes brought about by the river itself and not those changes that are due to large inputs of sediment from landslides or other sources marginal to the channel. To be complete, the concept of channel recovery must therefore, also include the effects of large sediment inputs to headwater channels, which the above results show, is propagated through the river system at rates that depend on (1) the magnitude of the initial perturbation, (2) the rate at which sediment is supplied from upstream, and (3) the frequency of flows that are capable of moving sediment in subsequent years. Recovery may be very rapid (decades) in the proximal reaches of a river inundated with fine-grained sediment that is mobile over a wide range of discharges but much slower (centuries) in the distal reaches of a river continually subjected to high sediment input from upstream. The concept of channel recovery as related to spatially and temporally varying sediment transport rates is explored at a larger scale in the next section through an analysis of degradation in rivers draining the Sierra Nevada that were inundated with sand and gravel tailings from the hydraulic gold mines of the California Mother Lode.

6.2 Recovery of Sierra Nevada Rivers from the Effects of Hydraulic Mining

Approximately 100 years ago, large-scale hydraulic mining was outlawed as a means of extracting placer gold from the Tertiary auriferous gravels of the Sierra Nevada foothills. The disposal of mine tailings in valley bottoms, which had been standard practice for years, had greatly increased the sediment loads of rivers draining the region, and caused massive aggradation in headwater streams. However, the larger Sierra Nevada rivers were able to flush this debris relatively quickly from the foothills, and much of it was deposited in piedmont reaches where these rivers traverse the Sacramento Valley to San Francisco Bay. The loss of farmland productivity and the degradation of the fishery resource of the Sacramento River and its tributaries led to the 1884 decision prohibiting large-scale hydraulic mining and the disposal of tailings in river channels. Clandestine mining operations probably carried on through the turn of the century, but at a much smaller scale.

The streams and rivers of this region provide an unusual opportunity to examine the processes of stream channel recovery over a period of nearly a century. While there is little evidence to be found on larger rivers within the Sierra Nevada foothills, the effects of hydraulic mining are vividly displayed on some of the smaller streams of the region. Decades of incision in the headwater reaches of these streams has left flights of terraces that are tens-of-meters high. The number and height of these terraces generally diminishes downstream, and it is obvious that the process of degradation is proceeding at ever decreasing rates from proximal to distal reaches. The streams in this region, therefore, provide an excellent, if unnatural, analog for other fluvial systems where degradation is initiated from upstream.

Surprisingly little research has been conducted on rivers in this area since hydraulic mining ceased. The earliest studies were undertaken by the State of California and the U.S. Army to determine the extent to which the mining debris posed a threat to downstream navigation and flood control. G.K. Gilbert traversed the Sierra Nevada foothills between 1905 and 1908, and he provided a vivid account on the status of rivers at that time. Gilbert (1917) reported that, by the turn of the century, the larger rivers had passed

the peak of maximum aggradation in their piedmont reaches. His account of conditions in smaller streams suggests that degradation was in progress in the headwater reaches by that time, but incision was proceeding at variable rates. Gilbert's photographs reveal that some headwater streams had degraded several meters by 1900 while other streams remained choked with debris and no degradation was evident.

Subsequent to the publication of Gilbert's work, most of the research on the placer deposits in the Sierra Nevada foothills has been aimed at revitalizing the mining industry (Wildman, 1981). Little attention has been given to the processes and problems associated with the erosion of mining waste in small streams of this region until recently. Wildman (1981) interpreted the development of multiple, unpaired terraces on tributaries of the Bear and Yuba Rivers in terms of the episodic erosion processes envisioned by Schumm (1977). These rivers have not been studied with long-term recovery processes as the main focus.

Study Area: The foothills of the Sierra Nevada consist of intrusive and metamorphic rocks that are overlain by Tertiary sedimentary and volcaniclastic rocks. The Tertiary sediments were the primary source of placer gold and they form the present-day interfluvies separating deeply-incised canyons of the major rivers. The average annual precipitation varies from about 1300 mm to 1700 mm as the foothills rise in elevation from west to east; the density of the coniferous forest mimics this precipitation gradient.

The streams examined in this study are located just east of Nevada City, California. Scotchman Creek is a 4th order stream that drains 15 km² at its confluence with the South Fork Yuba River (Fig. 6.6). Greenhorn Creek is a 5th order tributary of the Bear River and drains about 100 km² where it empties into Rollins Reservoir (Fig. 6.6); this creek was also examined by Wildman (1981) in her study of episodic erosion of mining debris.

Methods: These streams were first visited by this author in 1985 at which time 3 cross sections were surveyed on Scotchman Creek, and 4 cross sections were surveyed on Greenhorn Creek. Bulk samples of the terrace sediments and grid-by-number samples of the present bed material were taken at the same time these cross sections were surveyed.

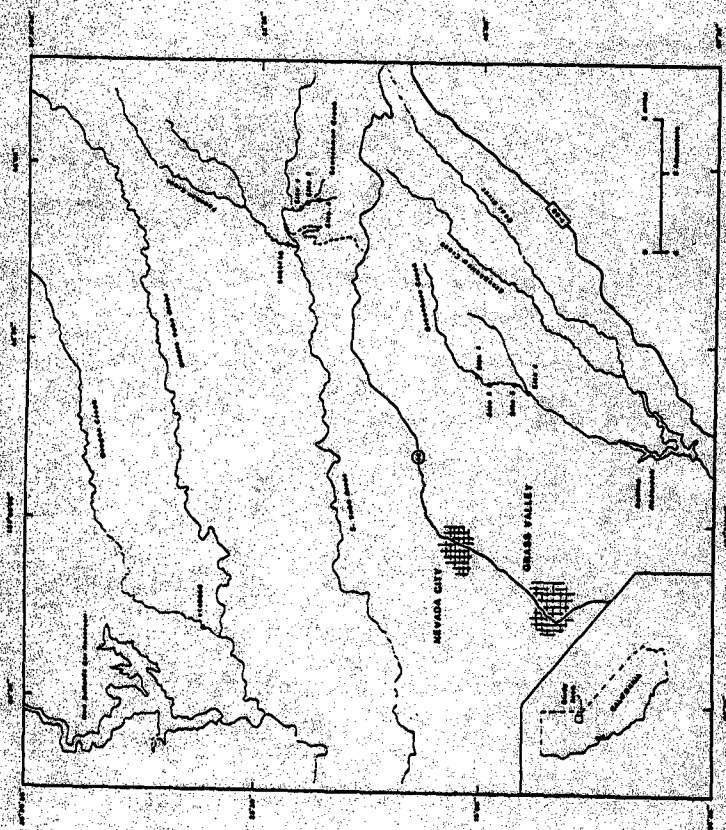


Figure 6.6. Location map of streams draining the foothills of the Sierra Nevada.

The ages of different terrace surfaces were determined with tree-ring cores. Tree ages represent minimum dates for when the terrace surface was last occupied because it likely took some time for a tree to become established once the surface was abandoned. A series of aerial photographs dating from 1939 were checked to verify the age of terrace surfaces.

The time when degradation began at a site would depend on its proximity to a mine and obviously could not be specified explicitly. For the purposes of the present study, 1900 was arbitrarily taken as the earliest date when channel recovery could have begun on these headwater streams. This date was chosen for convenience, but given that hydraulic mining was not outlawed until 1884, and that high erosion rates probably continued for at least a decade thereafter, 1900 was probably about the time when the mines ceased to be the primary sediment sources for headwater streams. The data and photographs presented by Gilbert (1917) suggest that this is not a bad, if oversimplified approximation.

Results: Erosion of the hydraulic mining debris in these streams has proceeded from upstream to downstream as illustrated by three valley cross sections on Greenhorn Creek (Fig. 6.7). At the most upstream locality (Site 1, Fig. 6.7), nearly all of the mine tailings had been removed by 1970 to expose the boulder and cobble bed of the former channel. The depth of incision at Site 2, located about 1.5 km downstream, is about the same (25 m) as at Site 1 (Fig. 6.7), but the elevation of the former channel bed has not yet been reached because of the greater depth of fill at this locality. Site 3 is located another 2 km downstream, and incision at this locality has only been about 10 meters (Fig. 6.7).

Incision of the mining debris in these creeks has left numerous terraces, the approximate ages of which were determined from trees and aerial photo interpretation. By knowing the approximate age when a surface was last active, the incision rate at each site could be calculated for different times (Fig. 6.8), but because the age of most terrace surfaces was uncertain, the incision rates for a given time period were best expressed as a range. From the data in Figure 6.8, it is apparent that incision at the upstream site reached a maximum rate earlier than sites downstream. The incision rate at the upstream site reached

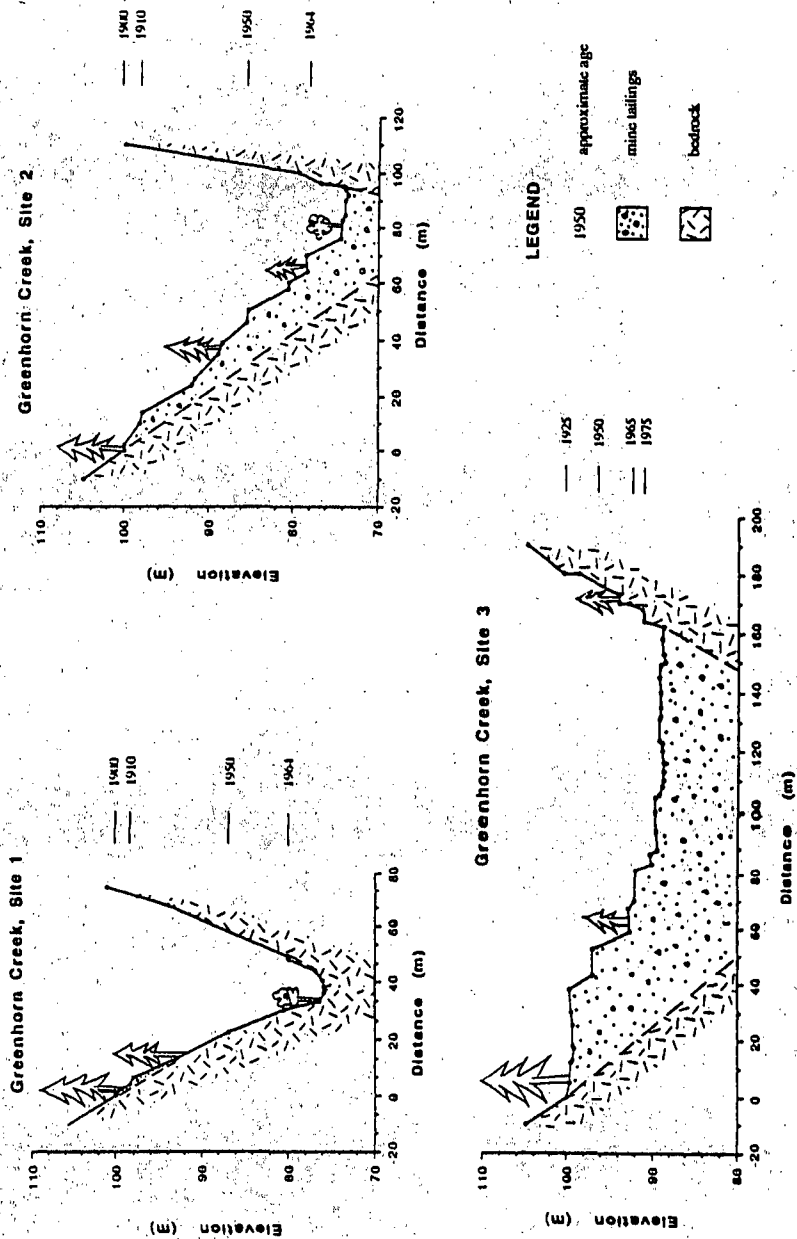


Figure 6.7 Channel cross sections on Greenhorn Creek showing different terrace levels and the approximate time when they were last occupied.

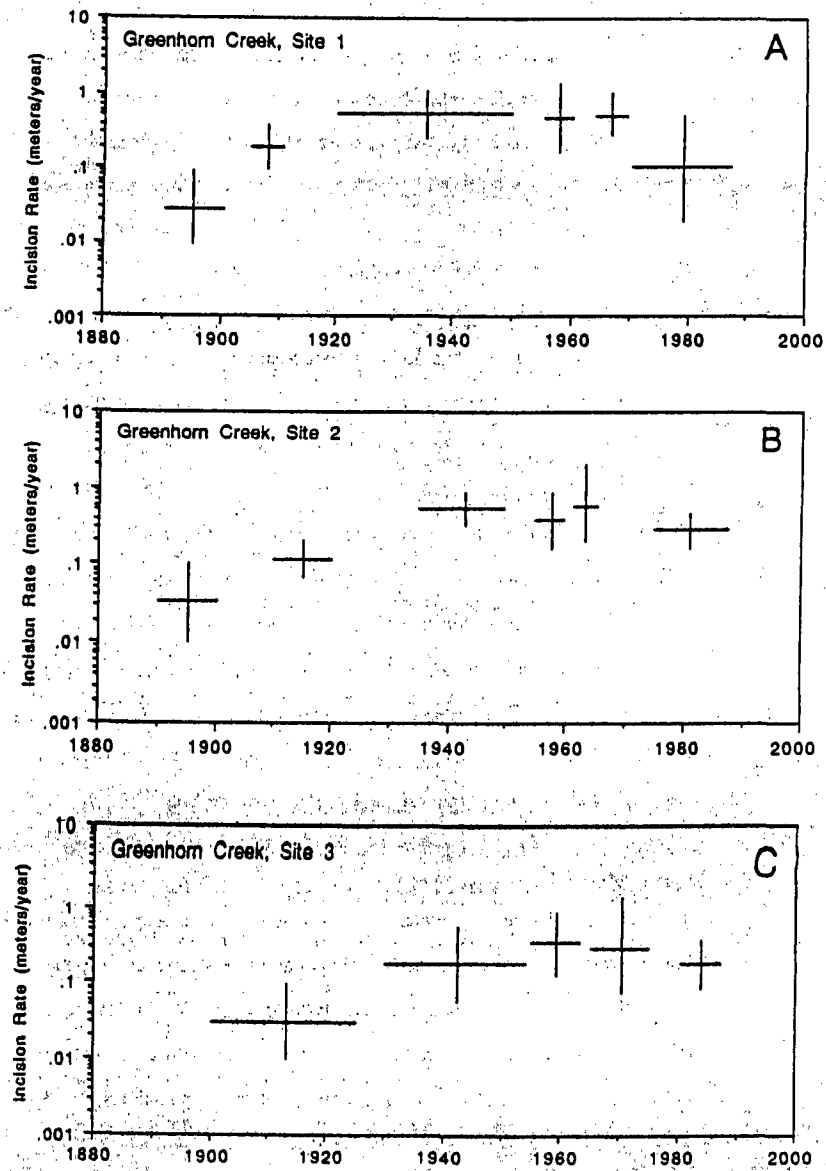


Figure 6.8. Temporal changes in incision rates from (A) upstream to (C) downstream reaches of Greenhorn Creek. Error bars indicate maximum and minimum age of terraces.

a maximum in about 1940 and declined relatively rapidly thereafter. Incision rates at the two sites farther downstream did not reach their peak until several decades later and appear to be declining, if they are declining at all, at slower rates than at the site upstream.

The downstream-progressing trend in degradation of the mining waste has been described in other streams of the Sierra Nevada foothills (Wildman, 1981) and is very similar to the trend described on Fall River in the preceding section. On Fall River, sites within the upstream part of the sediment storage zone reached a peak in degradation very early in their recovery period and sites further downstream were slower to respond. The streams of the Sierra Nevada have responded to the disposal of mining waste in similar fashion. The recovery of proximal channel reaches has been rapid while recovery of distal reaches has only recently begun. Rapid recovery in the proximal reaches of the Sierra Nevada streams is enhanced by their steep slope and because supply of sediment from upstream sources has diminished. Distal reaches of these streams have lower channel gradients, and recovery is slower because of the continued influx of sediment from upstream. Further, these headwater streams are confined within relatively narrow valleys and for a given discharge, can optimize stream power and sediment transport; in their distal reaches, these channels flow over broad, low-gradient valley floors that disperse flows over a much broader area and thereby reduce the efficiency of sediment transport.

6.3 A General Model for Recovery of Streams with High Sediment Loads

Channel recovery, whether expressed in terms of sediment transport, changes in bed elevation, or the adjustment of channel morphology cannot be adequately assessed without a knowledge of the frequency and magnitude of hydrologic events. In this section, a model for channel recovery is developed by considering the frequency of hydrologic events and the spatially-dependant flux of sediment as discussed above. The analysis uses data from streams that have been inundated with sediment in their headwaters and have subsequently been degrading, but it could also be applied to streams that have been scoured and are now in the process of filling. The analysis has potentially significant implications for studies of the fluvial response to high sediment loads that results from tectonism or climate change.

The preceding discussions of degradation on Fall River and on the Sierra Nevada streams illustrate that recovery rates depend partly on how frequently flows occur that are competent to move sediment. Assessing the frequency of sediment transport events would be a straightforward task on rivers with continuous sediment and water discharge records, but most streams lack this type of information, and gage records rarely span the full length of the recovery period. In the more common case where few data are available, the hydrologic and sediment transport characteristics of a recovering stream must be derived indirectly with the use of proxy hydrologic records and empirical sediment transport relations. The following analysis makes use of indirect methods and applies them to Fall River, the Sierra Nevada streams and several sites in the Redwood Creek Basin, northwestern California. At each of these sites, there is sufficient data to describe when these degrading streams reached a certain stage in their recovery.

Long-term hydrologic records were constructed for the ungaged sites using data from nearby gaging stations on rivers draining basins with similar hydrologic characteristics. Of the data that are available from a gage record, the flow duration curve, which expresses the percentage of time that flows within specified discharge classes are equalled or exceeded, is particularly useful in this analysis. The flow duration curves from the gaged sites were first converted to dimensionless form by dividing the flows in each discharge class by the mean annual flood. The nondimensional flow duration curves of the three stations that were used as proxies for the ungaged sites are given in Figure 6.9.

To use the non-dimensional flow duration curve at the ungaged sites then required that their mean annual flood be known. None of these sites are gaged however, so the mean annual flood was estimated with a regional regression equation that allows for computation of the T-year flood from climate and drainage basin characteristics (Waananen and Crippen, 1977). The mean annual flood was taken as the 2-year flood computed from this relation and the dimensionless flow duration curve was then be used to determine the percentage of time that a flow of given magnitude was equalled or exceeded at each of the ungaged sites.

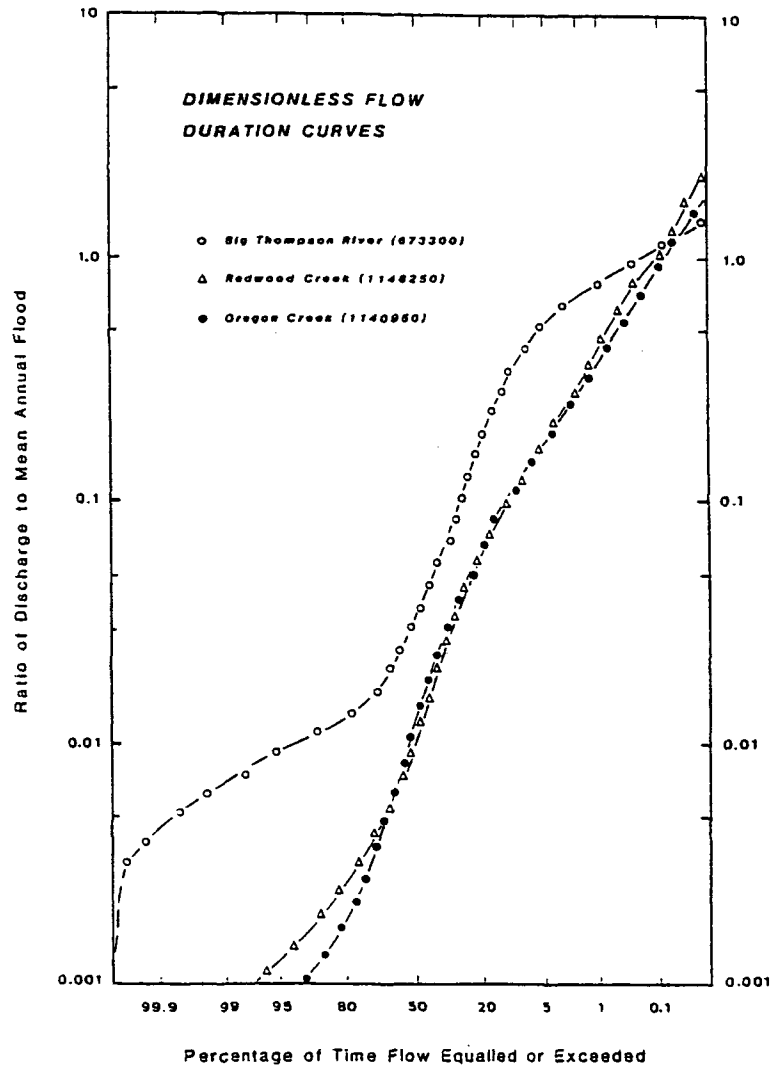


Figure 6.9. Non-dimensional flow duration curves used for determining the frequency of competent flows on (A) Fall River, (B) the Sierra Nevada streams, and (C) the tributaries of Redwood Creek.

In terms of the processes of channel recovery, the flows of interest are, of course, those that exceed the critical discharge for sediment transport. A number of empirical relations are available for estimating the critical conditions for sediment movement but the equation of Schoklitsch (Bathurst, et al., 1987) was best suited for this analysis because it does not require that a critical depth or a critical velocity be specified as in tractive force formulae. For a given discharge and channel width, the critical depth cannot be explicitly defined without knowing the flow velocity, or vice versa, so that the unique solution of a tractive force equation is not possible. At the ungaged sites, the only component of discharge that could be specified with any accuracy was the channel width. The Schoklitsch equation defines the critical condition in terms of unit discharge, (i.e. depth \times velocity) and by estimating the channel width from the cross section surveys, this equation could then be used to estimate the discharge required to move sediment of a given size on a given slope. The size of sediment available at the time when the bed was at a particular elevation was determined from samples of terrace sediments, and the reach slope was assumed to be the same as that of the present channel. At each site, the Schoklitsch equation was used in this way to compute the discharge required to move the median grain size during each of the time intervals defined by the ages of the upper and lower terrace surfaces or bed elevations. The data used to compute degradation rates, and the number of days that the critical discharge was exceeded during specified time intervals are listed for each site in Table 6.2.

This analysis makes use of some data with low resolution and several assumptions that are probably oversimplified. For example, the ages of the terraces along the Sierra Nevada streams are probably accurate to within no less than a decade because the trees that were used to date these surfaces probably did not get established until well after the surface was abandoned. The growth of vegetation on these surfaces is slow because the terrace sediments are well drained and are probably nutrient-poor. Another problem involves the choice of width in computing discharges because as these channels incised, their widths decreased significantly. In this analysis, the channel width during an interval of incision was taken as the average of the initial and final widths as defined by breaks in slope on the

Table 6.2 Summary data for recovery rates at selected sites on streams in Colorado and California

Reference No.	location	interval	years	change in width (m)	change in bed elevation (m)	degradation rate (m/yr)	D ₅₀ (mm)	Q _{crit} ⁽¹⁾ (m ³ /s)	Q _{crit} ⁽²⁾ / Q _{maf}	% time flow exceeded	days/yr exceeded
1	Fall River, XS 42	1984	1	0	0.64	0.640	2.0	0.3	0.0	48.0	175
2	Fall River, XS 54	1984-1985	2	0	0.04	0.020	5.5	4.0	0.54	5.0	18
3	"	1986-1987	2	0	0.35	0.175	8.0	7.0	0.94	0.8	3
4	Fall River, XS 57	1984-1985	2	0	0.21	0.105	1.0	0.4	0.06	40.0	146
5	"	1986-1987	2	0	0.20	0.100	2.0	1.2	0.16	23.0	84
6	Greenhorn Creek, 1	1901-1950	50	32	10.5	0.210	8.0	2.5	0.22	3.5	13
7	"	1951-1965	15	23	9.5	0.633	24	7.4	0.64	0.5	2
8	"	1966-1979	14	8	4.0	0.286	24	3.4	0.29	2.0	7
9	Greenhorn Creek, 2	1901-1940	40	50	15.0	0.375	8.0	9.3	0.75	0.3	1
10	"	1941-1960	20	26	4.5	0.225	24	24.0	1.94	0.02	0.1
11	"	1961-1987	27	5	6.5	0.241	24	11.5	0.93	0.2	1
12	Greenhorn Creek, 3	1901-1955	55	37	7.5	0.136	10	16.2	1.05	0.1	0.4
13	"	1956-1965	10	6	1.5	0.150	24	42.3	2.74	0.01	0.04
14	"	1966-1987	22	8	2.0	0.091	24	39.4	2.55	0.01	0.04
15	Greenhorn Creek, 4	1901-1970	70	8	4.0	0.057	10	11.4	0.56	0.6	2
16	"	1971-1987	17	6	1.5	0.088	24	38.0	1.86	0.02	0.1
17	Scotchman Creek, 2	1901-1960	60	6	2.0	0.033	0.8	0.2	0.03	34.0	124
18	"	1961-1965	5	2	2.0	0.400	4.0	1.8	0.27	2.5	9
19	"	1966-1987	22	16	1.3	0.059	46	2.4	0.37	1.3	5
20	Scotchman Creek, 3	1901-1965	65	1	3.0	0.046	0.5	0.1	0.01	52.0	190
21	"	1966-1975	10	8	0.5	0.050	4.0	1.5	0.21	4.0	15
22	"	1976-1987	12	0.1	0.2	0.017	6.0	2.4	0.34	1.6	6
23	Bridge Creek	1975-1976	1	5	0.7	0.740	34	9.7	0.32	1.4	5
24	"	1976-1986	10	3	0.9	0.090	34	13.8	0.45	0.65	2
25	Tbn McDonald Creek	1965-1969	4	4	1.3	0.333	45	18.5	0.93	0.1	0.4

(1) critical discharge for sediment transport as computed from the critical motion equation of Scholditsch.

(2) ratio of critical discharge to the mean annual flood; values of the mean annual flood were computed from regional regression equations.

terrace profiles. Finally, the number of days during a time interval that the critical discharge was exceeded was computed as the percent of time that the flow was exceeded multiplied by the length of the time interval and thus represents the "expected" number of days, rather than the actual number of days that the critical flow was exceeded. The actual number of days that the critical flow was exceeded during a time interval may have been greater or less than the expected number but this technique provided a means of computing the frequency of flows during periods when no discharge records were available.

Results: The results of this analysis are presented in Figure 6.10 with the data qualitatively distinguished on the basis of whether the sediment input to a reach remained high during a time interval or whether the sediment supply from upstream was low. At sites where the upstream supply of sediment was low (closed circles, Fig. 6.10), the rate of channel degradation increased as the frequency of the critical discharge increased. This is entirely as expected and reflects the ability of high gradient, proximal streams to evacuate sediment rapidly if it is fine grained and is in limited supply. At sites where the upstream supply of sediment was high (open circles, Fig. 6.10), the rate of degradation bears no relation to the number of days the critical discharge was exceeded. These sites are on low-gradient, distal reaches, and even though the sediment in the channel is relatively mobile, degradation has been minimal because the upstream sediment flux has remained high.

The importance of scale and sediment transport frequency can be illustrated by tracking the position of the sites on Greenhorn Creek as shown in Figure 6.10. Degradation at Site 1, the most upstream locality on Greenhorn Creek, has been relatively rapid because the sediment comprising the channel fill was transported several days per year (6-8, Fig. 6.10). Degradation at Site 2, the next locality downstream, has proceeded at lower rates than at the upstream site because the valley floor is wider and the critical discharge is exceeded only a few days per year (9-11, Fig. 6.10). Degradation at Site 3, still farther downstream, has proceeded at even lower rates (12-14, Fig. 6.10) because sediment transport occurs infrequently due to the reduced slope and increased valley width. At Site 4, the most

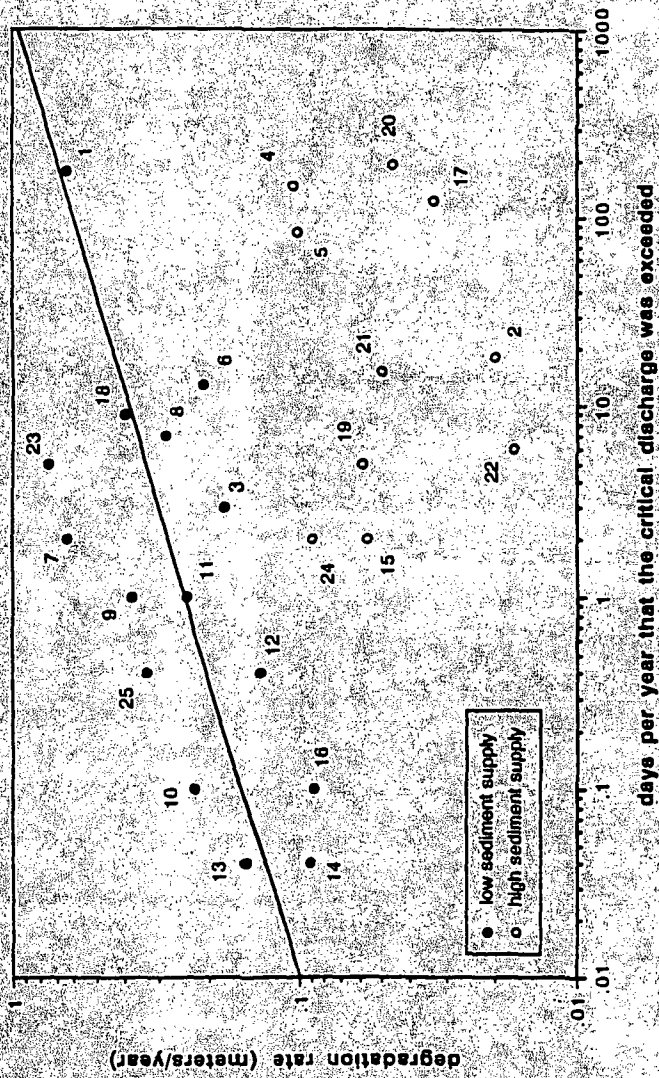


Figure 6.10. Degradation rate as a function of the exceedence of the critical discharge for sediment transport. Open circles indicate sites where continued sediment input from upstream sources prohibited degradation. Closed circles represent sites where sediment supply from upstream diminished rapidly and recovery proceeded thereafter at rates that depended on the frequency of flows that were competent to move sediment. Data are keyed to localities listed in Table 6.1

downstream locality on Greenhorn Creek, there has been minimal degradation even though flows that were competent to move the sand-sized sediment occurred relatively frequently (15, Fig. 6.10). The Fall River sites show a similar trend of rapid incision taking place in the proximal reaches where competent flows occurred frequently and sediment supply from upstream was low, moderate incision taking place in medial reaches with a gradually diminishing sediment supply, and little incision occurring in distal reaches where competent flows occurred very frequently, but sediment supply from upstream remained high.

These results can be used to formulate a general model of channel recovery that considers the spatial and temporal variability of sediment transport in channel subjected to high sediment loads from upstream sources. In this model, channel recovery is represented by the change in bed elevation (Δy) through time (Fig. 6.11). As discussed previously, and shown in the foregoing analysis, the point in time when channel recovery begins is scale dependent, and proximal reaches may respond faster than distal reaches. Recovery on a proximal reach inundated with fine-grained sediment begins almost immediately (Curve A, Fig. 6.11) and because this sediment is mobile at discharges that occur frequently, recovery is very rapid. Recovery on a distal reach does not occur until some time (Δt) later when the sediment supply from upstream wanes. Once initiated, recovery at the distal site will likely proceed at a slower rate than upstream because sediment transport occurs less frequently due to the reduced slope and greater channel width (Curve B, Fig. 6.11).

This semi-quantitative model was developed using data from degrading streams but could be applied equally well to rivers in the process of re-filling, or to channels that are adjusting their planforms. The point in time at which recovery begins at the site depends on the availability and proximity of upstream sources that can supply the site with sediment to remould its channel. From that point on, the rate at which planform or bed elevation adjustments take place is dependent partly on the flux of sediment from upstream, but also on the frequency of events that are competent to move the available sediment.

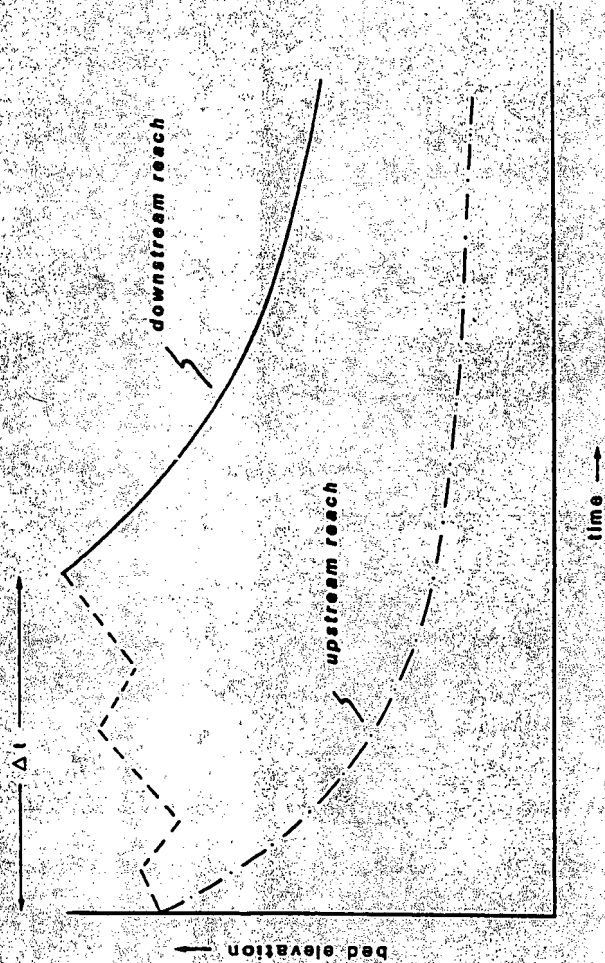


Figure 6.11. Conceptual model of changes in bed elevation as a function of time and location. Recovery begins almost immediately on a headwater stream (curve A); recovery on the downstream reach begins some later time (Δt) and thereafter proceeds at a slower rate than upstream because of continued influx of sediment from upstream reaches.

6.5 Summary

This chapter explored the concept of geomorphic recovery on rivers affected by large floods and catastrophic sediment inputs. The results of extensive field measurements on Fall River following the 1982 Lawn Lake flood in Rocky Mountain National Park indicate that sediment loads in upstream channel reaches returned to near-background levels within 5 years of the initial disturbance. The fine-grained sediment in these proximal reaches was quickly removed and transported to distal reaches of the study area where it has been conveyed at much slower rates. The sediment supplied to the distal reaches of Fall River is mobile much of the time but, because of the reduced slope, it moves at slower rates and the return to pre-flood conditions is delayed.

The spatial and temporal variability in recovery rates was examined at a much larger scale on streams in the Sierra Nevada, California that were severely impacted by the deposition of hydraulic mining waste in their valley bottoms. Since the late 1800's, these streams have incised into the mining debris at rates that decrease in the downstream direction. The mine tailings have been rapidly eroded from headwater reaches because the supply of sediment from upstream sources diminished soon after mining stopped. Degradation rates in proximal reaches probably reached their maximum several decades into the recovery period when the particular combination of channel width and sediment size optimized sediment transport. The mine tailings have been eroded more slowly from distal reaches because of the continued influx of sediment from upstream and because channel width increases and valley slope decreases thereby reducing the efficiency of sediment transport in the downstream direction.

Finally, a general model was presented to show that, at any given location, a river will recover from the effects of a flood or a catastrophic sediment input at rates that will vary depending on (1) the magnitude of the initial perturbation, (2) the rate at which sediment is supplied from upstream, and (3) the frequency of flows in subsequent years that are competent to move the available sediment.

CHAPTER VII

SUMMARY AND CONCLUSIONS

In attempting to bring together data and observations from many different rivers, this study represents a significant departure from previous lines of research in flood geomorphology. This study is the first to quantitatively integrate a large number of hydrologic and geologic factors that influence the geomorphic effectiveness of large floods. The effort is by no means exhaustive, but it addresses the importance of rare floods in the context of their exceedence of more frequent hydrologic events, as well as their ability to overcome the resistance offered by a river's morphology and perimeter sediments. To restate, the specific objectives of this study were:

- (1) to consider the flood frequency characteristics of different climatic regimes,
- (2) to assess the geomorphic effects that floods have on coarse-bed streams and to determine what factors were most important in explaining the response,
- (3) to examine the relationship between the frequency of coarse sediment transport and the morphology of high gradient streams and,
- (4) to address channel recovery processes following large floods or sediment inputs.

The rivers examined are primarily high-gradient, coarse-bed streams draining small to intermediate size basins ($< 1,000 \text{ km}^2$) in mountainous areas of Colorado and northern California. These study regions represent a wide spectrum of climatic regimes where floods are generated by localized thunderstorms, large-scale frontal storms, and snowmelt runoff. The results of the study are briefly summarized below.

7.1 Flood Frequency Characteristics

Floods are the result of hydrologic processes that vary in scale and intensity depending on the climatic characteristics of a region. Floods that occur in climatic regimes where precipitation and runoff is widely distributed over time and space are not large relative to "normal" hydrologic events. Thus, peak flows on the snowmelt-fed streams draining the Alpine Region of the Colorado Front Range fall within a narrow range of discharges and the 100-year flood is less than twice the mean annual flood (Fig. 3.4). However, the localized nature of precipitation in semi-arid regions such as the Foothills of the Colorado Front Range results in highly variable streamflow and a 100-year flood may be 10-times larger than the mean annual flood (Fig. 3.4). Precipitation in the mountainous areas of California may also be very intense but runoff is slower and more spatially-distributed so that floods have magnitudes intermediate to those produced by snowmelt or thunderstorms.

Floods in the regions studied here appear to bear little or no relation to the morphometric characteristics of drainage basins. In the semi-arid Foothills Region of Colorado, drainage basins have thin, rocky soils and abundant bedrock exposures. Although runoff is rapid and relief is high, hillslopes in this region are not highly susceptible to erosion and do not have fine textured drainage networks because they are comprised of bedrock and coarse-grained soils. In the humid environments of northern California, much of the rainfall may be routed to channels as subsurface storm flow because soils are relatively permeable. As a result of this process, precipitation can be very intense in this region, but flood peaks may not be extraordinarily high. Transient runoff process (variable source areas, after Dunne, 1978), may also contribute to the flood characteristics in northern California. These runoff processes involve little surficial erosion however, and may not manifest themselves as part of the channel network. Thus in humid, high relief environments, like those of northern California, drainage basin characteristics may provide limited evidence for the geomorphic importance of rare hydrologic events.

7.2 Geomorphic Effects of Floods

The geomorphic effects of floods were assessed using discharge, grain size and cross section data from 25 sites in California and Colorado that recently experienced large floods. These floods were not exceptional in terms of their discharge per unit drainage area or in terms of their unit stream power but, in many cases, significant geomorphic changes took place. The complex reasons for these changes were explained in terms of the local conditions of channel morphology, flow resistance and sediment transport.

Many of the sites experienced no significant change as the result of floods that were several times larger than a mean annual flood and it was suggested that mountain streams may be in adjustment with these rare events. The conditions that led to scour, fill, or changes in channel width at other sites depended on the local channel gradient, sediment size and floodplain width (Fig. 4.7). Channel scour occurred on high gradient reaches where the flood greatly exceeded the mean annual flood. Sites with intermediate gradients, gravel-sized bed material, and wide valley floors experienced lateral erosion. Deposition occurred at sites with low gradients and high sand and gravel sediment loads.

A detailed analysis of the relationship between flow resistance and channel changes showed that the hydraulic and sediment transport conditions of floods cannot be simply represented. In streams with bouldery sediments and low relative submergence of the bed, much of the total shear stress is unavailable for sediment movement due to spill resistance induced by large boulders. As a result, floods on high gradient ($> 1\%$) streams may entrain sediment far smaller than would be predicted with available competence relations. Floods on low gradient rivers are generally deeper and the total flow resistance is lower because of the high relative submergence of the bed. However, the bed forms associated with high sediment loads may reduce the proportion of shear stress available for sediment transport and aggradation occurs (Fig. 4.11). Both conditions commonly occur in floods but they have generally not been accounted for in previous studies.

7.3 Magnitude and Frequency of Coarse Sediment Transport

Indirect evidence for the geomorphic effectiveness of large floods was provided by an analysis of the magnitude and frequency of coarse sediment transport on high gradient rivers. Using an empirical sediment transport equation and the flow frequency characteristics of 7 gaging stations in northern California, the discharge that was most effective for transporting bed material was found to be an increasingly rare event as the channel gradient and size of the bed material increased. The return period of the effective discharge was less than 2 years on rivers with fine-gravel beds and channel slopes much less than 1% but exceeded the length of the gage record on a boulder bed river with a 2% slope (Fig. 5.5). These results and the discussion of large particle movement in the preceding chapter suggest that, in high gradient rivers, only the largest flows are capable of moving the bed material.

The discharge that is most effective for bed material transport is often very different from the bankfull discharge in high gradient, cobble-bed rivers. It was suggested that the morphology of many high gradient rivers is relict from past floods of extraordinary return period that have extensively reworked the valley floor. Large floods produce low-flow channels that, by coincidence, may be filled to the bankfull capacity by more common events (Fig. 5.6). It would be erroneous in these cases to assume that the "bankfull" flows are the dominant or channel forming events.

These results do not refute the findings of previous workers but suggest that the magnitude and frequency concept proposed by Wolman and Miller (1960) is not readily applied to high gradient rivers with bed material that is mobilized only during rare floods. Further, if rare floods do not greatly exceed the mean annual flood as in the case of snowmelt-fed rivers, then it is possible that nothing short of a climate change or greatly different runoff and sediment transport regimes will effect the morphology of these high gradient rivers.

7.4 Geomorphic Recovery From the Effects of Floods

Rivers that have been affected by large floods and catastrophic sediment inputs recover at rates that vary depending on the frequency of competent flows and the location of the site relative to active sediment source areas. The results of extensive field measurements on Fall River following the 1982 Lawn Lake flood in Rocky Mountain National Park indicate that the initially high sediment loads in the upstream reaches of Fall River declined nearly to background levels in 5 years (Fig. 6.3). The fine-grained sediment in these proximal reaches was quickly removed and transported to distal reaches of the study area where it has been conveyed at much slower rates. Fall River discharges are competent to move this sand-sized sediment much of the time but, because of the reduced slope, it moves at slower rates and the return to pre-flood conditions in the downstream reaches has been delayed.

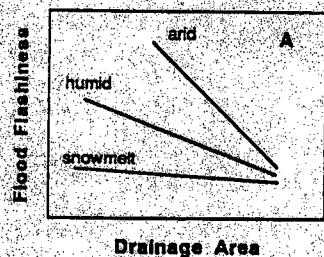
Streams in the Sierra Nevada have responded to the deposition of hydraulic mining waste in their valley bottoms in ways that are similar to Fall River. Since the late 1800's, these streams have incised into the mining debris at rates that decrease in the downstream direction. Tens-of-meters of mine tailings have been eroded from the headwater reaches of these streams and they are now flowing on their former beds. Incision was rapid in headwater reaches because the supply of sediment from upstream diminished soon after mining stopped and flows that were competent to move the mining debris occurred frequently thereafter (Fig. 6.8). The mine tailings have been eroded more slowly from distal reaches because of continued sediment supply from upstream, because the down-valley increase in width allows for sediment storage, and because the channel slope is lower thereby reducing the efficiency of sediment transport. Therefore, at any given location, a river will recover from the effects of a flood or a large sediment input at rates that will vary depending on (1) the magnitude of the initial perturbation, (2) the rate at which sediment is supplied from upstream, (3) the sediment storage potential of the reach, and (4) the frequency of flows in subsequent years that are competent to move the available sediment (Fig. 6.11).

7.5. Summary

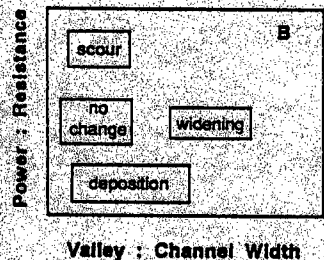
The flood-induced geomorphic responses of rivers are partly explained by large-scale factors of basin size, relief, climate, geology, and vegetation. This study has verified the important effects of scale and climate as emphasized by Baker (1977) and Wolman and Gerson (1978). More importantly, the results of this study can be used to set approximate limits for where the effects of scale and climate are most important for understanding flood magnitudes, the geomorphic changes brought about by floods, and the post-flood recovery processes. The effects of scale can be explored through the variables of drainage basin area, channel slope, and sediment size, while the effects of climate can be explored through variables that account for the amount and areal distribution of runoff. The combined interaction of these factors are discussed below with the aid of Figure 7.1.

High magnitude floods (say those that exceed the mean annual flood by a factor of 5 or more) occur in smaller drainage basins, and this effect of scale is most important in climates where single rainfall events produce more than about 10% of the total annual precipitation. The areal distribution and intensity of rainfall are less important in basins much larger than about 1,000 km² (Fig. 7.1a), because at that scale, hydrologic processes are attenuated.

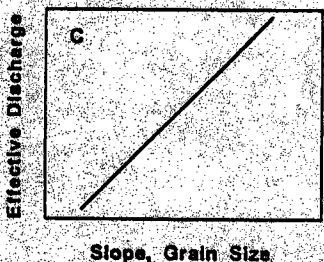
The geomorphic responses to floods are also climate- and scale-dependent (Fig. 7.1b). Climate controls the amount of runoff and the degree of weathering or sediment availability; channel slope and sediment size are scalar variables that influence the ratio between driving and resisting forces. High-gradient streams that drain small basins may withstand erosion by all but the largest floods because their beds are very coarse, and because more easily-eroded sediment is available only in discontinuous floodplains and terraces. This may be particularly true in arid climates where slower weathering rates and shallow soils limit the availability of sediment which, in more temperate climates, provides the potential for a more catastrophic geomorphic response. These conclusions are at odds with those of Baker (1977) and Wolman and Gerson (1978) who perhaps placed more emphasis on the controls that climate exerted on flood magnitude than on sediment availability.



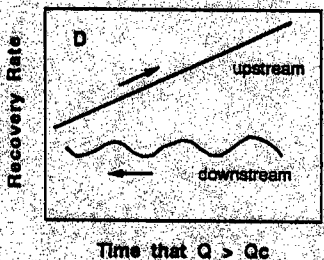
Both climate and scale control the intensity of rainfall and the magnitude of runoff.



Climate controls runoff intensity and sediment availability; the effect of scale is represented by slope, sediment size and channel dimensions.



Climate controls the magnitude and frequency of flows; sediment transport scaled by grain size and slope.



Climate controls the availability of sediment and frequency of flows; sediment transport scaled by grain size, slope and channel dimensions

Figure 7.1. Summary of the effects of scale and climate on (A) flood variability, (B) channel changes, (C) sediment yield, and (D) channel recovery.

The amount of coarse sediment yielded by a river is clearly dependent on the scale of the river as represented by either bed material size or the slope of the channel (Fig. 7.1c). Only the larger magnitude floods are capable of exceeding the thresholds for sediment transport in high gradient streams. Not only are larger magnitude floods more likely in small drainage basins, but these flows may dominate the long-term sediment yield of a small basin. Therefore, the slope of the channel and size of the bed material may be wholly in adjustment with these infrequent events. In terms of coarse sediment yield, climate enhances the effects of scale because a 5-year flood is equivalent in magnitude, and may yield as much sediment from a small, semi-arid basin, as a 50-year flood yields from a larger, humid region basin.

Lastly, the effects of scale and climate clearly influence the recovery of channels affected by large floods or sediment inputs, but perhaps not in the manner suggested by Wolman and Gerson (1978). These authors suggested that small-size or arid region streams would recover more slowly because hydrologic and geomorphic processes were more episodic therein. This conclusion overlooks the fact that intensity and degree of weathering is greater in humid climates, which therefore, causes a greater susceptibility for the catastrophic introduction of sediment from hillslopes. The present study is somewhat biased in this sense, but the results presented earlier clearly demonstrate the need to account for large sediment inputs in headwater areas, that because they propagate downstream, will lead to slower recovery rates with increasing scale. In this case, the time when recovery begins is scale-dependent, with the recovery beginning very soon after the initial perturbation in headwater streams and at a much later time in downstream river reaches (Fig. 7.1d). Both scale and climate determine the rate at which recovery proceeds because the frequency of sediment transport is a function of both scalar factors, such as grain size or channel slope, and climatic factors that determine the flow frequency characteristics of the stream (Fig. 7.1d).

7.4 Future Work

This research has focused on the general topics of flood hydrology, hydraulics, sediment transport, and channel recovery. In addition to our general understanding of floods and their geomorphic effects, this research has raised a number of important issues that merit further study.

This study was unable to establish a strong link between floods and drainage basin characteristics, but clearly, such a link must exist between the climatic processes that generate precipitation and the hillslope and channel processes that transmit runoff. Simply stated, "where does the water go?" The measurement scales used in this study were conventional, but perhaps too coarse to discern true process links. The topography and morphometry of drainage basins may be more adequately, and more easily represented by digital terrain models. The spatial and temporal heterogeneity of rainfall and antecedent soil moisture conditions may be more accurately resolved at the watershed scale using "real time" satellite imagery. When combined with field experiments and ground verification, remotely-sensed data may ultimately provide the quickest and most accurate information on the hydrologic and physical conditions that lead to the generation of a large flood.

This study did not rigorously account for the fact that a river's response to a large flood depends on the upstream supply or storage of sediment. As numerous "sediment budget" studies have shown, quantifying the amount of erosion or deposition at the basin-wide scale is by no means a simple task. However, future studies in flood geomorphology might account for upstream sediment inputs indirectly through proxy variables describing the amount of upstream disturbance of hillslopes or channels. For example, by examining pre- and post-flood aerial photographs, the length of stream channel affected by landslides could be quantified, or the amount of bottomland vegetation that was disturbed by bank erosion could be measured. These measurements would provide indirect, but perhaps, meaningful indices of the amount disturbance upstream of a site while avoiding the laborious task of gathering such data in the field.

Much of our current understanding of river hydraulics and sediment transport is derived from empirical studies conducted under moderate or even low-flow conditions. The results of this study clearly indicated a potential for gross error when applying relations that were developed under flow and sediment transport conditions that are very different from those experienced during floods. The difficulty of making streamflow measurements during floods will likely preclude the field as the most productive avenue for future research. The effects of high sediment loads and flow resistance can be partly accounted for theoretically, and through the use of proxy variables. Carefully controlled flume experiments could also be used to explore the relative importance of high Reynolds numbers, high bed material loads, and large channel bed undulations, all of which have the effect of increasing the total resistance to flow. Using a fixed bed of coarse sediment, the different elements of flow resistance could be adjusted incrementally, and their additive influence could be measured.

A general model for channel recovery was presented that accounted for the lag time between when a disturbance occurred and when the channel began to restore its pre-event condition. No useful criteria were presented for establishing the scale of this lag time although it was suggested that it was distance dependent. Disturbances that propagate in a downstream direction are relatively common (e.g. deforestation caused by fire or land use, volcanic catastrophes, etc.), and a scaling criterion would be most useful if the general model were to be applied to a large-scale disturbance such as a glaciation. The surfaces used to date glacial events are often assumed to be time-equivalent but the results of this and other studies have demonstrated that this is unlikely to be true in systems with high sediment loading in their headwaters. To what extent this presents a problem for Quaternary studies is unknown, but if the lag time is of the same order as the interglacial time period, then correlation between glacial units will be highly suspect.

REFERENCES

- Abrahams, A.D., 1984. Channel networks: a geomorphological perspective, *Water Resources Research*, v. 20, p. 161-188.
- Abrahams, A.D., and Ponczynski, J.J., 1984. Drainage density in relation to precipitation intensity in the U.S.A., *Journal of Hydrology*, v. 75, p. 383-388.
- Anderson, M.G. and Calver, A., 1977. On the persistence of landscape features formed by a large flood, *Transaction of the Institute of British Geographers, New Series*, v. 2, p. 243-254.
- Andrews, E.D., 1980. Effective and bankfull discharge of streams in the Yampa River Basin, *Journal of Hydrology*, v. 46, p. 311-330.
- Andrews, E.D., 1983. Entrainment of gravel from naturally sorted riverbed material, *Geological Society of America Bulletin*, v. 94, p. 1225-1231.
- Ashida, K. and Bayazit, M. 1973. Initiation of motion and roughness of flows in steep channels, *Proceedings, 15th Congress of the International Association for Hydraulic Research*, Istanbul, Turkey, v. 1, p. 475-484.
- Ashmore, P.E. and Day, T.J., 1988. Effective discharge for suspended sediment transport in streams of the Saskatchewan River Basin, *Water Resources Research*, v. 24, p. 864-870.
- Bagnold, R.A., 1966. An approach to the sediment transport problem from general physics, *U.S. Geological Survey Professional Paper 422-I*, 37 pp.
- Baker, V.R., 1977. Stream channel response to floods, with examples from central Texas, *Geological Society of America Bulletin*, v. 88, p. 1057-1071.
- Baker, V.R. and Ritter, D.F., 1975. Competence of rivers to transport coarse bedload material, *Geological Society of America Bulletin*, v. 86, p. 975-978.
- Baker, V.R. and Costa, J.E., 1987. Flood power, in Mayer, L. and Nash, D. (eds), *Catastrophic Flooding*. Allen & Unwin, Boston, p. 1-21.
- Bateman, P.C. and Wahrhaftig, C., 1966. Geology of the Sierra Nevada, in Baily, E.H. (ed), *Geology of Northern California, California Division of Mines and Geology Bulletin 190*, p. 107-171.
- Bathurst, J.C., 1982. Flow resistance in boulder-bed streams, in Hey, R., Bathurst, J.C. and Thorne, C.R. (eds), *Gravel-bed Rivers*. Wiley & Sons, New York, p. 443-465.
- Bathurst, J.C., Graff, W.H. and Cao, H.H., 1987. Bed load discharge equations for steep mountain rivers, in Thorne, C.R., Bathurst, J.C. and Hey, R.D. (eds), *Sediment Transport in Gravel-Bed Rivers*, John Wiley and Sons, New York, p. 453-491.
- Benson, M.A., 1964. Factors affecting floods in the Southwest, *U.S. Geological Survey Water Supply Paper 1580-D*, 72 pp.
- Benson, M.A. and Thomas, D.M., 1966. A definition of dominant discharge, *International Association of Hydrologic Sciences Bulletin*, v. 11, p. 76-80.
- Best, D. W., 1984. Land-use in the Redwood Creek Basin, *Redwood National Park Technical Report No. 9*, 24 pp.
- Beschta, R.L., 1983. Long-term changes in channel widths of the Kowai River, Torlesse Range, New Zealand, *Journal of Hydrology (N.Z.)*, v. 22, p. 112-122.
- Blair, T.C., 1987. Sedimentary processes, vertical stratification sequences and geomorphology of the Roaring River alluvial fan, Rocky Mountain National Park, Colorado, *Journal of Sedimentary Petrology*, v. 57, p. 1-18.
- Brown, W.M. and Ritter, J.R., 1971. Sediment transport and turbidity in the Eel River Basin, California, *U.S. Geological Survey Water Supply Paper 1968*, 67 pp.
- Bull, W.B., 1979. Threshold of critical power in streams, *Geological Society of America Bulletin*, v. 90, p. 453-464.
- Burkham, D.E., 1972. Channel changes of the Gila River in Safford Valley, Arizona, 1846-1970, *U.S. Geological Survey Professional Paper 655-G*, 24 pp.
- Carling, P. A. 1983. Threshold of coarse sediment transport in broad and narrow natural streams, *Earth Surface Processes and Landforms*, v. 8, p. 1-18.
- Carlston, C.W., 1963. Drainage density and streamflow, *U.S. Geological Survey Professional Paper, 422-C*, p.1-8
- Carlston, C.W. and Langbein, W.F., 1960. Rapid approximation of drainage density: line intersection method, *U.S. Geological Survey Water Resources Bulletin 11*
- Carson, M.A. and Griffiths, G.A., 1985. Tractive stress and the onset of bed particle movement in gravel stream channels: different equations for different purposes, *Journal of Hydrology*, v. 79, p. 375-388.
- Chorley, R.J. and Morgan, M.A., 1962. Comparison of morphometric features, Unaka Mountains, Tennessee and North Carolina, and Dartmoor, England, *Geological Society of America Bulletin*, v. 73, p. 17-34.
- Chorley, R.J., Schumm, S.A. and Sugden, D.E., 1985. *Geomorphology*. Methuen & Co., New York, 605 pp.
- Collins, B.D. and Dunne, T., 1986. Erosion of tephra from the 1980 eruption of Mount St. Helens, *Geological Society of America Bulletin*, v. 97, p. 896-905.
- Costa, J.E., 1983. Paleohydraulic reconstruction of flash-flood peaks from boulder deposits in the Colorado Front Range, *Geological Society of America Bulletin*, v. 94, p. 986-1004.
- Costa, J.E., 1987. Hydraulics and basin morphometry of the largest flash floods in the conterminous United States, *Journal of Hydrology*, v. 93, p. 313-338.
- Dalrymple, T. and Benson, M.A., 1967. Measurement of peak discharge by the slope area method, *U.S. Geological Survey Techniques in Water Resources Investigations 3*, Chapter A2, 12 pp.
- Dietrich, W.E., Wilson, C.J., and Reneau, S.L., 1986. Hollows, colluvium and landslides in soil-mantled landscapes, in Abrahams, A.D. (ed), *Hillslope Processes*. Allen and Unwin, Boston, p.361-388.
- Dunne, T., 1978. Field studies of hillslope flow processes, in Kirkby, M.J., (ed) *Hillslope Hydrology*. Wiley-Interscience, New York, p. 227-293.
- Einstein, H.A., 1950. The bed load function for sediment transport in open channel flows, *Technical Bulletin 1026, U.S. Department of Agriculture*
- Elliott, J.G., Jarrett, R.D. and Ebling, J.L., 1982. Annual snowmelt and rainfall peak flow data on selected foothills region streams, South Platte River, Arkansas River and Colorado River Basins, Colorado, *U.S. Geological Survey Open-File Report 82-426*, 86 p.
- Fahnestock, R.K., 1963. Morphology and hydrology of a glacial stream- White River, Mt. Rainier, Washington, *U.S. Geological Survey Professional Paper 422-A*, 70 pp.
- Freeze, R.A., 1980. A stochastic-conceptual analysis of rainfall-runoff processes on a hillslope, *Water Resources Research*, v. 16, p. 391-408.
- Gilbert, G.K., 1917. Hydraulic mining debris in the Sierra Nevada, *U.S. Geological Survey Professional Paper 105*, 154 pp.
- Giancy, P.A. and Harmsen, L., 1975. A hydrologic assessment of the September 14, 1974 flood in Eldorado Canyon, Nevada, *U.S. Geological Survey Professional Paper 930*
- Gregory, K.J., 1976. Drainage networks and climate, in Derbyshire, E. (Ed), *Climatic Geomorphology*. MacMillan, London, p. 289-315.
- Graf, W.A., 1983. Downstream changes in stream power in the Henry Mountains, Utah, *Annals, Association of American Geographers*, v. 73, p. 373-387.
- Griffiths, G.A., 1979. Recent sedimentation history of the Waimakariri River, New Zealand, *Journal of Hydrology (N.Z.)*, v. 18, p. 6-28.

- Hack and Goodlett, 1960. Geomorphology and forest ecology of a mountain region in the central Appalachians, *U.S. Geological Survey Professional Paper 347*, 66 pp.
- Hadley, R.F. and Schumm, S.A., 1961. Sediment sources and drainage-basin characteristics in the upper Cheyenne River basin, *U.S. Geological Survey Water Supply Paper 1531-B*, p. 157-196.
- Hardin, D.R., Janda, R.J. and Nolan, K.M., 1978. Mass movement and storms in the drainage basin of Redwood Creek, Humboldt County, California: A progress report, *U.S. Geological Survey Open File Report 78-486*, 161 pp.
- Harvey, A.M., 1984. Geomorphic response to an extreme flood: a case from southeast Spain, *Earth Surface Processes*, v. 9, p. 267-279.
- Harvey, M.D., Pitlick, J., and Hagans, D.K., 1987. Adjustments of point bar morphology during a snowmelt runoff period, *EOS, Transactions, American Geophysical Union*, v. 68, p. 1297.
- Hey, R.D., 1978. Determinate hydraulic geometry of river channels, *Journal of the Hydraulics Division, American Society of Civil Engineers*, v. 104, p. 869-885.
- Hey, R.D., 1979. Flow resistance in gravel-bed rivers, *Journal of the Hydraulics Division, American Society of Civil Engineers*, v. 105, p. 365-379.
- Hickey, J.J., 1969. Variations in low-water streambed elevations at selected gaging stations in northwestern California, *U.S. Geological Survey Water Supply Paper 1879-E*, 33 pp.
- Horton, R.E., 1933. The role of infiltration in the hydrologic cycle, *Eos, Transactions of the American Geophysical Union*, v. 14, p. 446-460.
- Horton, R.E., 1945. Erosional development of streams and their drainage basins: Hydrophysical approach to quantitative morphology, *Geological Society of America*, v. 56, p. 275-370.
- Hosking, J.R.M. and Wallis, J.R., 1986a. Paleoflood hydrology and flood frequency analysis, *Water Resources Research*, v. 22, p. 543-550.
- Hosking, J.R.M. and Wallis, J.R., 1986b. The value of historical data in flood frequency analysis, *Water Resources Research*, v. 22, p. 1606-1612.
- Huber, N.K., 1981. Amount and timing of late Cenozoic uplift and tilt of the central Sierra Nevada, California - evidence from the upper San Joaquin River Basin, *U.S. Geological Survey Professional Paper 1197*, 28 pp.
- Hubbell, D.W., 1987. Bed load sampling and analysis, in Thorne, C.R., Bathurst, J.C. and Hey, R.D. (eds), *Sediment Transport in Gravel-Bed Rivers*, Wiley & Sons, New York, p. 89-105.
- Irwin, W.P., 1966. Geology of the Klamath Mountains Province, *California Division of Mines and Geology Bulletin*, v. 190, p. 19-38.
- Jarrett, R.D. and Costa, J.E., 1986. Hydrology, geomorphology and dam-break modeling of the July 15, 1982 Lawn Lake Dam and Cascade Lake Dam failure, Larimer County, Colorado, *U.S. Geological Survey Professional Paper 1369*, 78 pp.
- Jarrett, R.D., 1983. Hydraulics of high-gradient streams, *Journal of the Hydraulics Division, American Society of Civil Engineers*, v. 110, p. 1519-1539.
- Jarrett, R.D., 1987a. Errors in slope-area computations of peak discharges in mountain streams, *Journal of Hydrology*, v. 96, p. 53-67.
- Jarrett, R.D., 1987b. Flood hydrology of foothill and mountain streams in Colorado, unpublished Ph.D. dissertation, Colorado State University, Fort Collins, 239 pp.
- Judson, S.R. and Ritter, D.F., 1964. Rates of regional denudation in the United States, *Journal of Geophysical Research*, v. 69, p. 3395-3401.
- Kelsey, H.M., 1980. A sediment budget and an analysis of geomorphic process in the Van Duzen River Basin, northcoastal California, 1941-1975, *Geological Society of America Bulletin*, v. 91, p. 1119-1216.
- Kelsey, H.M., Coghlan, M., Pitlick, J., Best, D. Geomorphic analysis of streamside landsliding in the Redwood Creek basin, in Nolan, K.M., Kelsey, H.M. and Marron, D.C. (eds), Geomorphic processes and aquatic habitat in the Redwood Creek basin, Northwestern California, *U.S. Geological Survey Professional Paper 1454*, (in press)

- Kirby, W.H., 1987. Linear error analysis of slope-area discharge determinations, *Journal of Hydrology*, v. 96, p. 125-138.
- Kircher, J.E., Choquette, A.F. and Richter, B.D., 1985. Estimation of natural streamflow characteristics in western Colorado, *U.S. Geological Survey Water Resources Investigations Report 85-4086*, 28 pp.
- Kochel, R.C., and Johnson, R.A., 1984. Geomorphology and sedimentology of humid-temperate alluvial fans, central Virginia, in Koster, E.H. and Steele, R.J. (eds), *Sedimentology of Gravels and Conglomerates*, Canadian Society of Petroleum Geologists Memoir 10, p. 109-122.
- Kochel, C.R., Baker, V.R., and Patton, P.C., 1982. Paleohydrology of Southwestern Texas, *Water Resources Research*, v. 18, p. 1165-1183.
- Komar, P.D., 1987. Selective gravel entrainment and the empirical evaluation of flow competence, *Sedimentology*, v. 34, p. 1165-1176.
- Leopold, L.B. and Wolman, M.G., 1960. River Meanders, *Geological Society of America Bulletin*, v. 71, p. 769-794.
- Leopold, L.B., Bagnold, R.A., Wolman, M.G., and Brush, L.M., 1960. Flow resistance in sinuous or irregular channels, *U.S. Geological Survey Professional Paper 282-D*, p. 111-135.
- Leopold, L.B., Wolman, M.G. and Miller, J.P., 1964. *Fluvial Processes in Geomorphology*, Freeman, San Francisco, 522 pp.
- Limerinos, J.T. 1970. Determination of the Manning coefficient from measured bed roughness in natural channels, *U.S. Geological Survey Water Supply Paper 1898-B*, 45 pp.
- Lisle, T.E., 1982. Effects of aggradation and degradation on pool-riffle morphology in natural gravel channels, northwestern California, *Water Resources Research*, v. 18, p. 1643-1651.
- Lustig, L.K., 1965. Sediment yield of the Castaic watershed, western Los Angeles County, California - a quantitative geomorphic approach, *U.S. Geological Survey Professional Paper 422-F*, 23 pp.
- Madej, M.A., 1984. Recent changes in channel-stored sediment, Redwood Creek, California, *Technical Report 11*, Redwood National Park, Arcata, California, 54 pp.
- Maddock, T., 1970. Indeterminate hydraulics of alluvial channels, *Journal of the Hydraulics Division, American Society of Civil Engineers*, v. 96, p. 2309-2323.
- Madole, R.F. and Shroba, R.R., 1979. Till sequence and soil development in the North St. Vrain Drainage Basin, east slope, Front Range, Colorado, in Etridge, F.G. (ed), *Field Guide for the Northern Front Range and Northwest Denver Basin, Colorado, Geological Society of America, Rocky Mountain Section, Spring Meeting*, May, 1979, Fort Collins, p. 123-178.
- McCain, J.F., Hoxit, L.R., Maddox, R.A., Chappell, C.F. and Caracena, F. 1979. Storm and flood of July 31-August 1, 1976, in the Big Thompson River and Cache la Poudre River basins, Larimer and Weld Counties, Colorado, *U.S. Geological Survey Professional Paper 1115, Part A*, 82 pp.
- Mathai, H.F., 1969. Floods of June, 1965 in South Platte River Basin, Colorado, *U.S. Geological Survey Water Supply Paper 1850-B*, 64 pp.
- Meyer-Peter, E. and Müller, R., 1948. Formulas for bed-load transport, *Proceedings of the International Association of Hydraulic Research, 3rd Annual Conference, Stockholm*, p. 39-64.
- Milhou, R.T., 1973. Sediment transport in a gravel-bottomed stream, unpublished Ph.D. thesis, Oregon State University, Corvallis, Oregon, 232 pp.
- Nanson, G.M., 1986. Episodes of vertical accretion and catastrophic stripping: a model of disequilibrium flood-plain development, *Geological Society of America Bulletin*, v. 97, p. 1467-1475.
- Nanson, G.M. and Hickin, E.J., 1986. A statistical analysis of bank erosion and channel migration in western Canada, *Geological Society of America Bulletin*, v. 97, p. 497-504.

- Newson, M.D., 1978. Drainage basin characteristics, their selection, derivation and analysis for a flood study in the British Isles, *Earth Surface Processes*, v. 3, p. 277-293.
- Newson, M.D., 1980. The geomorphological effectiveness of floods- a contribution stimulated by two recent events in Mid-Wales, *Earth Surface Processes*, v. 5, p. 1-16.
- Nolan, K.M., Lisle, T. E. and Kelsey, H.M., 1987. Bankfull discharge and sediment transport in northwestern California, *Erosion and Sedimentation in the Pacific Rim*, International Association of Hydrologic Sciences Special Publication 165, p. 439-449.
- Osterkamp, W.R. and Costa, J.E., 1987. Changes accompanying an extraordinary flood on a sand-bed stream, in Mayer, L. and Nash, D. (eds), *Catastrophic Flooding*. Allen & Unwin, Boston, p. 201-224.
- Paine, A.D.M., 1984. Canyon and terrace formation near Mount St. Helens, Washington, unpublished M.S. Thesis, Colorado State University, Fort Collins, 157 pp.
- Parker, G., Klingeman, P.C., and Mclean, D., 1982. Bed load and size distributions in paved gravel-bed streams, *Journal of the Hydraulics Division, American Society of Civil Engineers*, v. 108, p. 544-571.
- Patton, P.C. and Baker, V.R., 1976. Morphometry and floods in small drainage basins subject to diverse hydrogeomorphic controls, *Water Resources Research*, v. 12, p. 941-952.
- Pickup, G., Higgins, R. J., and Grant, L., 1983. Modelling sediment transport as a moving wave- the transfer and deposition of mining waste, *Journal of Hydrology*, v. 60, p. 281-301.
- Pickup, G. and Warner, R.F., 1976. Effects of hydrologic regime on magnitude and frequency of dominant discharge, *Journal of Hydrology*, v. 29, p. 51-75.
- Pitlick, J. and Thorne, C.R., 1987. Sediment supply, movement and storage in an unstable gravel-bed river, in Thorne, C.R., Bathurst, J.C. and Hey, R.D. (eds), *Sediment Transport in Gravel-Bed Rivers*. John Wiley and Sons, New York, p. 151-178.
- Pitlick, J. 1988. Variability of bed load measurement, *Water Resources Research*, v. 24, p. 173-177
- Pitlick, J., (in press). Sediment routing in tributaries of Redwood Creek, in Nolan, K.M., Kelsey, H.M. and Marron, D.C. (eds), *Geomorphic processes and aquatic habitat in the Redwood Creek basin, Northwestern California*, U.S. Geological Survey Professional Paper 1454.
- Potter, K.E., 1987. Research on flood frequency analysis: 1983-1986, *Reviews of Geophysics*, v. 25, p. 113-118.
- Potter, K.E. and Walker, J.F., 1985. An empirical study of flood measurement error, *Water Resources Research*, v. 21, p. 403-406.
- Prestegaard, K.L., 1983. Bar resistance in gravel-bed streams at bankfull stage, *Water Resources Research*, v. 19, p. 472-476.
- Ritter, J.R., 1974. The effects of the Hurricane Agnes flood on channel geometry and sediment discharge of selected streams in the Susquehanna River Basin, Pennsylvania, *U.S. Geological Survey Journal of Research*, v. 2, p. 753-761.
- Schick, A.P., 1974. Formation and obliteration of desert stream terraces- a conceptual analysis, *Zeitschrift fur Geomorphologie, Supplement 21*, p. 88-105.
- Schumm, S.A., 1977. *The Fluvial System*. Wiley, New York, 338 pp.
- Schumm, S.A., 1985. Explanation and extrapolation in geomorphology: Seven reasons for geologic uncertainty, *Transactions of the Japanese Geomorphological Union*, 6, p.1-18.
- Schumm, S.A. and Lichty, R.W., 1963. Channel widening and floodplain construction along Cimarron River in Southern Kansas, *U.S. Geological Survey Professional Paper 352-D*, p. 71-88.
- Scott, G.R., 1975. Cenozoic surfaces and deposits in the Southern Rocky Mountains, in Curtis, B.F. (ed), *Geological Society of America Memoir 144*, p. 227-248.
- Scott, K.M. and Gravelee, G.C., 1968. Flood surge on the Rubicon River, California- hydrology, hydraulics and boulder transport, *U.S. Geological Survey Professional Paper 422-M*, 40 pp.

- Shroba, R.R., Schmidt, P.W., Crosby, E.J. and Hansen, W.R., 1979. Geologic and geomorphic effects in the Big Thompson Canyon area, Larimer County, U.S. Geological Survey Professional Paper 1115, Part B, p. 87-152.
- Simons, D.B., Al-Shaikh-Ali, K.S., and Li, R.M., 1979. Flow Resistance in cobble and boulder riverbeds, *Journal of the Hydraulics Division, American Society of Civil Engineers*, v. 105, pp. 477-488.
- Stedinger, J.R. and Cohn, T.A., 1986. The value of historical and paleoflood information in flood frequency analysis, *Water Resources Research*, v. 22, pp.
- Stewart, J.H. and LaMarche, V.C., 1967. Erosion and deposition in the flood of December 1964 on Coffee Creek, Trinity County, California, *U.S. Geological Survey Professional Paper 422-K*, 22 pp.
- Thomas, D.M. and Benson, M.A., 1970. Generalization of streamflow characteristics from drainage basin characteristics, *U.S. Geological Survey Water Supply Paper 1975*, 55 pp.
- United States Department of Commerce, National Oceanic and Atmospheric Administration, *Climatological Data for California*, U.S. Government Printing Office, Washington, D.C. (published monthly).
- United States Water Resources Council Hydrology Committee, 1982. *Guidelines for determining flood flow frequency, Bulletin 17B*, U.S. Government Printing Office, Washington, D.C.
- Waananen, A.O. and Crippen, J.R., 1977. Magnitude and frequency of floods in California, *U.S. Geological Survey Water Resources Investigation 77-21*, 96 pp.
- Wildman, N.A., 1981. Episodic removal of hydraulic mining debris, Yuba and Bear River basins, California, unpublished M.S. thesis, Colorado State University, Fort Collins, 107 pp.
- Williams, G.P., 1978. Bankfull discharge of rivers, *Water Resources Research*, v. 14, p. 1141-1154.
- Williams, G.P., 1983. Paleohydrological methods and some examples from Swedish fluvial environments, *Geographiska Annaler*, v. 65A, p. 227-243.
- Williams, G.P. and Guy, H.P., 1973. Erosional and depositional aspects of hurricane Camille in Virginia, 1969, *U.S. Geological Survey Professional Paper 804*, 80 pp.
- Wolman, M.G., 1954. A method of sampling coarse bed material, *Transactions of the American Geophysical Union*, v.35, p.951-956.
- Wolman, M.G. and Eiler, J.P., 1958. Reconnaissance study of erosion and deposition produced by the flood of August 1955 in Connecticut, *Transactions American Geophysical Union*, v. 39, p. 1-14.
- Wolman, M.G. and Miller, J.P., 1960. Magnitude and frequency of forces in geomorphic processes, *Journal of Geology*, v. 68, p. 54-74.
- Wolman, M.G. and Gerson, R., 1978. Relative scales of time and effectiveness of climate in watershed geomorphology, *Earth Surface Processes*, v. 3, p. 189-208.
- Zimpfer, G.L., 1982. Hydrology and geomorphology of an experimental drainage basin, unpublished Ph.D. dissertation, Colorado State University, Fort Collins, 185 pp.